Fuzzy Logic Control of Torsional Lateral Modal Response in Offset Geared Machine Trains

by

Henry Keith Laskey P Eng

A thesis
presented to the University of Waterloo
in fulfilment of the
thesis requirement for the degree of
Doctor of Philosophy
in
Mechanical Engineering

Waterloo, Ontario, Canada, 1998

© H K Laskey 1998

National Library of Canada
Acquisitions and Bibliographic Services
395 Wellington Street
Ottawa ON K1A 0N4
Canada

Bibliothèque nationale du Canada
Acquisitions et services bibliographiques
395, rue Wellington
Ottawa ON K1A 0N4
Canada

Your file Votre référence

Our file Notre référence

The author has granted a non-exclusive licence allowing the National Library of Canada to reproduce, loan, distribute or sell copies of this thesis in microform, paper or electronic formats.

The author retains ownership of the copyright in this thesis. Neither the thesis nor substantial extracts from it may be printed or otherwise reproduced without the author's permission.

L'auteur a accordé une licence non exclusive permettant à la Bibliothèque nationale du Canada de reproduire, prêter, distribuer ou vendre des copies de cette thèse sous la forme de microfiche/film, de reproduction sur papier ou sur format électronique.

L'auteur conserve la propriété du droit d'auteur qui protège cette thèse. Ni la thèse ni des extraits substantiels de celle-ci ne doivent être imprimés ou autrement reproduits sans son autorisation.

0-612-32837-6

Canada

The University of Waterloo requires the signatures of all persons using or photocopying this thesis. Please sign below, and give address and date.

To Norma

ABSTRACT

Fuzzy Logic Control of Torsional Lateral Modal Response in Offset Geared Machine Trains

Energy conservation is providing the driving force behind the development of variable frequency drives for medium voltage AC motors. Significant energy savings can be realized by varying the speed of a turbomachine to provide a better match with the application specific system requirements. Many of these drives will be retrofitted to existing equipment which normally run at fixed operating speeds. Energy saving measures for future automated plants will require these machines to operate smoothly over a significant speed range. Resonance response at certain "critical" speeds will inevitably lead to excessive vibration for many of these applications.

This work concentrates on machine trains containing a parallel shaft offset gearbox which results in a coupling of the torsional and lateral dynamic regimes of the rotating elements. This is manifested most significantly through the physical offset of the shaft centerlines giving rise to both lateral and torsional forcing functions.

The new development introduced herein is an extension to the concept of the well known Lanchester damper combined with a fuzzy logic controller. A semi-active damper / absorber is used to provide an optimal damping / inertia torque for control of the machine train response using artificial intelligence techniques. The result is a very effective and economical control responding to the lateral vibration via the coupled torsional regime. The unique control is basically a three step procedure to locate the minimum lateral response of the gearbox by varying inertia addition and torsional damping. The torsional damper / absorber is attached to the free end of the high speed shaft.

This is a general development which can be readily applied to offset geared machine trains in industry. This represents a major step forward in the provision of a convenient new method which combines and extends known technology to solve a complex problem that has plagued industry for years.

ACKNOWLEDGMENTS

I would like to express my appreciation to my initial supervisor, Dr Raj Dubey and my present supervisors, Dr. H R Martin and Dr. J Huissoon for their instructive guidance and helpful support throughout the course of this work.

I would like to thank my family for their patience and encouragement during this time period. I would also like to express my total admiration and appreciation for the undying support and patience shown by Norma. I am forever indebted to her for making life appear normal during the years of this work effort. Lastly, but by no means least, I would like to give thanks to my Lord and Savior Jesus Christ for the strength and ability to complete the work.

TABLE OF CONTENTS

List of Tables xi

List Of Figures xii

Nomenclature xv

Chapter 1

Introduction

1.1 Energy Conservation 1

1.2 Forcing Functions 2

1.3 Torsional Lateral Coupled Response 3

Chapter 2

Literature Review

2.1 Passive Control 9

2.2 Active Control 12

2.3 Fuzzy Logic 16

2.4 Summary of Literature Relevance 20

Chapter 3

Theory

3.1 Introduction 21

3.2 Torsional Lateral Coupling 21

3.2.1 Single Shaft Rotor 22

3.2.2 Two Rotors with Offset Gearing 25

3.3 Bondgraph Solution 26
3.4 State Space Control 28
3.5 Fuzzy Control 31
3.5.1 Fuzzy Set Theory 31
3.5.2 Membership Functions 32
3.5.3 Fuzzy Logic 33

Chapter 4

Application

4.1 Torsional /Lateral Modeling 38
4.2 Mathematical Model 40
4.2.1 Lagrange Method 43
4.2.2 Bondgraph Method 46
4.2.2.1 Constitutive Equations 53
4.3 Control of Torsional Vibration 60
4.3.1 Passive Control 60
4.3.1.1 Flexible Couplings 60
4.3.1.2 Absorbers and Dampers 61
4.3.2 Active Control 62

Chapter 5

Experimental

5.1 Prototype Development 64
5.1.1 Machine Train 64
5.1.2 Instrumentation 67
5.1.2.1 Lateral Vibration Measurement 67
5.1.2.2 Prototype Speed Measurement 68
5.1.2.3 Torsional Vibration Measurement 71
5.1.3 Data Acquisition 73

5.1.4 Control Hardware 73
5.1.4.2 Amplifier 76
5.2 Control Development 79
5.2.1 Classical Control Considerations 79
5.2.2 Fuzzy Software 83
Level 1. Approximate Speed Correction 90
Level 2. Pre-Minimization 98
Level 3. Minimization Through Fuzzy Inferencing 102
5.3 Final Result 107

Chapter 6

Discussion of Results

6.1 Prototype 109
6.2 Computer Simulation 115
6.3 Relevance to a Real Machine Train 126

Chapter 7

Conclusions and Recommendations 128

References 132

Bibliography 136

Appendix I

Prototype: Equations of Motion 138
Lagrange Method 138
Bondgraph Method 140
Reconciliation of Methods 142

Prototype with Damper 145

Appendix II

Prototype State Space Matrices 146

Appendix III

Fuzzy Control Software 149

Appendix IV

Torsional Lateral Mode Shapes 165

Appendix V

Metrabyte Model DAS-16 Card 179

LIST OF TABLES

Table 3.1: Orderly Rotations about the x_o, y_o, z_o Axes 23

Table 4.1: Bondgraph Model Elements 52
Table 4.2: Prototype Stiffness Parameters 56
Table 4.3: Shaft Section Parameters 57
Table 4.4: Prototype Mass / Inertia Parameters 58
Table 4.5: Prototype System Frequency Comparison 59

Table 5.1: Metrabyte Das-16 Data Acquisition Board Settings 74
Table 5.2: Initial Estimated Voltage Correction Function 91
Table 5.3: Second Estimated Voltage Correction Function 92
Table 5.4: Third Estimated Voltage Correction Function 95
Table 5.5: Fuzzy Associative Matrix (FAM) 103

Table 6.1: Damping and Inertia Distribution with Voltage 117

Table A-IV 1: Relative Node Displacements (free mode 2) 169
Table A-IV 2: Relative Node Displacements (free mode 3) 171
Table A-IV 3: Relative Node Displacements (locked mode 2) 173
Table A-IV 4: Relative Node Displacements (locked mode 3) 175
Table A-IV 5: Relative Node Displacements (locked mode 4) 177

LIST OF FIGURES

Figure 1.1: Typical Offset Gear Machine Train 4
Figure 1.2: Offset Torques and Forces 5

Figure 3.1: Disk on Flexible Shaft 24
Figure 3.2: A Normal Fuzzy Set 33

Figure 4.1: Mathematical Model of Prototype 42
Figure 4.2: Prototype Machine Train 48
Figure 4.3: Bondgraph Diagram 49

Figure 5.1: Experimental Rig 65
Figure 5.2: Proximeter Calibration 68
Figure 5.3: Tachometer Calibration 69
Figure 5.4: Trigger / Tachometer Circuit 70
Figure 5.5: Main Gear Torsional Deflection 72
Figure 5.6: Output Amplifier Calibration 75
Figure 5.7: Output Amplifier Circuit 77
Figure 5.8: Prototype Control Configuration 78
Figure 5.9: Active Vibration Control 81
Figure 5.10: Universe of Discourse 84
Figure 5.11: Locked vs Free Damper 86
Figure 5.12: Lateral Response at Constant Clutch Voltage 87
Figure 5.13: Lateral Response at Constant Clutch Voltage 88
Figure 5.14: Lateral Response at Constant Clutch Voltage 88
Figure 5.15: Lateral Response at Constant Clutch Voltage 89

Figure 5.16: Response vs. Voltage at Constant Speed 89
Figure 5.17: Lateral Response with Initial Estimated Function 93
Figure 5.18: Clutch Voltage with Initial Estimated Function 93
Figure 5.19: Lateral Response with Second Estimated Function 94
Figure 5.20: Clutch Voltage with Second Estimated Function 94
Figure 5.21: Lateral Response with Third Estimated Function (i) 96
Figure 5.22: Clutch Voltage with Third Estimated Function (i) 96
Figure 5.23: Lateral Response with Third Estimated Function (ii) 97
Figure 5.24: Clutch Voltage with Third Estimated Function (ii) 97
Figure 5.25: Pre-Minimize Procedure 101
Figure 5.26: Fuzzy Control Flow Diagram 105
Figure 5.27: Instability From Over-Correction 106
Figure 5.28: Ineffective Under-Correction 106
Figure 5.29: Lateral Response with Active Fuzzy Control 108

Figure 6.1: Interference Diagram for Free Damper 113
Figure 6.2: Interference Diagram Locked Damper 114
Figure 6.3: Sum and Difference Frequency Exciters 114
Figure 6.4: Rotor Response Simulation (64.5 Hz) 118
Figure 6.5: Rotor Response Simulation (53.8 Hz) 120
Figure 6.6: Composite Simulation Response (53 Hz) 121
Figure 6.7: Composite Simulation Response (64.5 Hz) 122
Figure 6.8: Composite Simulation Response (67 Hz) 123
Figure 6.9: Composite Simulation Response (68 Hz) 124
Figure 6.10: Composite Simulation Response (69 Hz) 125

Figure A-IV 1: Finite Element Model 166
Figure A-IV 2: Free Mode 2, Coupled Mode Shape 170
Figure A-IV 3: Free Mode 2, Relative Shaft Twist 170

Figure A-IV 4: Free Mode 3, Coupled Mode Shape 172
Figure A-IV 5: Free Mode 3, Relative Shaft Twist 172
Figure A-IV 6: Locked Mode 2, Coupled Mode Shape 174
Figure A-IV 7: Locked Mode 2, Relative Shaft Twist 174
Figure A-IV 8: Locked Mode 3, Coupled Mode Shape 176
Figure A-IV 9: Locked Mode 3, Relative Shaft Twist 176
Figure A-IV 10: Locked Mode 4, Coupled Mode Shape
..... 178
Figure A-IV 11: Locked Mode 4, Relative Shaft Twist 178

NOMENCLATURE

torsional and bending symbols:

ϕ	rotation about x
ψ	rotation about y
θ	rotation about z
u	displacement along x_o
v	displacement along y_o
w	displacement along z_o
e_x, e_y	eccentricity in the x y z frame for respective axes
s	arc length along deflected shaft
r	position vector for point along deformed central line
r	disk, gear radius
N_x, N_y	transverse shear forces in the respective axes
M_x, M_y	bending moments in the respective axes
M_z	torsional moment
$I = I_x = I_y$	transverse area moment of inertia
ρ	mass density per unit volume
m	mass per unit length
T	applied torque
q	generalized coordinate

energy and lumped parameter symbols:

y	excursion along the y axis
θ	rotation about z
d	diameter
Q	non-conservative forces
T	kinetic energy
V	potential energy
U	strain energy
L	Lagrangian (L = T - V)
I_x, I_y, I_z	moment of inertia about the applicable axis
m	mass
R	internal damping
b	friction or work related damping (to ground)
G	shear modulus
J	polar area moment of inertia of shaft cross-section
ℓ	length of the beam, lumped parameter
E	modulus of elasticity
λ	wavelength
a	celerity, speed of sound
f	frequency

bondgraph symbols:

ω	rotational velocity
I	mass moment of inertia of rotating body
C_t	torsional flexibility
K_t	torsional stiffness
SE	source of effort
SF	source of flow
R	damping (resistance)
TF	transformer
p	parallel junction
s	series junction
f	flow (general)
e	effort (general)
r	pinion, gear radius

state space symbols:

M	mass matrix
K	stiffness matrix
R	damping matrix
A	system matrix
B	input coefficient matrix
F	disturbance coefficient matrix
C	state output coefficient matrix
D	output coefficient matrix
E	disturbance output coefficient matrix
x	state vector
x_s	transduced state vector
r	input vector
w	disturbance vector
y	output vector
S	controllability matrix
V	observability matrix
G	feedback gain matrix
f	actuator force vector
T_1	coordinate transformation of control force to actuator force
T_2	coordinate transformation of state vector transducers
u	control force vector

fuzzy control symbols:

X	input universe of discourse
Y	output universe of discourse
x	elements contained in X (input)
y	elements contained in Y (output)
A, B	fuzzy sets defined on the universe of discourse
μ	fuzzy membership value

pre-minimize and simulation symbols:

SR	slope ratio
V_1	vibration at step 1
s_1	difference in vibration level for step 1
SIR	slip inertia ratio

sum & difference frequency symbols:

F_{ex}	combined exciting frequency
F_a	varying frequency
F_b	fixed frequency

Chapter 1

Introduction

1.1 Energy Conservation

The trend toward faster running, lighter machines in industry today results in many vibration problems associated with the basic structure of machines as well as with the dynamics of rotating elements. There is also a definite need in industry today to conserve energy, creating a demand for the development of medium voltage (2.3 kV-6 kV) high horsepower (1000-6000 HP) alternating current variable speed drives. Drives of this description will be installed to optimize power usage in the process and utility industries.

The driving force behind the development of these variable frequency drives for medium voltage AC motors is energy conservation. Significant energy savings can be realized by varying the speed of a turbomachine to provide a better match with the specific application system requirements. The power requirement of a positive displacement machine (pump or compressor) is directly proportional to the speed of operation. These are constant torque machines for which speed can be varied to directly follow flow change requirements. The power required by a centrifugal machine is a direct function of the varying torque. Torque is related directly to the developed head of the machine which varies as the square of the speed. Power is directly proportional to both torque and speed

resulting in the power requirement related to the speed ratio cubed. These facts can lead to dramatic energy saving opportunities for those applications which may not need full speed operation throughout the load duty cycle of the turbomachine.

It is estimated [1] that an overall 45% of industrial and commercial energy consumption is by fan, pump, and blower systems. A further 30% of energy is consumed by constant torque machines. The estimated potential savings available in these systems by use of variable speed drives will range from 20 to 50% of present day consumption. Many of these drives will be retrofitted to existing equipment which have been designed and operated successfully at a fixed operating speed. Energy saving measures as well as future automated plant requirements will require these machines to operate over a significant speed range. In the case of automated plants, the machine will likely be controlled remotely by a process variable which itself will be determined by prevailing market conditions. This control will have indiscriminate requirements for operation at all possible speeds within a specified operating range.

Resonance can occur, as a result of a speed change, when an inherent forcing frequency associated with the operating machine matches a natural frequency. Resonance response at certain speeds will inevitably lead to excessive vibration in many of these applications. Future automated plant requirements will no longer accept stepping over resonances electronically, as the resulting stepwise speed changes will not deliver the smooth process output dictated by quality control of the end product.

1.2 Forcing Functions

In many cases, variable speed capability may be incorporated with existing fixed speed AC systems without changing motors, conduit or wiring. Until just recently, only three

basic inverter types existed for use with squirrel cage induction motors: the voltage source (VSI or VVI), the current source (CSI), and the pulse width modulated source (PWM). For more recent designs, these simple designations do not adequately characterize the available configurations. However, both multi-step and PWM inverters induce torque variations on the output shaft of the associated drive motor during operation. These variations occur at different frequencies as a result of harmonics in the supply waveform between the inverter and the motor. Inverters do not produce sine wave outputs. Six step inverters may produce significant exciting harmonics at 6x, 12x, and 18x the supply frequency. Therefore, the construction of inverter bridge components together with varied control modes, can result in the excitation of torsional and lateral modes of the driven equipment.

This is not by any means the only source of excitation. Excitation may be inertially based such as unbalance with driving amplitudes varying as the square of speed. Other sources of excitation may result from shaft misalignment as well as from the nature of the driven machine such as pulsing associated with reciprocating machines, and blade passing frequencies of turbomachines.

1.3 Torsional Lateral Coupled Response

The thrust of this research concentrates on multi-element machine trains having a set of parallel shaft offset gears, see Fig 1.1. As a result of this gearing, there will be a strong coupling of the torsional and lateral dynamic regimes associated with the rotating elements of the train. The industry standard analytical approach [12] for such a machine train would normally entail a lateral analysis of each individual machine with a torsional analysis of the assembled train. In many cases, analysis may not be done at all unless

specifically requested by the end user. Moreover, the lateral and torsional analysis when conducted, would be executed independently of each other.

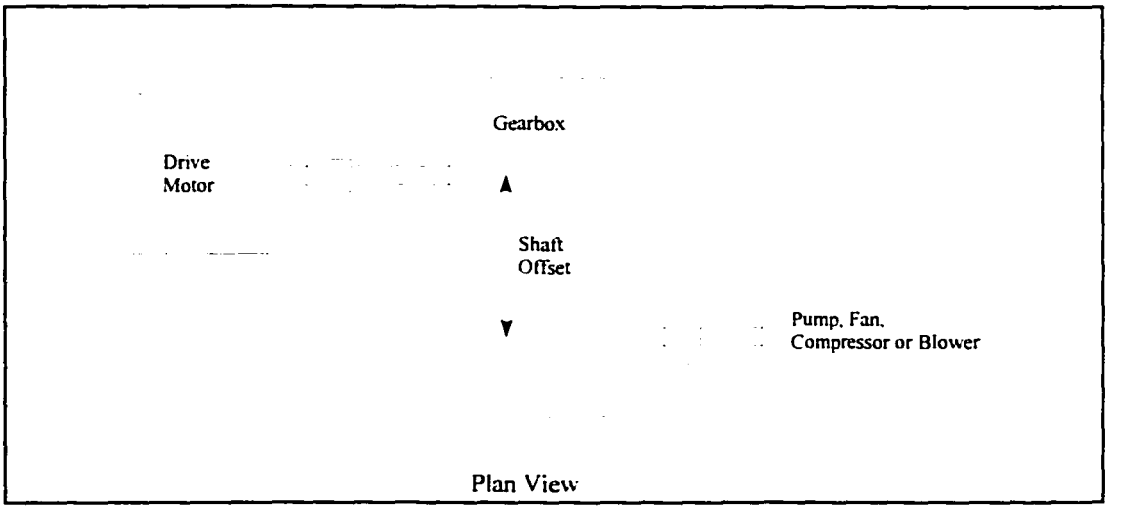


Figure 1.1: Typical Offset Gear Machine Train

Recent investigations [11, 12, 13, 14] have shown that the dynamic behaviour of multi-element machine trains with offset gearing exhibits significant coupling between the torsional and lateral modes. This is manifested most significantly through the physical offset of the shaft centerlines giving rise to an offset forcing function. A force (causing bending) as well as a moment (causing torsion) is evident on each of the pinion and gear shafts as indicated in Fig 1.2.

Torsional vibration can be a silent destroyer as there are generally no operating characteristic tell-tale symptoms that provide prior warning of impending damage as with radial vibration. Torsional vibration, allowed to develop unheeded, can lead to disastrous, if not catastrophic, consequences. Without special monitoring instrumentation, it is impossible to know how significant the torsional motion might be on a given machine component. Also, transducers must be judiciously placed to ensure meaningful information for the modes of interest. Transducers placed at a node point

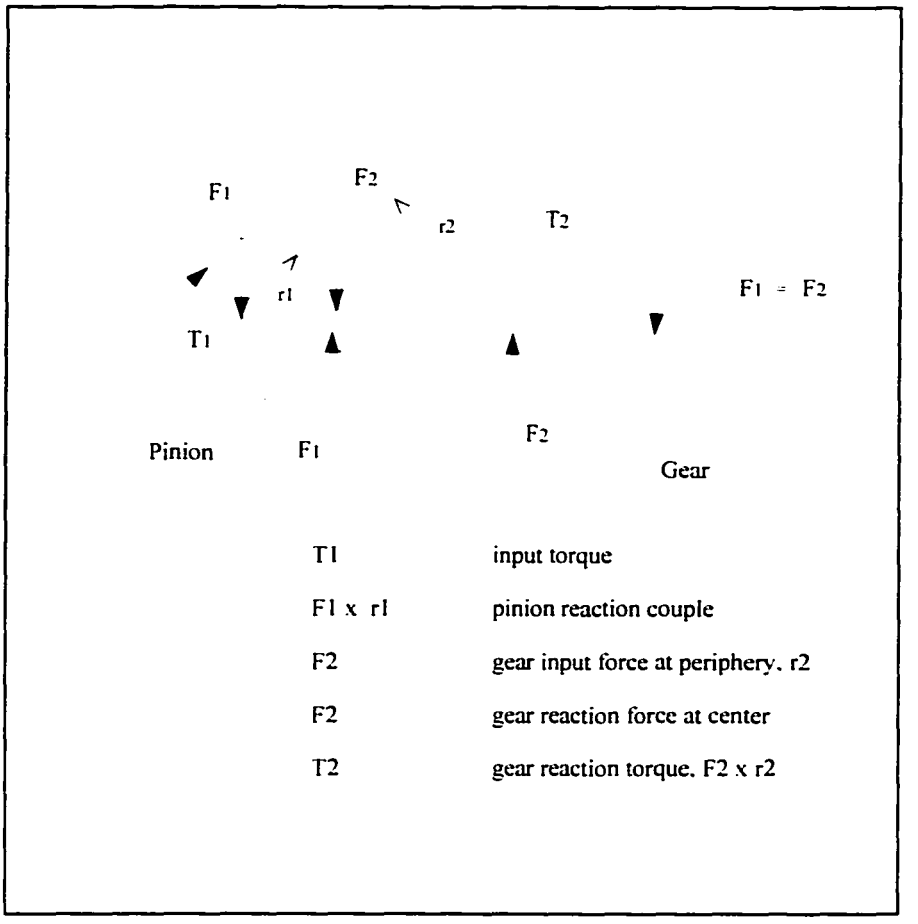


Figure 1.2: Offset Torques and Forces

may lead to a false sense of security for an operating speed. Constant monitoring should be considered if effective protection of machinery is desired. A machine train with a protective device of some description (torsionally soft couplings or a vibration absorber) may operate successfully at its rated speed for many hours, yet will give little warning prior to failure of the protection device, resulting in a disastrous operating condition for the machine train.

Generally, the first line of defence for a torsional problem is the application of a torsionally soft coupling or the introduction of a flywheel. These modifications can shift natural frequencies down; however, the effect may be localized without the ability to be

easily extended to other modes. Many problems exist with torsionally flexible couplings by way of a shortened lifespan through hysteretic heating and consequent fatigue of the flexible member. Also, nonlinearities, usually associated with these devices, make it very difficult to design a system which will be predictable exactly. The only thing which can be predicted, with some certainty, is the direction of resonance frequency shift.

For variable speed machine trains, shifting of the natural frequency down by the introduction of either a flywheel or a soft coupling will not eliminate the resonance problem, but merely shift its location. Shifting the frequency upward is difficult to achieve since, in general, mass cannot be eliminated easily and it is difficult to select a coupling which will exhibit stiffness properties significantly greater than a standard coupling. For instance, in the case of a reciprocating pump / compressor driven by an adjustable speed drive, it may be impossible to shift the resonant frequencies up or down and avoid all possible forcing functions when traversing a significant speed range. Depending on the characteristics of the load and the drive, there will be exciting torques associated with the fundamental frequency as well as with several higher harmonics.

The problem of control of torsional vibration in a variable speed application is somewhat complex. For a fixed speed machine, it is conceivable to select suitable devices to attenuate the effects of vibratory torque at the one speed. However, when the system requires speed to be varied over an operating range, especially in the retrofit market, the unknowns associated with crossing several natural frequencies with various forcing functions can create significant problems. Passive absorbers and dampers are limited since they are designed or selected for a single speed and will be most effective in attenuating the system response at that speed.

The new concept introduced herein is an extension to the application of the well known Lanchester damper by controlling the effective damping / inertia torque with artificial intelligence techniques. This results in a very effective and economical control

responding to the lateral vibration via the coupled torsional regime. The response of the system is a function of the transport velocity and as such, does not lend itself to simple linear characterization since the instituted control shifts the resonant response peaks away from the operating speed by modifying the mass and elastic properties of the train. In addition, significant damping is introduced, as required, over the speed range to reduce unwanted torsional variations. These effects are accomplished by the automatic selection of additive torsional inertia via the controlled magnetically actuated friction clutch with flywheel assembly. This arrangement is attached to the open end of the high speed gear shaft. The flywheel inertia attachment to the system is through the clutch friction effect only. The stronger the magnetic clamping force, the greater the inertia influence. The torsional damping effect due to slip will have its greatest influence somewhere in the midrange of clamping forces, while tapering off at either extreme.

The torsional damper has been used successfully, but not optimally, for years in reciprocating engines to reduce the torsional response excited by the crank-effort driving functions. The normal application procedure is to determine a suitable mass and damping factor based on the intersection of response curves for the case of no damper, as well as the case of the damper fully locked into the system [2]. A selection is then made from commercially available units.

The method developed herein constitutes a semi-active type of control which is unable to input energy to the system. The control can only dissipate energy while also modifying the temporary energy storage distribution throughout the operating machine train.

No attempt has been made to apply classical control methods to this problem because of the complex nature of the combined actuator and system response characteristic. This fact however renders the artificial intelligence approach, because of its flexible nature, quite useful in realizing a successful control. The fuzzy control developed herein is not a routine application of fuzzy logic to a well defined type of problem (eg. inverted

pendulum), but serves to illustrate the relative convenience and flexibility of exploiting these methods in developing a useful and economical control for systems having distinct characteristics which are difficult to describe mathematically.

This is a general development which can be readily applied to machine trains in industry. The major step forward is in the provision of a convenient new method which combines and extends known technology to solve a complex problem which has plagued industry for years. The control of the output parameter is realized with artificial intelligence techniques utilizing a fuzzy logic controller. A fuzzy logic controller is an expert type system based on a number of fuzzy operating If ...Then ... type of rules. The output modification is determined through inferencing techniques developed in fuzzy set theory. The fuzzy system provides the required control with the same control logic for all resonant frequencies which may be excited within the operating range. This is accomplished without the need for a mathematical model of the system to determine the proper tuning parameters as would be the case with a conventional control system. The conventional PID control would require modification or tuning for each peak encountered in the speed range.

The fuzzy logic controlled damper system, applied as described in this document, precludes the development of significant torsional vibration energy with associated coupled lateral motion of the gearbox shafting and bearing supports, at all speeds throughout the operating range of an offset geared machine train.

Chapter 2

Literature Review

2.1 Passive Control

The initiating work of developing a theory for vibration absorbers was published in 1928 by Ormandroyd and Den Hartog [3]. This work considered the special analysis of a two degree of freedom system dealing with the case of adding a small spring-mass system tuned to the resonant frequency of the primary single degree of freedom system. The predicted annihilation of vibration at resonance was shown to be true experimentally. However, the system now had two resonant frequencies, one below and one above the original frequency. It was realized at the inception of these theoretical explanations, and stated by the authors, that this device would only be suitable for attachment to a fixed speed machine.

A further work by the same authors [4] developed the theory of the Lanchester damper for torsional systems and for specific application to reciprocating engines. The Lanchester damper is a rotating mass attached to the primary system by damping only. This type of damper originated with dry, or coulomb friction, but because of inconsistencies of the frictional torque, soon became constructed using a viscous fluid encased in a close-clearance housing. This allowed for better mathematical treatment

as well as more predictable and reliable results.

Brock [5] extended the Den Hartog work by developing the formulas for optimum damping for three specific cases of absorber tuning:

(1) optimum tuning
(2) constant tuning (i.e. absorber natural frequency matches the primary system)
(3) no tuning

In another work, Brock [6] also developed formulas for optimum damping for the case of inertial disturbance. The original theory assumed a constant amplitude forcing function for all frequencies. For inertial disturbance the amplitude varies as the rotating speed squared (e.g. unbalance). This type of forcing function is generally not a problem for torsional systems; however for offset geared systems, it may become significant for the case of lateral unbalance response causing a torsional forcing function through the coupling phenomenon.

All of the foregoing theory has been developed for an auxiliary system attachment to a single degree of freedom system. A real machine train will have a continuum of mass and stiffness and therefore many degrees of freedom. Lewis [7] extended the theory of the viscous vibration absorber by developing a method of determining optimum damping for a multi-mass, multiple degree of freedom system. The method is based on producing a sequence table (i.e. a Holzer calculation) for the specific resonance and shaft section of concern. For the untuned damper, a plot of the applicable amplitude through resonance for the case of no damping and infinite damping will define the point of intersection from which the amplitude ratio of dynamic to static displacement of primary mass, x_o/δ_{st}, can be determined. If greater attenuation is required, a larger mass must be considered. Otherwise, for the case of the untuned damper, a sequence table is constructed for a frequency, ω^2, equidistant above and below the intersection point and with damping

introduced as a complex stiffness ($j\omega b$). A mean value of the damping coefficient b, determined from these two points, should be adequate for most practical cases involving single speed operation.

The difficulty with all of the theoretical methods presented, is that the optimum is found for one frequency only. In the case of a real machine train having multiple degrees of freedom, there will also be multiple resonances. Several of these frequencies may be excited when traversing the operating speed range as required in a variable speed arrangement. Szenasi and Bloggett [8] present a field example of a 4 cylinder compressor driven through a gearbox by a 16 cylinder reciprocating engine. The operational speed range for the engine is 1000-1700 rpm. They show 15 crossings of the first three natural frequencies by orders of the engine fundamental and compressor harmonics on a Campbell diagram. Their analysis of the problem is commendable; however, no real solution is proposed.

The effect of torsional response of a real machine train having offset gearing cannot be treated adequately in an independent analysis without due consideration given to the lateral response of the system. Wachel and Szenasi [9] present a field problem where torsional oscillations were observed together with unstable lateral vibration. They point out the importance of offset gearing in the energy exchange between the torsional and lateral modes.

Iannuzzelli and Elward [10] observed that some measured eigenfrequencies of a compressor train can only be calculated using a torsional-lateral coupling analysis across the offset gear.

Simmons and Smalley [11] pointed out the lack of reliable damping and excitation data which has led to rule of thumb assumptions and predictions for torsional systems. They found by experiment and analysis of a gas turbine compressor train, that the torsional

modes, with superimposed bending component at the offset gear, can be significantly damped via the radial motion in the oil film bearings. Their measured damping was nearly double that predicted from a damped eigenvalue analysis of the gear lateral motion alone. This is explained by a coupling of the torsional and lateral modes.

The effect of the coupling phenomenon is to shift the frequencies for resonance as well as the onset of rotor instabilities. Schwibinger and Nordmann [12] found that in a classical eigenvalue analysis, where the coupling effect is ignored, serious errors may result in the prediction of critical speeds and the speeds for the onset of instability. If the strong coupling effect is neglected, no account is made for torsional mode damping contributed by lateral motion in the fluid film bearings. Sensitivity analyses have also shown the significant effects of bending and torsional parameters on the calculated damping constants and stability threshold speeds.

2.2 Active Control

Much work has been done toward controlling lateral vibration in flexible rotors by modifying dynamics through magnetic bearings or by the implementation of linear actuators which act independently of the bearing supports.

In the case of a general industrial machine train, the costs associated with either of these methods may be prohibitive and thus a new approach is warranted. Historically, just as in the case of dynamic analysis, the control of lateral and torsional vibration has been treated as separate entities.

Stanway and Burrows [13] examine the state variable feedback control of flexible rotors mounted in flexibly supported journal bearings, through eigenvalue assignment.

Vibration control of rotating or translating systems was investigated by Ulsoy [14] for the effects of observation and control spillover caused by high frequency dynamics. This control strategy also utilized pole assignment.

Direct control of lateral vibrations through state variable feedback will lead to very large numbers of state variables which must be measured or estimated. To measure all of these is unrealistic from a cost and accessibility standpoint and to estimate each one requires many calculations which must be accomplished in real time. This, too, can be quite expensive or even impractical. Therefore, in most cases, the model is reduced to control the number of modes of interest while ignoring the higher frequencies.

Firoozian and Stanway [15] extend their own finite element program, for the lateral analysis of turbomachinery rotors, to an integrated approach to state variable feedback control. They follow the modal approach in which the modes to be controlled are arbitrarily chosen while the residual (higher frequency) modes are ignored. This can, and usually does, lead to spillover problems with high frequency contamination of the controller and transducer signals. As in most cases, the control forces are introduced at an outside position, at or near the bearings, and not at the most effective point of the rotor span. This is a limitation imposed by the lack of accessibility to most turbomachine shafts while in operation.

Raju and Sun [16] studied the modal control of a flexible system with multiple sensors and actuators. There was improvement in the control for an increased number of sensors and actuators; however, the complexity of the controller grows rapidly. Even for a simple cantilever beam there is considerable difficulty in finding optimal locations for the sensors and actuators. Again, with the modal approach, a realistic cutoff of frequencies must be chosen and the higher modes either filtered out or ignored. It has been noted that a larger number of sensors and actuators appear to reduce the destabilizing effects of spillover.

Ulbrich [17] discusses several strategies for the control of flexible rotor dynamics. His experiment involved imparting control forces via actuators attached to the bearing housings. He showed distinct improvement of control with proceeding from one velocity feedback, to velocity plus displacement feedback, to velocity and displacement feedback from two locations. Again, the control forces are restricted to being input at some non-optimum location (i.e. externally at bearing housings instead of at the maximum excursion point of the shaft).

In the general implementation of state variable feedback control, a state observer will be used to estimate those variables which are not available due to accessibility or cost. Burdess and Metcalfe [18][19] develop an approach for observer design based on disturbance cancellation having no a-priori knowledge of the disturbance. This single degree of freedom concept is expanded to a two degree of freedom system in [20], by the same authors, with limited success in controlling both modes. A big advantage of their formulation is the elimination of the requirement to model the system exactly. Disadvantages are the large gains required to maintain stability of the closed loop system and the limited ability to place poles arbitrarily. Large gains incorporated with sensor and actuator dynamics generally lead to instability. In most practical systems the dynamics will be considerably more complex, however, no inherent ability to handle spillover or unmodeled dynamics or to provide decoupling from other modes is indicated in this work.

Large systems are generally plagued by significant dynamic coupling of modes. One method to alleviate this difficulty is to apply decoupling filters. This works well when the plant parameters are well defined and unchanging with time. If changes do occur, this solution is not robust and the filters actually become extra dynamical elements in the system [21].

Maday and Johnson [21] outline a method of decentralizing control of large mechanical systems from a complex integrated central controller to multiple autonomous single-input single-output (siso) controllers. The control algorithm utilizes cascaded integral error compensation with state variable feedback (IESF).

Their control was developed using a decentralized non-collocated active vibration control system. Active vibration control of large mechanical systems is generally an application for multi-input multi-output control (mimo). Implementation of mimo control for high order systems can lead to considerable complexity and unreliability with the operation of the total system dependant on a central controller.

For a rotating machine train the advantages of decentralization are several: improved reliability, lower cost of implementation, and a modular type of design which will allow add-on systems for possible future branch expansions. The basic methodology involves performing row and column partition of the overall system "A" matrix to separate the component systems into autonomous units, with the influence of all connected systems treated as disturbance. The regulator format of this control then attempts to reduce the effects of the disturbance to zero.

The control algorithm has strong decoupling capability and does not require separate decoupling filters. Stable control is assured through pole assignment. The example utilized is a very low frequency system (< 1 Hz) for which the gains of the controller are reasonable. However, when applied to a more realistic system with operating frequencies up to 100 Hz, the dynamic range of the controller gains quickly becomes unmanageable. At around 5 Hz the required gain is approximately 10^7 for all poles placed at -5. This situation would obviously have to be improved if this control method were to be adapted for use with industrial equipment.

Zhu, Castelazo and Nelson [22] developed an optimal control strategy for rotor vibrations excited by synchronous rotating unbalances. They show that almost complete vibration cancellation can be achieved even when less actuators than degrees of freedom of the system are used in the presence of coordinate coupling.

2.3 Fuzzy Logic

The first thinker to grapple seriously with the concept of vagueness was Charles Sanders Pierce. He advanced Boolean logic and was the first to apply it to electric circuits; the basis of the digital computer.

Bertrand Russell [23] also probed the topic of vagueness from the standpoint of language. He maintained that vagueness and precision were features of language, not reality.

Max Black [24] pioneered the concept of fuzzy sets. Black outlined his proto-fuzzy sets in a 1937 article. He agreed with Pierce that vagueness stems from a continuum, and with Russell that it has degrees. He postulated that a continuum implies degree to properly identify or define the entity within the continuum. Imagine an infinite line of chairs beginning with a lump of wood and ending with a finished Chippendale and with each step along the way having minor indistinguishable changes from the previous unit. At what point does the unit become a chair and for any individual unit, in the line, how much is it a chair and how much is it not a chair?

Jan Lukasiewicz [25] took the first step toward a formal model of vagueness. He originated the substructure of fuzzy sets and early logic based on the significant step of three valued logic which incorporated 1 for true, 0 for false, and ½ for possible.

In his 1965 paper, Zadeh [26] identified vagueness and set forth the mechanics of fuzzy set theory. The key insight was that a set contained members which belonged only partly to the set. This led to the development of multi-valued logic in use today. In it he distinguished fuzziness from probability.

Zadeh [27] first described possibility theory in **System Theory**, the main journal in the field. Possibility is distinct from fuzziness although possibility distribution is essentially the same as membership function. He described possibility as the degree of ease with which an event may occur. Probability is the likelihood of occurrence.

Mamdani [28] described the initial application of fuzzy logic to the control of a real machine. The device was a steam engine with boiler and piston drive. The control objective was to maintain the boiler pressure and shaft output speed constant. The control was invoked as a set of linguistic rules which essentially modelled how a human expert operator would react to the various conditions. This proved to be very effective in reaching the set targets and maintaining them.

Recent literature contains many applications of fuzzy logic to various control systems. The application to the control of complex processes which are poorly defined or which may have nonlinear components is developing as a fruitful area of research. In his paper, Lee [29] presents an excellent summary of the general application of fuzzy logic controllers. Application pursuits have been broad-based ranging from the fields of finance to earthquake engineering. He notes that in many cases the fuzzy logic based systems have proven to be superior to classical methods. Some more notable applications referenced by the author are as follows:

a) activated sludge process
b) heat exchanger process
c) aircraft flight control
d) automobile speed control

e) automobile parking

f) traffic control

g) fuzzy automatic train operation

h) elevator control

i) cement kiln operation

j) power system and nuclear reactor control

Murayana et al. [30] applied fuzzy control concepts to the operation of a main diesel engine. The authors develop a new method of obtaining empirical rules for smooth engine operation. The objective of their work was to minimize fuel consumption regardless of changing operating conditions. Observations after implementation of the fuzzy control indicated a reduced time to reach optimum point without sacrificing accuracy, and with no evidence of unstable back and forth response through the run up.

Larkin [31] described a model of an aircraft auto-pilot controller based on fuzzy algorithms. The controller manoeuvres the aircraft from level flight onto the descent glide path and into final approach until just before touchdown. The effect of varying parameters and different defuzzification strategies on controller performance and aircraft response is analysed using flight simulation techniques.

In their work, Yasunobu and Miyamoto [32] developed a fuzzy predictive controller which uses expert rules culled from the experience of a skilled human operator for automatic train operation. The controller selects the most likely control command based on predictions of control results and direct evaluations of control objectives. This control was applied to a train system from the standpoint of riding comfort, running time, accuracy of stop gap, energy consumption, and safety. The predictive fuzzy controller showed significant improvements over classical control systems. Robust operation under changing grades as well as a 10% energy saving were also realized.

Yagishita et al. [33] applied fuzzy theory to the control of coagulant addition in a water purification plant. Mathematical modelling of the relationship between chemical addition and water turbidity is very complex. Normally, the amount of chemical used would depend significantly on the experience and judgement of skilled operators. Using fuzzy reasoning this judgement can be quantified using imprecise linguistic descriptors to provide corrective modification to a base statistical amount. It was demonstrated that the chemical control using fuzzy reasoning is as good as a skilled operator and gave a definite improvement compared with the results obtained with a regression model.

Murakami and Maeda [34] present a synthesis of a fuzzy logic control following Lukasiewicz logic for application to an automobile speed control system. The controller is composed of linguistic control rules which are conditional statements expressing the relationship between inputs and outputs. Algorithms for computing values of the two manipulated variables are developed in order to effect speed control of the automobile in real time. Results of computer simulations and road testing of an automobile equipped with a dedicated microprocessor are discussed as well as the usefulness of the fuzzy logic controller for automobile speed control.

In their paper, Bartolini et al. [35] present a performance adaptive fuzzy control algorithm for application to a continuous casting plant. The adaptive procedure consists of modifications to the membership functions of the fuzzy subsets for input and output variables. Such modifications are executed on the basis of the overall control system performance. The algorithm results are comparable with those obtained by using self tuning algorithms with classical control methods.

Scharf and Mandic [36] described the application of a self organizing fuzzy controller to movements of a commercially produced revolute joint robot arm. The fuzzy self organizing controller often gives superior results compared with a conventional PID

controller. Step response investigations of pick and place operations demonstrate the ability of the controller to deal effectively with the transient portion of the response.

2.4 Summary of Literature Relevance

Classical control methods have not as yet offered an adequate control of the combined torsional and lateral response of complex industrial machine trains which are required to operate at or near a resonant frequency. To date, the complete system of machines in the train has not been treated as a whole from a control standpoint.

The torsional damper / absorber is a known solution for fixed speed applications but has not previously been implemented as a control actuator device. Implementation of this device results in a time variable system. The realm of fuzzy logic is the application of fuzzy set theory and expert system rules to the control of time varying or non-linear systems.

Chapter 3

Theory

3.1 Introduction

This chapter will set out the underlying theory for the mathematical modeling of the plant as well as the fundamental concepts of state space and fuzzy logic control. The rigor of the dynamic model of the plant for determination of natural frequencies and computer simulations is required only to such a degree as to demonstrate the functionality of the control. The purpose of the work is adequately served with a relatively close dynamic representation of the physical prototype, and therefore such concepts as gyroscopics, rotary inertia and shear deflection will not be considered in the mathematical model.

3.2 Torsional Lateral Coupling

The concept of modeling torsional lateral coupling has been developed by others for the single shaft rotordynamics model [37] as well as the two shaft system incorporating an offset gear box [10] [12]. The actual equations of motion forming the mathematical

model of the prototype plant for this project are developed in Chapter 4, Application, using both the Lagrange approach and bondgraph method to represent the energy exchange across the gear mesh for the simple two shaft plant. Although there is coupling between the torsional and lateral regimes in a single shaft rotor, this will not be the main focus of this work. Of greater interest here is the strong coupling which occurs through the energy exchange mechanism associated with a parallel shaft horizontal offset gearbox (ref Fig 1.1 and 1.2).

3.2.1 Single Shaft Rotor

Diken and Tadjbakhsh [37] developed a model for a continuous flexible shaft rotor which carries a disk and is supported by isotropic flexible damped bearings at the ends. It is assumed that the mass center of the shaft does not coincide with the axis of rotation giving rise to a mass eccentricity distribution along the axis. External damping proportional to the velocity of the transverse motion of the shaft and external rotational damping proportional to the angular velocity of the cross section are included in their development of the equations of motion. Internal damping, gyroscopics, rotary intertia and shear effects are also taken into account.

The kinematical description of the rotating and deformed shaft and disk was achieved by referring to a sequence of reference frames in relative motion with respect to each other. Referring to Fig 3.1, the x, y, z frame is attached to the rotating shaft, the x_o, y_o, z_o is rotating with constant angular speed Ω with respect to the X, Y, Z inertial frame. To describe the action of bending and torsional motion in the vibrating shaft, orderly rotations about the x_o, y_o, z_o axes are allowed as given in Table 3.1.

Table 3.1: Orderly Rotations about the x_o, y_o, z_o Axes

Rotation angle	Applicable axis
ϕ	x_o
ψ	y_o (rotated)
θ	z_o (rotated)

The position vector of a point along the shaft, in the x_o, y_o, z_o frame, is given as

$$\mathbf{r} = u\mathbf{i}_o + v\mathbf{j}_o + (s+w)\mathbf{k}_o \quad \ldots\ldots\ldots\ldots\ldots\ldots\ldots\ldots\ldots\ldots \quad (3\text{-}1)$$

where u and v are the displacements in the transverse x_o and y_o directions respectively, w is the displacement in the longitudinal direction, and s is the arc length along the shaft to the point of interest (ref Fig 3.1).

The eccentricity vector **e** referred to the x, y, z frame is defined as

$$\mathbf{e} = e_x(s)\mathbf{i} + e_y(s)\mathbf{j} \quad \ldots\ldots\ldots\ldots\ldots\ldots\ldots\ldots\ldots\ldots\ldots\ldots \quad (3\text{-}2)$$

The following set of linear equations were developed [37] using the principles of linear and angular momentum (damping terms have been omitted here).

$$\partial N_x/\partial s = m[\ddot{u} - e_y\ddot{\theta} - \Omega^2 (u - e_y\theta) - 2\Omega (\dot{v} + e_x\dot{\theta}) - e_x\Omega^2] \quad \ldots\ldots\ldots\ldots\ldots \quad (3\text{-}3)$$

$$\partial N_y/\partial s = m[\ddot{v} - e_x\ddot{\theta} - \Omega^2 (v - e_x\theta) + 2\Omega (\dot{u} - e_y\dot{\theta}) - e_y\Omega^2] \quad \ldots\ldots\ldots\ldots\ldots \quad (3\text{-}4)$$

$$\partial M_x/\partial s - N_y = (\rho I + 2m\, e_y^2)(\ddot{\phi} + \Omega^2\phi) - 2m\, e_x\, e_y\, (\ddot{\psi} + \Omega^2\psi) \quad \ldots\ldots\ldots\ldots \quad (3\text{-}5)$$

$$\partial M_y/\partial s + N_x = (\rho I + 2m\, e_x^2)(\ddot{\psi} + \Omega^2\psi) - 2m\, e_x\, e_y\, (\ddot{\phi} + \Omega^2\phi) \quad \ldots\ldots\ldots\ldots \quad (3\text{-}6)$$

$$\partial M_z/\partial s = [2\,\rho I + 2m(e_y^2 + e_x^2)]\ddot{\theta} + m\, e_x\, (\ddot{v} - \Omega^2 v + 2\Omega\dot{u})$$

$$- m\, e_y(\ddot{u} - \Omega^2 u - 2\Omega\dot{v}) + \partial T/\partial s \quad \ldots\ldots\ldots\ldots \quad (3\text{-}7)$$

where	N_x, N_y	transverse shear forces in the respective axes
	M_x, M_y	bending moments in the respective axes
	M_z	torsional moment
	$I = I_x = I_y$	transverse area moment of inertia
	ρ	mass density per unit volume
	m	mass per unit length
	T	applied torque

Linear momentum in the z_o direction for axial vibration along the shaft is neglected. The shaft cross section is assumed to be round. In the above equations, torsional lateral coupling is evident through the effect of the mass eccentricity.

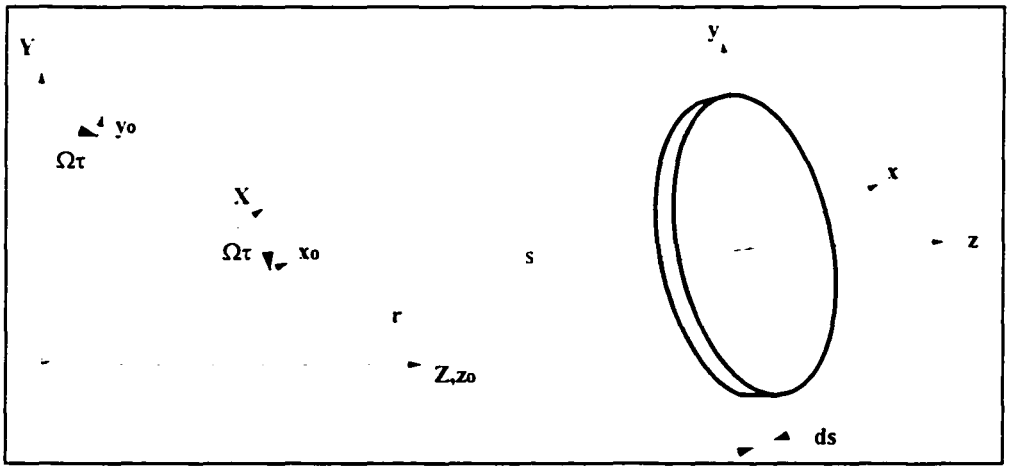


Figure 3.1: Disk on Flexible Shaft

3.2.2 Two Rotors with Offset Gearing

A model for the simple two shaft system is developed by Schwibinger et al [12] where the equation of motion with 'n' degrees of freedom is stated using the principle of virtual work. Static deflection functions were utilized to approximate displacements and allowing discretization of the model with continuous mass and stiffness distribution into disk-, shaft- and bearing- elements connected at their nodes. Noting that the sum of virtual work done by the inertia, damping, stiffness and external forces is equal to zero, the following energy equation may be stated

$$\delta q^T \{ M\ddot{q} + R\dot{q} + K\,q - F(t) \} = 0 \quad \ldots\ldots\ldots\ldots\ldots\ldots\ldots\ldots \quad (3\text{-}8)$$

where M (n x n) mass matrix
R (n x n) damping matrix
K (n x n) stiffness matrix
q (n x 1) vector of displacements
F (n x 1) vector of external forces

A constraint equation is introduced to connect the shafts allowing the coupling of the torsional-lateral dynamics as follows.

$$r_1 q_1 + q_3 = r_2 q_2 + q_4 \quad \ldots\ldots\ldots\ldots\ldots\ldots\ldots\ldots\ldots\ldots\ldots\ldots \quad (3\text{-}9)$$

where r_1, r_2 pinion, gear radius respectively
q_1 rotational displacement of the pinion
q_2 rotational displacement of the gear
q_3 lateral displacement of the pinion
q_4 lateral displacement of the gear

In this relatively simple model, no account of the gyroscopic, rotary inertia or shear deformation effects on the model are taken into account. These effects are small with respect to the low frequency (< 200 Hz) dynamic behavior of the overall lumped parameter torsional lateral model.

3.3 Bondgraph Solution

The bondgraph method writes the model equations into a straightforward setup of the system matrix for which eigenvalues may be readily determined. The state of a system may be described by a set of first order differential equations written in terms of state variables $[q_1, q_2, q_3...q_n]$ which are a function of time. The state variables are the smallest set of variables which determine the state of the dynamic system. These variables can be used to predict the future state of the system, when its present state and the excitation are known.

A set of first order differential equations may be written as

$$\dot{q}_1 = a_{11}\, q_1 + a_{12}q_2 + ...a_{1n}q_n + b_{11}\, u_1 + ... \, b_{1m}\, u_m$$

$$\dot{q}_2 = a_{21}\, q_1 + a_{22}q_2 + ...a_{2n}q_n + b_{21}\, u_1 + ... \, b_{2m}\, u_m$$

$$\vdots$$

$$\dot{q}_n = a_{n1}\, q_1 + a_{n2}q_2 + ...a_{nn}q_n + b_{n1}\, u_1 + ... \, b_{1m}\, u_m \quad \text{(3-10)}$$

which may be expressed in matrix equation form as

$$\begin{vmatrix} \dot{q}_1 \\ \dot{q}_2 \\ . \\ . \\ . \\ \dot{q}_n \end{vmatrix} = \begin{vmatrix} a_{11}\ a_{12}\ ....a_{1n} \\ a_{21}\ a_{22}\ ....a_{2n} \\ .\qquad . \\ .\qquad . \\ .\qquad . \\ a_{n1}\ a_{n2}\ ....a_{nn} \end{vmatrix} \begin{vmatrix} q_1 \\ q_2 \\ . \\ . \\ . \\ q_n \end{vmatrix} + \begin{vmatrix} b_{11}\ ....b_{1m} \\ b_{21}\ ....b_{2m} \\ . \\ . \\ . \\ b_{n1}\ ....b_{nm} \end{vmatrix} \begin{vmatrix} u_1 \\ u_2 \\ . \\ . \\ . \\ u_m \end{vmatrix} \quad \ldots\ldots\ldots\ldots\ldots \quad (3\text{-}11)$$

The first column matrix on the RHS is the state vector. The second column matrix represents the input signals. The [A] (n x n) coefficient matrix is the dynamic system matrix of the model containing the eigenvalues of the system. The system vector differential equation can be written as

$$[\dot{q}] = [A]\{q\} + [B]\{u\} \quad \ldots\ldots\ldots\ldots\ldots\ldots\ldots\ldots\ldots\ldots \quad (3\text{-}12)$$

and relates the rate of change of the state of the system, to the present state of the system and the input signals.

3.4 State Space Control

Modern control theory utilizes vector matrix representation to establish control realizations. The state variable selection is not unique and may be conveniently made for each application.

Again, the state equations may be written for a linear time invariant system as

$$\dot{q}(t) = A\,q(t) + B\,r(t) + F\,w(t) \quad \ldots\ldots\ldots\ldots\ldots\ldots\ldots\ldots\ldots\ldots \quad (3\text{-}13)$$

with output equations

$$y(t) = C\,q(t) + D\,r(t) + E\,w(t) \quad \ldots\ldots\ldots\ldots\ldots\ldots\ldots\ldots\ldots\ldots \quad (3\text{-}14)$$

where all coefficient matrices are constant values

A = system matrix (n x n)

B = input coefficient matrix (n x p)

C = state output coefficient matrix (q x n)

D = output coefficient matrix (q x p)

E = disturbance output coefficient matrix (q x v)

F = disturbance coefficient matrix (n x v)

q = state vector (n x 1)

r = input vector (p x 1)

w = disturbance vector (q x 1)

y = output vector (q x 1)

In the case of active vibration control r = 0. The disturbance is an unknown quantity and the function of the active control system will be to operate on the state vector as a regulator attempting to reduce the effects of external disturbances to zero. The equations are therefore reduced to

$$\dot{q}(t) = A\,q(t) + F\,w(t) \quad \ldots\ldots\ldots\ldots\ldots\ldots\ldots\ldots\ldots\ldots\ldots\ldots\ldots\ldots \quad (3\text{-}13a)$$

$$y(t) = C\,q(t) + E\,w(t) \quad \ldots\ldots\ldots\ldots\ldots\ldots\ldots\ldots\ldots\ldots\ldots\ldots\ldots\ldots \quad (3\text{-}14a)$$

The above system will be controllable if there exists a piecewise continuous input u(t) that will drive the state to any final state in a finite time interval. This may be tested by inspection of the matrix [S] defined as

$$S = [B\ AB\ A^2B\ \ldots A^{n-1}B]$$

It is necessary and sufficient for this matrix to have a rank equal to the dimension of the system [A] matrix (n).

For state variable control, it will be necessary to have available the full selected set of state variables to achieve control. It is not always possible, or convenient, to measure these values, in which case an "observer" will be utilized. The observer will use the available variables to estimate the missing variables. In order for this to be possible the system must be observable.

A system is completely observable if every state variable of the system affects some of the outputs. Similar to controllability, a test for observability can be made by inspection of the matrix [V] defined as

$$V = [C^T\ A^TC^T\ (A^T)^2C^T\ \ldots(A^T)^{n-1}C^T]$$

It is a necessary and sufficient condition for the rank of [V] to be equal to the dimension of the system [A] matrix (n).

One of the fortunate and most attractive aspects of the state variable method is the ability to arbitrarily place the poles of the closed loop system. To investigate the condition

required for arbitrary pole placement, consider a process described by the following state equation

$$\dot{q}(t) = A\, q(t) + B\, u(t) \quad \ldots\ldots\ldots\ldots\ldots\ldots\ldots\ldots\ldots\ldots\ldots\ldots\ldots\ldots \quad (3\text{-}15)$$

and the state feedback control is

$$u(t) = -G\, q(t) + r(t) \quad \ldots\ldots\ldots\ldots\ldots\ldots\ldots\ldots\ldots\ldots\ldots\ldots\ldots\ldots \quad (3\text{-}16)$$

then substituting (16) into (15)

$$\dot{q}(t) = (A\text{-}BG)\, q(t) + B\, r(t) \quad \ldots\ldots\ldots\ldots\ldots\ldots\ldots\ldots\ldots\ldots\ldots\ldots\ldots \quad (3\text{-}17)$$

This leads to the eigenvalue equation

$$| \lambda I - A + BG | = 0 \quad \ldots\ldots\ldots\ldots\ldots\ldots\ldots\ldots\ldots\ldots\ldots\ldots\ldots\ldots \quad (3\text{-}18)$$

for which arbitrary pole placement can be achieved through selection of appropriate values of [G].

A variation on pole placement would be to select values of [G] based on a minimization of some selected index (i.e. optimal control).

3.5 Fuzzy Control

3.5.1 Fuzzy Set Theory

Fuzzy set theory provides a means for representing uncertainty. Historically, probability theory has been the primary tool for representing uncertainty in mathematical models. Uncertainty was assumed to follow the characteristics of random distribution. However, not all uncertainty is random. Vagueness or qualitative descriptions are generally not random. Fuzziness describes the ambiguity of an event whereas randomness describes the uncertainty in the occurrence of the event.

The application of fuzzy set theory will provide a means of mapping the normal imprecise human language description of a process onto the precise format of computer coding allowing the computer to emulate a human operator. The need stems from the fact that very few engineering models of processes can be defined or measured precisely. Real processes can be vague and ill-defined, in general, lending to unreliability of the precise computer results which are based on forced precision in the input information.

A fuzzy logic proposition is a statement involving a concept descriptor with vaguely defined boundaries. The assigned membership value for the proposition indicates the degree of truth applicable.

Even though the arbitrary sets of linguistic descriptors are qualitative and somewhat vague, the consequent outcome of the inferencing process is translated into objective and quantifiable results. Fuzzy mathematical tools, based on "fired" (satisfied) antecedents and inferred consequents, provide a vehicle for automation utilizing an extensive body of expert knowledge, gained through experience, which is not available in classical or modern control theory.

3.5.2 Membership Functions

In classical sets the transition of set membership is crisp and abrupt. For fuzzy sets, membership transition will be gradual allowing the boundary of sets to be vague and ambiguous. Membership functions characterize the fuzziness or ambiguity in a fuzzy set. The graphical function shape is usually selected to allow ready mathematical manipulation in the formalism of fuzzy set theory. The geometric shape of the function will allow the boundary to describe the vagueness of the variable along the universe of discourse (an appropriate scale or space containing the variable).

The following definitions are applicable for membership functions (see Fig 3.3):

- The **support** is the total region on the universe of discourse for which the membership value is greater than 0 (i.e. $\mu_A>0$).
- The **core** is the region on the universe of discourse for which full membership applies (i.e. $\mu_A=1$).
- The **boundary** of the membership is the region on the universe of discourse for which the membership value falls between 0 and 1 (i.e. $0< \mu_A < 1$).
- A **normal fuzzy set** is defined as one for which the membership function contains at least one element with a value of unity.

Fuzzification is the process of making a crisp quantity fuzzy. Most deterministic information will have a degree of uncertainty associated with it. If this uncertainty is the result of ambiguity, vagueness, or measurement imprecision, then a fuzzy membership function may be a good descriptor of the quantity.

For the case described herein, a series of membership functions have been selected to partition a suitable portion of the universe of discourse to handle the normal excursions of

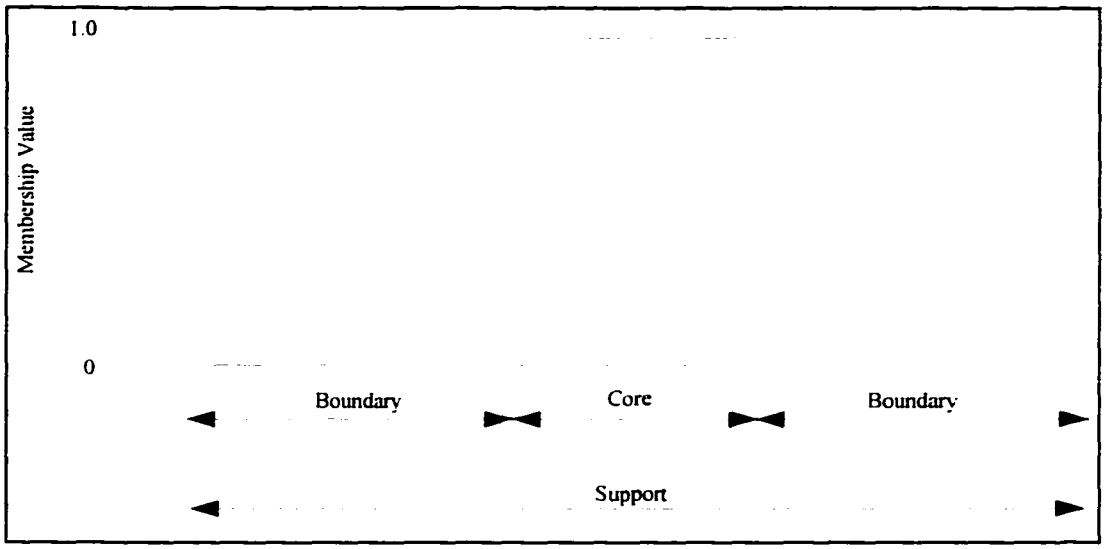


Figure 3.2: A Normal Fuzzy Set

the measured variable (vertical displacement of the pinion shaft). The membership functions are chosen to be normal and overlapping such that normality is maintained through the summation of adjacent function memberships.

3.5.3 Fuzzy Logic

Fuzzy logic is the basis for fuzzy logic controllers. Fuzzy logic captures and builds on the knowledge of a human operator or expert in a particular field. An essential part of the fuzzy logic controller is a linguistic set of rules defining that knowledge. Crisp input variables are fuzzified based on how well the value fits in the applicable subset, or membership function, defined on the input variable universe of discourse. The inferencing procedure, or mapping of input fuzzy sets to output fuzzy sets, has a basis in Boolean logic.

A fuzzy set is an extension or generalization of the classical set in which membership is characterized by either a value of 0 or 1. If a universe of discourse contains a collection of elements x which could be discrete or continuous, then a fuzzy set "A" in X is defined as the set of ordered pairs

$$A = \{ x, \mu_A(x) \mid x \in X \}$$

where $\mu_A(x)$ is the membership of x in A

The membership $\mu_A(x)$ takes on an appropriate value in the unit interval [0,1]. Fuzzy theory states that all things are a matter of degree. This violates the Aristotlean law of non-contradiction which states that an entity is Not {A And Not-A} at the same time (i.e. membership is either 0 or 1). At any given time, a fuzzy set can have membership in both A and Not-A. Also, fuzzy theory contradicts the law of the Excluded Middle (or the law of bivalence) which states that the entity is in either A or Not-A.

A fuzzy logic controller is comprised of four principal components:

i) fuzzification interface
ii) rules database
iii) inferencing or decision-making logic
iv) defuzzification interface

i) Fuzzify

The fuzzification interface involves measurement of the crisp input values followed by a determination of the applicable membership functions which associate numerical values within descriptive linguistic variables. A scale mapping is also performed for membership determination or to what level the value belongs to each linguistic variable on the universe of discourse. The input to this process is a crisp value and the output is a fuzzy set.

ii) Rules Database

The rules or knowledge database is the collection of known rules, based on experience or observation, which govern the process under control. This knowledge provides the mapping correspondence between the input space and the output space. Using the knowledge database, the input fuzzy sets are mapped to output fuzzy sets. These rules take the form "If A... Then B...". The fuzzy control rules provide a convenient way of defining the required control of the system or process in linguistic terms.

iii) Inferencing

Inferencing is the kernel of the decision making or mapping process used in the fuzzy logic controller. In approximate reasoning there are two important implication rules as developed below:

1. generalized modus ponens (forward inferencing)

   premise 1: x is A_1

   premise 2: if x is A_n then y is B_n

   consequence: y is B_1

2. generalized modus tollens (reverse inferencing)

   premise 1: x is B_1

   premise 2: if x is A_n then y is B_n

   consequence: y is A_1

where A_n is a group of antecedent or causal situations (input space)

B_n is the corresponding group of consequents or result situations (output space)

The generalized modus ponens or forward inferencing is normally the decision-making mechanism used in a fuzzy logic controller. The generalized modus tollens or reverse inferencing is the process generally used in Expert Systems to determine the possible causal situations for an observed result.

Fuzzy systems reason with parallel associative inferencing. When given an input, the fuzzy inferencing system will fire each fuzzy rule in parallel to a different degree (based on membership) to infer a conclusion or output. A rule fires when the antecedent conditions are satisfied.

Two basic paradigms exist in a forward driven inferencing structure. The first is accorded to Mamdani [28] and is based on the interpretation of a rule as the conjunction (And / Min) of the antecedents for determination of the degree of firing of the associated rule and inferring the consequent at that level. This method, known as the Mamdani method, uses disjunction (Or / Max) to aggregate the outputs of the individual rules. The second method, known as the logical method, is based on the interpretation of the rule as the disjunction of the antecedents negation determining the degree of firing of the associated rule and inferring the consequent fuzzy set at that level. In this case the fired rules connective for the output space is conjunction.

As noted above, the basic logic for antecedent / consequent and rules statement connectives can be modified, however the Mamdani approach will be followed herein. For each effected or 'fired' rule, the input fuzzy sets are connected to the output fuzzy sets by the intersection or pointwise minimum of the input fuzzy sets (i.e. corresponding to an 'And' operation in Boolean logic). For two inputs x_1 and x_2 defined on universes of discourse A and B, and a single output y defined on C, the inferred output fuzzy set can be written as follows:

$$\mu_C(y_i) = \mu_{A \wedge B} = \min \{\mu_A(x_1) , \mu_B(x_2)\}$$

iv) Defuzzify

The defuzzification interface converts the output fuzzy sets inferred by the applicable fired rules from the input space to crisp output values on the output universe of discourse. Each fired rule is connected by the union or pointwise maximum of the output fuzzy sets. For the above defined input / output scheme, the aggregation is defined as follows:

$$y = \max \{\mu_C(y_1), \ldots, \mu_C(y_R)\}$$

where: R = the number of fired rules

A more popular approach for the aggregation of all the fired rules is by the center of area method. Experience has shown that using a centroid or weighted combination method with all the applicable fired rules from the inferencing stage is more effective than using the strict maximum value. For a discrete series, the output signal is normally obtained using the following center of area method.

$$y = \frac{\sum \mu_C(y_j) * y_j}{\sum \mu_C(y_j)} \quad \ldots\ldots\ldots\ldots\ldots\ldots\ldots\ldots\ldots\ldots\ldots\ldots\ldots\ldots \quad (3\text{-}19)$$

This final crisp value is then transmitted to the control signal output amplifier for the actuator input to the plant.

Chapter 4

Application

4.1 Torsional /Lateral Modeling

Torsional vibration can cause serious problems in a rotating machine train if the phenomenon is not properly predicted and the equipment judiciously selected to avoid operation at or near a resonance. Turbomachine rotors are generally stiff enough within their own extents to put natural frequencies above the range of concern. However, machines with fairly long shafts carrying significant inertias should always be considered for investigation. As well, in the case of reciprocating engines, pumps or compressors, there are many higher order forcing functions which may be of concern. This will be particularly so when a variable speed AC motor is used to drive a reciprocating pump or compressor.

The weakest torsional link in a machine train will usually be the flexible drive couplings between the respective shafts. In a fixed speed situation, judicious selection of the shaft couplings can tune the system to avoid operation at or near a resonant condition.

Vibration problems, torsional or lateral, usually result from operation close to the coincidence of speed-related excitation frequencies with a natural frequency of the machine train.

The design objective in relation to torsional phenomenon, will be to attenuate alternating twist amplitudes to maintain shaft stress at an acceptable level and to avoid any pulsing unloading, or backlash, at the contact surfaces of gear teeth. In relation to bending response, the design objective will be to reduce shaft flexing in order to obtain a smooth running machine. The designer can achieve this objective in a number of ways

- controlling excitation amplitudes (design refinements, balancing, etc)
- controlling excitation frequencies (system modifications)
- controlling system natural frequencies (structural changes)
- controlling the level of effective damping in the system

The prime engineering objectives of a vibration analysis are to predict the natural frequencies and to compute the amplitudes and peak torques / forces under steady-state and transient (such as startup) excitations. The ability to predict natural frequencies and amplitudes for a given excitation is important in implementing any type of classical control.

An ability to identify relevant sources of excitation, as well as an awareness of the uncertainties of the predictive process, and an understanding of the significance of the uncertainties, is also important. It is necessary to interpret the mathematical results and to be able to apply them to the elimination of the vibration problem.

4.2 Mathematical Model

The mathematical model developed herein uses a lumped parameter approach. This allows a system description with ordinary differential equations and a matrix methods approach to the solution rather than dealing with the extra complication of a distributed system model with partial differential equations. The model developed here will follow after the simple two shaft system as noted in Section 3.2.2. The prototype is adequately represented for this work by one angular co-ordinate for each rotating inertia and one lateral co-ordinate for each of the pinion and gear masses. The use of lumped parameters is justified by noting that the wavelength associated with each of the frequencies of interest is significantly larger than the characteristic length of the modeled elements (>25 times suggested) [38]. Assuming the maximum frequency (f) of interest is 200 Hz and with a speed of sound in steel of a= 5100 m/sec, the shortest wavelength (λ) of interest is given by

$$\lambda = a / f \quad \ldots\ldots\ldots\ldots\ldots\ldots\ldots\ldots\ldots\ldots\ldots\ldots\ldots\ldots \quad (4.1)$$

$$= 5100 / 200 = 25.5 \text{ m}$$

This allows an element characteristic length of approximately 1 m for lumping of parameters. All of the component elements in the prototype model fall within this characteristic length limitation. In general, this range will allow the use of the lumped parameter modeling approach for most industrial machine train components.

Fig 4-1 indicates a lumped parameter model of the prototype which is representative of a typical drive train. All of the rotating inertia, with the exception of the damper / absorber is lumped into 4 discrete disks, each with a polar mass moment of inertia I_i. The inertia disks are considered to be connected by massless torsional springs K_i. These springs represent the torsional stiffness of the rotor shafting (combined with disk and coupling as applicable) between the respective stations of polar mass inertias. Shaft and coupling

inertia will be apportioned and included in the appropriate adjacent inertia stations. The number of divisions of the model will depend on the significance of the higher frequencies to the problem at hand.

For the prototype, torsional stiffness of the shaft sections is given by

$$K_i = (J_i G) / \ell_i \quad \ldots\ldots\ldots\ldots\ldots\ldots\ldots\ldots\ldots\ldots\ldots\ldots\ldots\ldots \quad (4.2)$$

or in the case of multiple diameter sections

$$K_i = (G/(\ell_1/J_1 + \ell_2/J_2 + \ldots)) \quad \ldots\ldots\ldots\ldots\ldots\ldots\ldots\ldots\ldots\ldots\ldots\ldots\ldots\ldots \quad (4.3)$$

where $J_i = \pi(d_i)^4 / 32$

G = shear modulus (7.69×10^{10} N/m^2 for steel)

ℓ_i = individual shaft section length

d_i = individual shaft section diameter

To account for the effect of the coupling of transverse vibration, the model of the prototype includes a mass acting at both the pinion and main gear stations. These masses are attached to lateral springs to represent shaft bending in the prototype. In an industrial machine train these springs would represent a combination of stiffness attributed to shaft bending, casing deflection, bearing oil film, and bearing housing, with the latter three being the more significant contributors. Gear tooth and mesh stiffness is also represented by a lateral spring, K_4, in the model. The bearings are modeled as stiff supports.

The number of mass stations should be at least one more than the number of frequencies of interest. This is always the case for such a semi-definite system since the first natural frequency is zero for the rigid body rotating mode. In this particular model of the

prototype, 6 mass stations have been included (ref Fig 4.1 without the attached damper), allowing 5 natural frequencies to be calculated.

Damping can be represented in the mathematical model in two forms

(1) structural damping within the components

R_i, $1 \leq i \leq 3$

(2) friction and work related damping

b_i, $1 \leq i \leq 4$

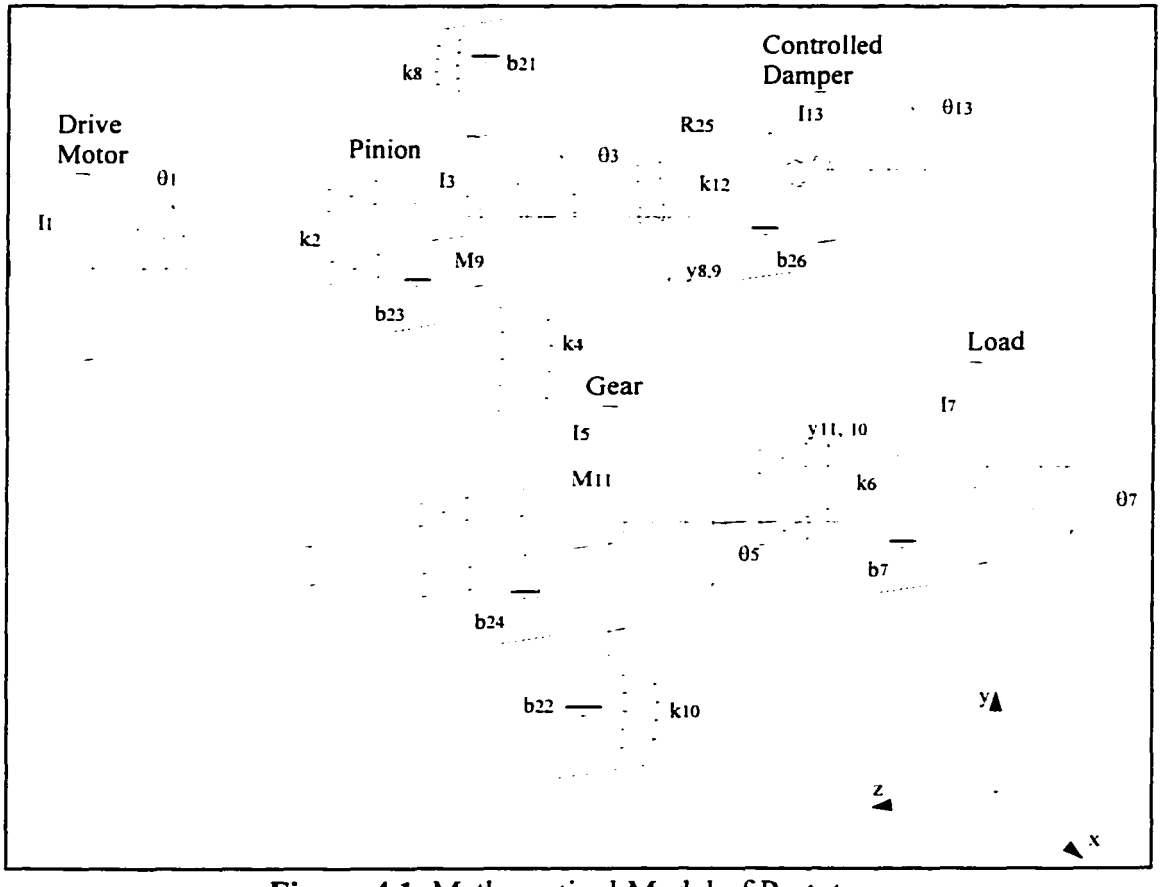


Figure 4.1: Mathematical Model of Prototype

The R_i damping represents energy dissipated between the elements in the system and the b_i represents energy associated with each disk which is dissipated to ground (e.g. windage and friction). For the analyzed model of the prototype, which will be used to establish the natural frequencies and mode shapes of the studied system, no damping has been included. This represents no real loss of generality since damping is usually quite small in torsional systems. For completeness, the damping terms are included in the equations developed in this section.

4.2.1 Lagrange Method

The generalized displacement co-ordinate will be q_i, with θ_i being the angular displacement of the i^{th} rotating inertia, ($1 \leq i \leq 4$), and y_j the rectilinear co-ordinate of the j^{th} mass, ($1 \leq j \leq 2$). Only the vertical displacement (y) direction is considered for the prototype as the transverse horizontal (x) direction will have the associated greater stiffness of two shafts in parallel. The system has 6 degrees of freedom, for motion in the co-ordinate directions noted in Fig 4.1, and the prototype drive train dynamics can be represented by 6 second-order, ordinary differential equations of motion with constant coefficients.

For purposes of illustration and comparison with the actual simulation model, developed in the section following, these equations may be derived using the Lagrange method where each co-ordinate will have a motion $q_i(t)$ that satisfies

$$d/dt(\partial L/\partial \dot{q}_i) - \partial L/\partial q_i = Q_i \qquad (1 \leq i \leq 6) \quad \ldots\ldots\ldots\ldots\ldots\ldots\ldots\ldots \quad (4.4)$$

Referring to Fig 4-1 and using the given numbering scheme, the total kinetic energy, T, will be the sum of the kinetic energy for each mass and rotating inertia station. For the i^{th} inertia,

$$T_i = \tfrac{1}{2} I_i (\dot{\theta}_i)^2 \qquad i = 1, 3, 5 \,\&\, 7 \quad \ldots\ldots\ldots\ldots \quad (4.5)$$

and for the j^{th} mass

$$T_j = \tfrac{1}{2} M_j (\dot{y}_j)^2 \qquad j = 9 \,\&\, 11 \quad \ldots\ldots\ldots\ldots\ldots\ldots \quad (4.6)$$

The total kinetic energy is therefore

$$T = \tfrac{1}{2} \Sigma I_i (\dot{\theta}_i)^2 + \tfrac{1}{2} \Sigma M_j (\dot{y}_j)^2 \qquad \text{for i \& j as noted} \quad \ldots\ldots\ldots\ldots \quad (4.7)$$

The potential energy, V, is the sum of the strain energy in each of the torsional and lateral springs. For the shaft sections in torsion

$$V_i = \tfrac{1}{2} \Sigma K_i (\theta_{i-1} - \theta_{i+1})^2 \qquad i = 2 \,\&\, 6 \quad \ldots\ldots\ldots\ldots\ldots\ldots\ldots\ldots \quad (4.8)$$

For the lateral springs representing the prototype transverse stiffness, the potential energy is given by

$$V_j = \tfrac{1}{2} K_j (y_j)^2 \qquad j = 8 \,\&\, 9 \quad \ldots\ldots\ldots\ldots\ldots\ldots\ldots\ldots \quad (4.9)$$

For the gear tooth and mesh stiffness, the potential energy for small deflections is represented by

$$V_4 = \tfrac{1}{2} K_4 (r_3\theta_3 - r_5 \theta_5 - y_9 - y_{11})^2 \quad \ldots\ldots\ldots\ldots\ldots\ldots\ldots\ldots\ldots\ldots \quad (4.10)$$

The non-conservative torques are obtained from the virtual work δW of the damping torques, the drive torques, and the load torque.

$$\delta W = \Sigma Q_i \delta \theta_i \qquad \text{for } i = 1 \text{ to } N \quad \ldots\ldots\ldots\ldots\ldots\ldots \quad (4.11)$$

Applying the drive torque, $T_1(t)$, at the first station and the load at the last station, the non-conservative torques are

$$Q_1 = T_1(t) - b_1 \dot{\theta}_1 - R_2(\dot{\theta}_1 - \dot{\theta}_3) \quad \ldots\ldots\ldots\ldots\ldots\ldots\ldots\ldots\ldots\ldots\ldots\ldots\ldots \quad (4.12)$$

$$Q_2 = - b_3 \dot{\theta}_3 - R_2(\dot{\theta}_3 - \dot{\theta}_1) - r_3R_4 (r_3 \dot{\theta}_3 - r_5 \dot{\theta}_5 - \dot{y}_9 - \dot{y}_{11}) \quad \ldots\ldots\ldots\ldots\ldots\ldots \quad (4.13)$$

$$Q_3 = -b_5\dot{\theta}_5 - r_3R_4(r_5\dot{\theta}_5 + \dot{y}_9 + \dot{y}_{11} - r_3\dot{\theta}_3) - R_6(\dot{\theta}_5 - \dot{\theta}_7) \quad \ldots\ldots\ldots\ldots\ldots \quad (4.14)$$

$$Q_4 = -b'_7\dot{\theta}_7|\dot{\theta}_7| - b_7\dot{\theta}_7 + R_6(\dot{\theta}_7 - \dot{\theta}_5) \quad \ldots\ldots\ldots\ldots\ldots\ldots\ldots\ldots \quad (4.15)$$

$$Q_5 = -R_4(\dot{y}_9 + r_5\dot{\theta}_5 + \dot{y}_{11} - r_3\dot{\theta}_3) - R_8\dot{y}_9 \quad \ldots\ldots\ldots\ldots\ldots\ldots\ldots \quad (4.16)$$

$$Q_6 = -R_4(\dot{y}_{11} + r_5\dot{\theta}_5 + \dot{y}_9 - r_3\dot{\theta}_3) + R_{10}\dot{y}_{11} \quad \ldots\ldots\ldots\ldots\ldots\ldots\ldots \quad (4.17)$$

The term b'_7 is the load torque damping coefficient assumed here to be proportional to the speed squared, suitable for a centrifugal machine (i.e. pump, fan, etc.).

Now using the Lagrangian equation and the non-conservative torques, we can form the six equations of motion for the system.

$$I_1\ddot{\theta}_1 + b_1\dot{\theta}_1 + R_2(\dot{\theta}_1 - \dot{\theta}_3) + K_2(\theta_1 - \theta_3) = T_1(t) \quad \ldots\ldots\ldots\ldots\ldots\ldots \quad (4.18)$$

$$I_3\ddot{\theta}_3 + b_3\dot{\theta}_3 + R_2(\dot{\theta}_3 - \dot{\theta}_1) + r_3R_4(r_3\dot{\theta}_3 - r_5\dot{\theta}_5 - \dot{y}_9 - \dot{y}_{11}) + K_2(\theta_3 - \theta_1) + r_3K_4(r_3\theta_3 - r_5\theta_5 - y_9 - y_{11}) = 0 \quad \ldots\ldots\ldots\ldots\ldots\ldots \quad (4.19)$$

$$I_5\ddot{\theta}_5 + b_5\dot{\theta}_5 + r_3R_4(r_5\dot{\theta}_5 + \dot{y}_{11} + \dot{y}_9 - r_3\dot{\theta}_3) + R_6(\dot{\theta}_5 - \dot{\theta}_7) + r_3K_4(r_5\theta_5 + y_{11} + y_9 - r_3\theta_3) + K_6(\theta_5 - \theta_7) = 0 \quad \ldots\ldots\ldots\ldots\ldots\ldots \quad (4.20)$$

$$I_7\ddot{\theta}_7 + b_7\dot{\theta}_7 + R_6(\dot{\theta}_7 - \dot{\theta}_5) + K_6(\theta_7 - \theta_5) = -b'_7\dot{\theta}_7|\dot{\theta}_7| \quad \ldots\ldots\ldots\ldots\ldots\ldots \quad (4.21)$$

$$M_9\ddot{y}_9 + R_4(\dot{y}_9 + r_5\dot{\theta}_5 + \dot{y}_{11} - r_3\dot{\theta}_3) + R_8\dot{y}_9 + K_4(y_9 + r_5\theta_5 + y_{11} - r_3\theta_3) + K_8y_9 = 0 \quad \ldots\ldots\ldots\ldots\ldots\ldots \quad (4.22)$$

$$M_{11}\ddot{y}_{11} + R_4(\dot{y}_{11} + r_5\dot{\theta}_5 + \dot{y}_9 - r_3\dot{\theta}_3) + R_{10}\dot{y}_{11} + K_4(y_9 + r_5\theta_5 + y_{11} - r_3\theta_3) + K_{10}y_{11} = 0 \quad \ldots\ldots\ldots\ldots\ldots\ldots \quad (4.23)$$

The above equations of motion may also be formulated using Newton's laws directly; or as a series of first order differential equations in a state space format using a modeling

method such as bondgraph (section 4.2.2). Appendix I develops the torsional / lateral coupled equations for the prototype without the damping terms for clarity. In the first case the above Lagrangian method is employed. Secondly, the energy exchange format of bondgraph is used. The bondgraph method (which uses momentum and displacement as state variables) results in the same number of first order differential equations provided the constraint equation (3.9) is utilized with the first method having velocity and displacement as state variables. However, from a computer simulation standpoint, the bondgraph format results in a smaller and more efficient system [A] matrix.

4.2.2 Bondgraph Method

The approach selected for computer simulation study utilizes the bondgraph method together with the software program Simulink in the Matlab environment. This program provides the capability of time and frequency domain solutions of the state space variables for the lumped parameter model representation of the prototype. The output gives displacement of the various stiffnesses and momentum of the respective masses in the system. The mode shapes are a coupled mixture of the torsional response of the shafting between the disks and the linear response of the pinion and gear wheels resulting from bending of their respective supporting shafts (vertical direction only considered). The bondgraph sketch for the model is presented in Fig 4.3 for the physical prototype depicted in Fig 4.2. The associated A, B, C, and D state space matrices (ref section 3.5) are given in Appendix II. The [A] matrix is assembled directly from the equations for the bondgraph as developed and listed in Appendix I.

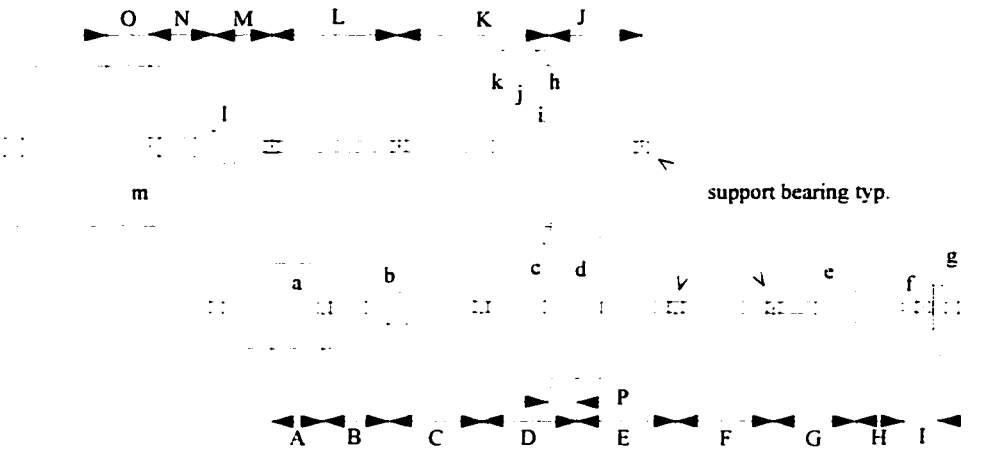
Simulation of the dynamics of a physical system can provide invaluable insight to the time domain response. The bondgraph model is developed from a basic understanding of the physics of the individual components usually laid out in a sketch or representation to simulate the function within the system. Several possible methods exist for solutions (i.e.

block diagram, vector network, linear graph); however, the bondgraph approach offers the significant advantage of a straight forward transition from the graphical representation, to equation listing, to the development of the state space system [A] matrix suitable for direct input to the Simulink program. The other methods mentioned require somewhat more work in formulation of the constitutive equations to form the system algorithm.

Within the Matlab environment, the state space system matrices can be quickly transformed into transfer function format for a study of the frequency response function. Eigenvalues and eigenvectors for the represented system can be found without difficulty.

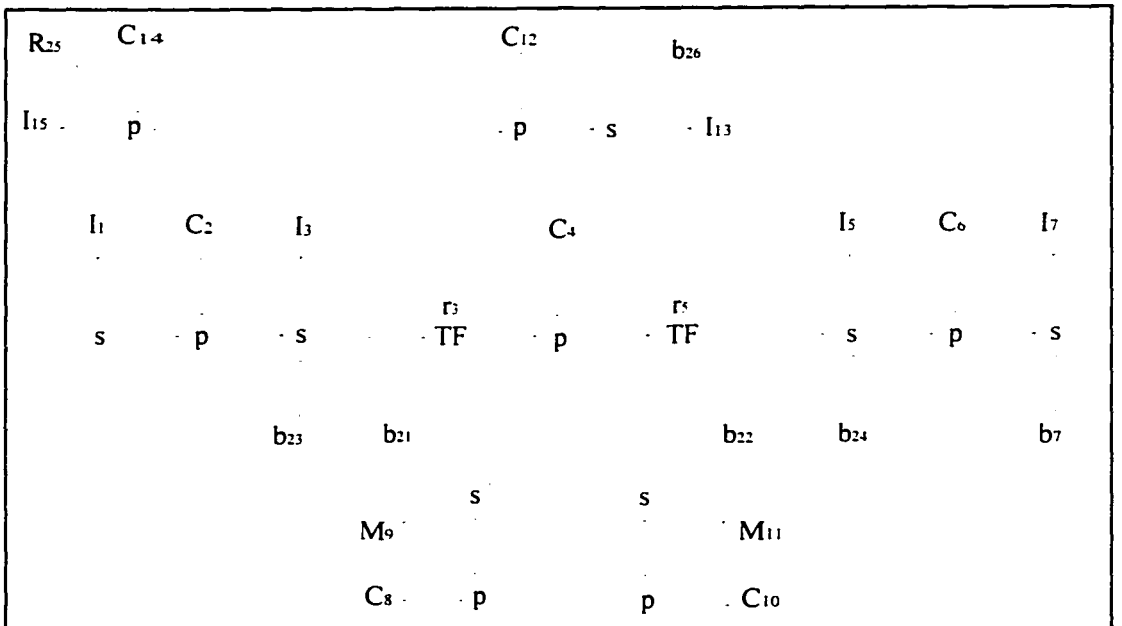
The Simulink program is a software package for use within the Matlab environment for modeling, simulating and analyzing dynamical systems in a continuous or sampled time format. The modeling environment is graphical using block diagrams for component assembly. Simulink allows movement beyond idealized linear models to explore more realistic nonlinear models. A significant library of nonlinear blocks is contained within the program including blocks for Coulombic friction, backlash, and deadzone components.

Because of the diversity of dynamic system models and behavior, several methods of simulation are offered. Integration methods include linsim - a method which extracts the linear dynamics; rk23 - a Runge-Kutta third order method; rk45 - a Runge-Kutta fifth order method; gear - Gear's predictor-corrector method for stiff systems; adams - the Adams predictor-corrector method; and euler - Euler's method. The most appropriate method in this case is linsim since the modeled system is essentially linear for each discrete control step. The control action updates the system matrices creating a nonlinear, time variant plant. The linsim method extracts the linear dynamics of the model leaving only the nonlinear portion for simulation. This allows a relatively fast simulation.



a	drive motor	
b	dry disc type double flex shaft coupling	
c	pinion gear	
d	inertia disk (pinion)	
e	dry disc type single flex shaft coupling	
f	magnetically actuated friction clutch	controlled
g	torsional damper flywheel mass	damper
h	main gear	
i	disc (gear rotor)	
j	disc (gear rotor)	
k	disc (gear rotor)	
l	dry disc type double flex shaft coupling	
m	load inertia / fan	

Figure 4.2: Prototype Machine Train



Notes:

Flexibility = reciprocal of Stiffness; C = 1/K

I_1	-	drive motor inertia
C_2	-	drive / pinion shaft torsional flexibility
I_3	-	pinion inertia
C_4	-	gear tooth / mesh flexibility
I_5	-	gear inertia
C_6	-	gear / load shaft torsional flexibility
I_7	-	load inertia
C_8	-	pinion shaft lateral flexibility
M_9	-	pinion mass
C_{10}	-	gear shaft lateral flexibility
M_{11}	-	gear mass
C_{12},C_{14}	-	damper connecting shaft torsional flexibility
I_{13}	-	damper inertia attached (variable)
I_{15}	-	damper inertia slipping (variable)
R_i	-	internal damping between elements
b_i	-	external damping to ground
r3, r5	-	transformer impedance ratio

Figure 4.3: Bondgraph Diagram

A maximum time step of 0.002 seconds was selected on the basis of achieving consistent and suitable plot results. This is approximately one half of the time step for which the simulation results began to deteriorate. In contrast, if the Runge Kutta methods were chosen, the maximum time step would be based on the highest frequency (i.e. 1/5 to 1/20 of the smallest period) increasing the simulation time quite considerably (> factor of 3). Also, the Runge Kutta methods do not work well with systems which have both fast and slow dynamics which is the case with the model simulated herein (slow at 64.5 Hz and fast at 255 Hz).

The bondgraph method uses lumped or multi-lumped representations of the basic modeling elements of mass, stiffness and damping. Elements of mechanical, fluid, electrical, magnetic, or thermodynamic systems can then be interpreted in terms of these concepts. These elements are then connected by power bonds, which identify power flow paths. Elements such as pipes, shafts, electrical wiring etc, are represented by bonds that carry power around a circuit. Power is the product of two components, generalized as effort and flow variables. For mechanical systems, these are assigned as force and velocity, respectively.

A bond connects two elements and carries effort and flow. A second type of bond called a signal bond, carries only one of the variables for information purposes. Energy flow is normally determined by the natural direction of flow around the system, from the driving point (active source) to the load point (passive sink). There are two types of sources available in the bondgraph structure; source of effort (SE) and source of flow (SF). Sources impose either an effort or a flow on a system, but not both. An effort source imposes an effort (e.g. torque) independent of the flow variable (e.g. angular velocity). Alternatively, a flow source imposes a flow independent of the effort variable.

The damping element (R), or the inverse (G), depending on causality, represents power dissipation. The compliance or capacitance element (C), which is the reciprocal of

stiffness, together with the mass or inertance element (I), store energy. This energy is exchanged back and forth during transient conditions. Like sources, these are all one port blocks and have only one bond attached.

An example of a two port element is a transformer (TF) which is used to model the transformation of power between two sets of physical quantities, such as the transformation of mechanical power across a gearbox (impedance transformer) or into another form such as hydraulic power (class transformer).

Elements are attached to applicable junctions, which may be either parallel "p" or series "s" formation. These junctions may be considered as analogous to junctions in an electrical circuit and the equivalent of Kirchoff's circuit laws may be applied to the bondgraph. For example, the parallel junction would have common effort (e.g. pressure), with the algebraic summation of flow, and the series junction would have common flow, with the algebraic summation of effort.

An important feature of the bondgraph is causality, which is indicated by the position of a short bar drawn at right angles across the bond. It is placed at the appropriate end of the bond to indicate which of the two power variables is the dependent or independent variable. A causal bar placed at the upstream end of the bond indicates that the flow is the independent variable in the formulation of the constitutive equation of the element. If the causal bar is placed at the downstream end then the effort becomes the independent variable.

To facilitate computation, integral causality is preferred. This automatically defines the constitutive equation setup for each element code. These are summarized in Table 4.1. Since the causality is fixed, with the exception of the (R) element, it becomes the job of the junctions to ensure consistency throughout the bondgraph model. In other words,

Table 4.1: Bondgraph Model Elements

Element Type	Code	Equation
Effort Source	SE	
Flow Source	SF	
Mass	I	$f = \frac{1}{I} \int e\, dt$
Compliance	C	$e = \frac{1}{C} \int f\, dt$
Damping	R causal bar may be placed at either end	$e = R\ f$
Transformer	TF or TF	$e_2 = n\ e_1$ $f_1 = n\ f_2$ n = fixed ratio
Parallel Junction	p (1, 2, 3, 4) can have only one bond with causal bar at junction	$f_1 = f_2 + f_3 + f_4$ $e_1 = e_2 = e_3 = e_4$
Series Junction	s (1, 2, 3, 4) can have only one bond without causal bar at junction	$e_1 = e_2 + e_3 + e_4$ $f_1 = f_2 = f_3 = f_4$

f = flow e = effort

following these simple rules, will force a correctly formatted bondgraph with automatic formulation of the correct "physics" for the problem.

4.2.2.1 Constitutive Equations

Considering first the torsional system, the constitutive equations for the angular velocity and torque are respectively, with $\dot{\theta}_x$ and $\dot{\theta}_y$ neglected as stated previously in section 4.1.

$$\dot{\theta}_z = 1/I \int T\,dt \quad \ldots\ldots\ldots\ldots\ldots\ldots\ldots\ldots\ldots\ldots\ldots\ldots\ldots\ldots \quad (4.24)$$

$$T = 1/C_t \int \dot{\theta}_z\,dt \quad \ldots\ldots\ldots\ldots\ldots\ldots\ldots\ldots\ldots\ldots\ldots\ldots\ldots\ldots \quad (4.25)$$

where :

C_t	$= 1/K_t$, torsional flexibility
T	= torque applied to the element
$\dot{\theta}_z$	= angular velocity of the rotating inertia
I	= polar mass moment of inertia

The torsional stiffness for each applicable shaft section is estimated based on the classical equation for shaft deflection in torsion.

$$\text{Torsional deflection} = \theta_z = \frac{T\,\ell}{G\,J} \quad \ldots\ldots\ldots\ldots\ldots\ldots\ldots\ldots\ldots\ldots \quad (4.26)$$

where :

ℓ = shaft length

G = shear modulus (7.69E10 N/m^2 - for steel)

J = polar area moment of inertia of the shaft cross-section

Torsional stiffness = $K_t = T/\theta = GJ/\ell$

Torsional flexibility = $C_t = \ell/GJ$

Referring to the mathematical model depicted in Fig 4.1 and the physical outline given in Fig 4.2, the torsional stiffness estimation for shaft section "C" is given below.

shaft length, $\ell = 0.105$ m

shaft diameter, $d = 0.0096$ m

$$J = \pi \frac{d^4}{32} = \frac{(0.0096)^4}{32} \qquad \ldots\ldots\ldots\ldots\ldots\ldots\ldots\ldots \quad (4.27)$$

$$= 8.34\text{E-}10 \ \text{m}^4$$

$$K_t = \frac{G\,J}{\ell} \qquad \ldots\ldots\ldots\ldots\ldots\ldots\ldots\ldots\ldots\ldots\ldots\ldots\ldots\ldots \quad (4.28)$$

$$\frac{7.69\text{E}10 \times 8.34\text{E-}10}{0.105} = 610.7 \ \text{N m/ Rad}$$

The estimated stiffness values for each shaft section is given in Table 4.2. For the shaft section between the pinion and the drive motor, the combined torsional stiffness will be based on a series combination of the shaft sections designated "A" through "D".

For bending, the stiffness for the pinion and the gear shafts has been estimated from the simple formula for a simply supported beam with point loading. The spans are designated as sections "D" and "E" for the pinion shaft and sections "J" and "K" for the gear shaft in Fig 4.2. These stiffnesses have been represented by single vertical lateral springs in the bondgraph model attaching the respective mass (pinion or gear) to ground. These simple supports offer no transverse rotational stiffness against bending. However, since the prototype pinion shaft for this model, continues through the bearings to further outboard supports, there will be a small influence on the natural frequencies due to the

added bending stiffness from this effect (see Table 4.5). The gear shaft has only one end for which there are further outboard supports.

Bending stiffness estimation for the pinion shaft:

total length = 0.145 m

shaft dia = 0.0096 m

modulus of elasticity = 2.0E11 N/m (steel)

mass density = 7800 Kg/ m^3 (steel)

shaft area = 0.7854 x $(0.0096)^2$ = 7.238E-5 m^2

bending stiffness (simply supported beam):

$$K_B = \frac{48\ E\ I}{\ell^3} \qquad \text{..... (4.29)}$$

$$= \frac{48 \times 2.0E11 \times (0.0096)^4 \times \pi}{(0.145)^3 \times 64}$$

$$= 1.31E6\ \text{N/ m}$$

or $C_B = 1 / K_B = 7.62E\text{-}7\ \text{m/N}$ ..... (4.30)

Elements are included in the model having lumped values representing both mass and inertia of the pinion and gear disks. The complete list of mass and moment of inertia information for the model of the prototype is presented in Table 4.4.

Table 4.2: Prototype Stiffness Parameters

Ref: Fig 4.1 & 4.2

shaft section	Length mm	Dia mm	Tor Stiff Nm/rad	Tor Stiff Nm/rad (combined sections)	Bend Stiff N/m
A	50	7.9	588.14		
B	65	7.9	452.42	(A,B,C,D)	
C	105	9.6	610.72	**k2**	(D,E)
D	85	9.6	754.41	145.48	**k8**
E	60	9.6	1068.75		1.31e6
F	90	9.6	712.50	(E,F,G,H,I)	
G	70	9.6	916.07	**k12**	
H	100	6.4	122.75	75.32	
I	50	7.9	773.87		(J,K)
J	60	9.6	392.09		**k9**
K	75	9.6	1068.75		1.63e6
L	200	9.6	320.63	(K,L,M,N,O)	
M	80	9.6	801.57	**k6**	
N	65	12.7	3021.66	164.73	
O	40	12.7	4910.2		
P	13	-			

Estimated Gear Mesh Stiffness	k4 = 1.84e8 N/m
Elastic Modulus	2.0e11 N/m^2
Torsional Modulus	7.69e10 N/m^2

Table 4.3: Shaft Section Parameters

Dia mm	Area $m^2 \times 10^{-5}$	Transverse Inertia $m^4 \times 10^{-10}$	Polar Inertia $m^4 \times 10^{-10}$
6.4	3.62	0.80	1.6
7.9	4.90	1.91	3.82
9.6	7.24	4.17	8.34
12.7	12.7	12.8	25.5

Elastic Modulus 2.0e11 N/m^2 (steel)
Torsional Modulus 7.69e10 N/m^2 (steel)

Natural frequencies have been found by mathematical modeling in two analysis programs, Matlab and a finite element code, CosmosM. In both cases lumped parameters have been used for the mass; however the elastic properties of the shafting in the finite element program have been modeled using beam elements. The finite element model was first run with the shaft extensions beyond the bearings having virtually no bending stiffness. In this case, the frequencies found were essentially identical to the Matlab solution. In a second run the shaft extensions had continuous bending stiffness beyond the bearing. In this case the frequencies are slightly influenced. The frequency results from both programs are given in Table 4.5.

Table 4.4: Prototype Mass / Inertia Parameters

Ref Item from Fig 4.2		Mass Kg	Inertia Kg m^2
a	motor	.356	.000071
b	coupling	.150	-
c	gear	.392	.00044
d	disk	.626	.00045
e	coupling	.150	-
f	clutch	.164	.00003
g	disk (damper)	.532	.00062
h	gear	.324	.00043
i	disk	.301	.00058
j	disk	.512	.00140
k	disk	.301	.00058
l	coupling	.150	-
m	load/fan	1.40	.00133

Table 4.5: Prototype System Frequency Comparison

		Matlab		CosmosM			
				first (no shaft ext.)		second (shaft ext. incl.)	
	mode	ω (rad/sec)	Hz	ω (rad/sec)	Hz	ω (rad/sec)	Hz
Free	2	405	64.5	404	64.4	405	64.4
	3	900	143.2	904	143.9	899	143.1
	4	1098	174.7	1116	177.7	1311	208.6
	5	1462	232.7	1480	235.5	1486	236.5
	6	1588	252.7	1600	254.8	1608	255.9
Locked	2	338	53.8	337	53.6	337	53.7
	3	427	67.9	426	67.8	426	67.8
	4	915	145.6	921	146.6	912	145.1
	5	1099	174.9	1117	177.8	1317	209.6
	6	1467	233.5	1488	236.8	1500	238.7

4.3 Control of Torsional Vibration

Control of torsional vibration can be effected by adding passive elements such as flex drive couplings, dynamic absorbers, or dampers.

4.3.1 Passive Control

4.3.1.1 Flexible Couplings

As mentioned earlier, flexible drive couplings, being the weakest of the various stiffness elements in the train, can be selected to tune the system by shifting the troublesome frequency away from the operating frequency. These couplings will, also, likely add damping which will attenuate the resonant buildup as the speed passes the resonance point on the startup or rundown. The normal amount of damping is considered to be in the order of 2 - 5% of critical.

When this type of shaft coupling is applied, the natural frequency of concern is shifted down so that the operating speed is well above the resonant peak. Such couplings having low stiffness yet high damping may still result in unsatisfactory operation due to greater transverse vibratory forces transmitted across the coupling at the normal high speed operation. Further improvement could be achieved with a similar coupling having both low stiffness and also low damping, however this is not readily available.

The actual prediction of frequencies becomes considerably more difficult as the stiffness and damping properties are usually not known exactly. These couplings, generally, behave in a nonlinear fashion, increasing the uncertainty of prediction and the solution of a problem at one particular frequency may lead directly to a similar or worse problem at a different frequency.

These couplings are generally constructed of elastomeric inserts which, because of hysteresis, may exhibit heating problems at the resonant condition. This introduces component life as another unknown for consideration. The component life will be dependent on the number of operational occurrences at the resonances and the dwell times at those points. Clearly, for a variable speed machine, merely causing a blind shift of the resonances does not provide a very secure or satisfactory operating approach for the long term.

A further complication, which may result from the use of flexible drive couplings, is brought about because these units are generally larger and heavier than their stiffer, all-metal, counterparts. This may lead to lateral response problems because of the increased shaft overhang weight.

4.3.1.2 Absorbers and Dampers

Another accepted method of passive control is the application of dynamic vibration absorbers and dampers to the system. The most effective attenuation of vibration is achieved with the application of a tuned absorber with damping, having optimum values for both stiffness and damping factors. Under these conditions, for a single operating speed, maximum attenuation of vibration is achieved. However, the situation can be made worse at other non-resonant speeds as compared with the case of no absorber [2]. Also, if the machine is a variable speed unit and another mode becomes a significant factor in the overall response, the values of stiffness and damping will not be optimum for this frequency and increased vibration may result.

Providing optimum stiffness and damping for a single speed by selection or design is a difficult task and becomes impossible when more that one critical frequency is excited within the operating range. Most industrial engine drive applications utilize a

hydroviscous variation of the Lanchester damper, which is a flywheel attached to the primary system by way of damping alone. The original Lanchester damper used dry or Coulomb friction as the damping mechanism. More recent applications use viscous shear damping provided by a liquid interface between the components in relative motion. In any case, optimum damping can be provided for one speed only. Furthermore, since the damper is generally a selection of available sizes, the situation may only approach optimum conditions at the chosen speed.

4.3.2 Active Control

The control approach taken in this work incorporates the implementation of a controllable Lanchester damper. The effect of this device is twofold:

- providing modification of the mass elastic properties of the system
- providing damping of unwanted torsional vibration.

The control realization involves the use of a fuzzy logic controller developed in software on the lab 80286 PC.

Fuzzy systems are typically used to simulate and control nonlinear plants or systems which are difficult to describe mathematically. In the general analytical case, to provide a classical controller for a physical plant, the first step will be to carefully calculate the mass elastic parameters of the plant. Many real plant systems do not lend themselves to easy linear quantification of parameters. Moreover, if for some reason, a parameter change were incorporated in the plant, either purposefully or through normal equipment maintenance, a controller parameter change would be required. The fuzzy control system operates independently of plant parameters reacting only to the resulting output state variables and as such is inherently self correcting for plant changes or nonlinearities. Typically, fuzzy systems degrade gracefully in that as rules are deleted from the matrix, the control response is a gradual deterioration and not an abrupt change as may result

from classical control. Fuzzy systems are indeed able to make decisions with only partial information. This is a robustness which far exceeds the conventional linear model based classical control system. A fuzzy system with incorporated "learning" would have the capability to modify itself on the fly, without external prodding, to produce the missing rules required to smooth out the control response.

The established theories for vibration dampers / absorbers are for neat capsulized single degree of freedom system or simplistic multi-degree of freedom systems [7] for which all input parameters are readily available. Real systems cannot be so neatly simplified so as to pick optimum damping or tuning. A more realistic approach will be to provide a controllable function which, through the use of fuzzy logic, is self optimizing for the real world parameters without the necessity of determination of these parameters. This mechanism will be self modifying across the operating speed range. The ease of fit to various systems makes the device quite appealing for complex machine trains where a "designed" or "selected" optimized damper / absorber may not historically have been considered as a solution. The appeal will be particularly so for variable speed applications in the retrofit market where the system parameters are not well defined and may be subject to change over time.

Herein, the fuzzy controlled torsional damper will be employed to counter the identified torsional lateral mode shapes of the rotor system. Chapter 5 presents experimental results for the prototype with and without the fuzzy control. Chapter 6 discusses the experimental results and presents comparative computer simulation outcomes based on the bondgraph model of the prototype.

Chapter 5

Experimental

5.1 Prototype Development

The laboratory prototype was constructed from a Bently Nevada rotordynamics study kit, (ref Fig 5.1). The basic kit has been modified to include an extra shaft, support bearings and gears to function as a parallel shaft offset geared arrangement as shown in Fig 4.2. Rotating inertia, gear and pinion mass has been selected (ref. Tables 4.2 and 4.4) with appropriate bearing support spans to place the first three natural frequencies below 200 Hz. This was done to obtain a response which would be representative of a real industrial machine train.

5.1.1 Machine Train

The drive motor is a Bodine, type NSE-12, 1/10 HP, 115 Vac/dc, variable speed universal motor. Top speed capability for the motor with very light load is 10,000 rpm (167 Hz). For the prototype arrangement, top speed is around 5000 rpm due to bearing and windage losses.

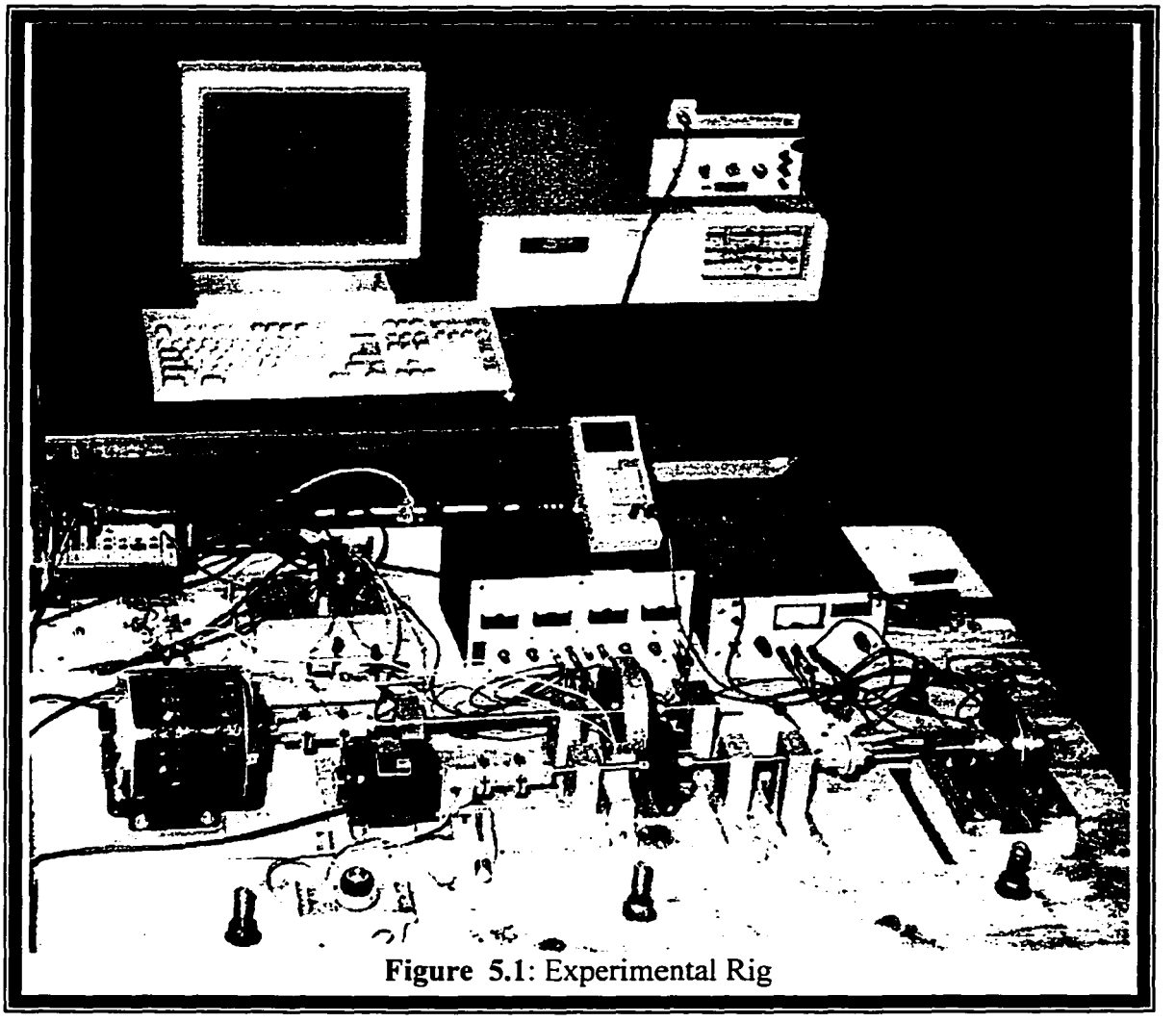


Figure 5.1: Experimental Rig

The pinion and gear shafts are 9.6 mm (⅜ in.) diameter. The bearing spans can be varied through a key-slide bearing support mounting arrangement on the machine base. The disks representing the gear and pinion mass / inertia are fastened to the shaft by a double set screw arrangement. Mass may be added or removed conveniently via this sliding disk provision. Dynamic unbalance can be readily adjusted with set screws selectively placed in a series of holes around the periphery of these inertia disks.

Flexible shaft couplings at the drive, load, and damper connection positions are a dry disc type and are also fastened with a double set screw arrangement. Both the drive and load couplings have double flex units while the damper coupling has a single flex disc. The double flex units require close lateral shaft support on either side of the coupling to maintain smooth running at high speed. These couplings are quite stiff torsionally while providing lateral discontinuity between connected shafts. These characteristics are typical of flexible disc couplings used in industry.

The bearings are cylindrical sleeve journal bearings which are oil lubricated. However, no continuous supply of lubrication is available nor is there any closure at the ends of the bearing sleeves. This leads to some variation and non-repeatability in the prototype response as the lubrication conditions change throughout a test run.

For convenience, the gear ratio was chosen to be 1:1. The gears are straight spur type each having 96 teeth on a pitch diameter of 101.6 mm (4.00 in). The face width is 6.4 mm (0.25 in). Both gear wheels are steel and are operated without lubrication. This introduces some damping (friction) at the gear mesh, however still quite light.

The load mass is provided by a 1/4 HP motor which is left unpowered. This unit provides both a rotating inertia and a quadratic load relationship with speed via the motor fan.

The complete prototype is mounted on a solid plywood base which in turn is mounted on a concrete inertia block of semi-infinite mass. Refer to Fig 4.2 for a plan outline and Fig 5.1 for a photograph of the prototype machine train utilized in this project.

5.1.2 Instrumentation

The purpose of the control is to reduce the lateral vibration associated with the offset gear mesh and as a consequence to also reduce the coupled torsional response of the machine train at the operation frequency. To implement the control and study the effects, two parameters were measured; the lateral (vertical) displacement of the pinion shaft and the speed of operation of the prototype.

5.1.2.1 Lateral Vibration Measurement

Lateral vibration of the pinion shaft was measured by a proximity probe placed as close as possible to the shaft center span. This transducer is a Bently Nevada, 190 series, rf proximity probe in conjunction with a series 3000 proximeter. The proximeter is powered by -18 volts dc as supplied by a Xantrex -Triple Output Laboratory Power Supply. The proximeter converts the -18 volts into an rf signal applied to the probe through a co-axial extension cable. The probe coil radiates the rf signal into the surrounding area as a magnetic field. If there is no conductive material within a specified distance to intercept the magnetic field, there is no loss of power in the rf signal. When a conductive material approaches the probe tip, eddy currents are generated on the surface of the material, resulting in a power loss in the rf signal. As the shaft moves in close proximity to the probe tip, the proximeter measures the magnitude of the rf signal, and provides a negative output voltage signal proportional to the peaks of the rf signal. The

linear range of these probes is for gaps of approximately 0.5 mm to 1.5 mm. Calibration sensitivity of the probe used is 9.815 V/mm (249 mV/ mil) as presented in Fig 5.2. The frequency response bandwidth for the combined probe and proximeter is dc to 10 kHz, however the useful upper range is generally limited to 1 kHz due to typically small displacement amplitudes experienced above this frequency. The output signal was attenuated by a factor of 6 for suitable input to the data acquisition unit.

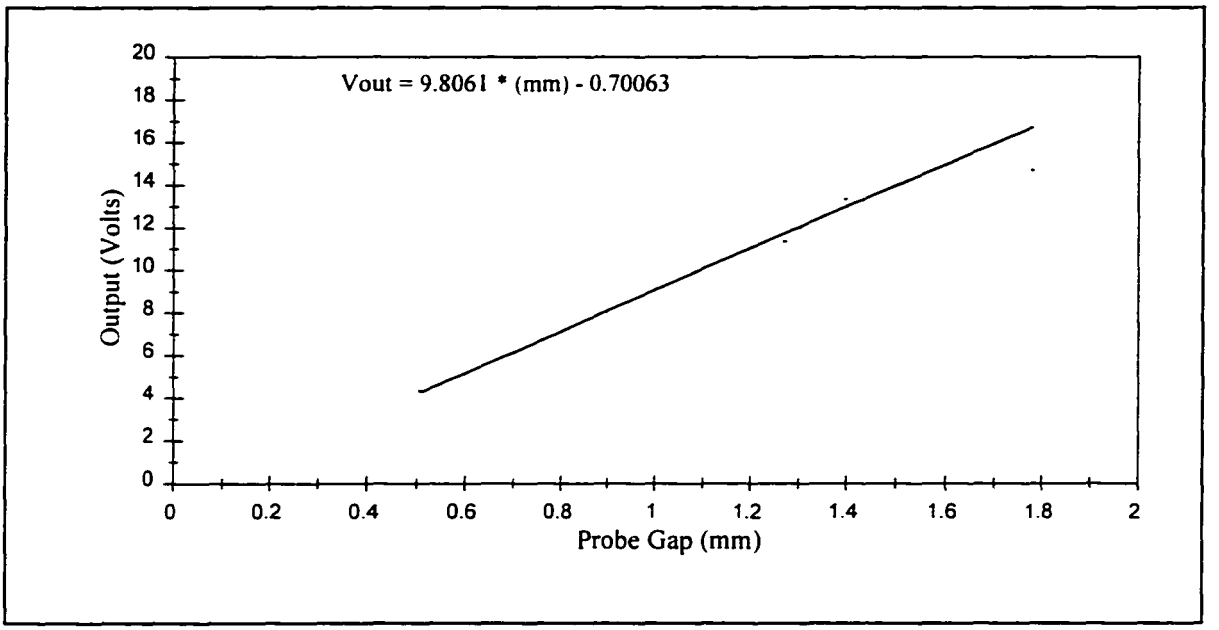


Figure 5.2: Proximeter Calibration

5.1.2.2 Prototype Speed Measurement

The speed of the operating prototype was monitored using an optical switch together with a voltage comparator circuit to provide a 1/rev pulse signal. This signal was input to a frequency to voltage conversion circuit which provided a linear dc voltage output proportional to shaft speed. The optical switch is a Motorola type 354A with a 3 mm (1/8

inch) gap width. Rise time for this switch is 8 μsec with a fall time of 50 μsec. The voltage comparator chip is a National Semiconductor, type LM393N, 8 pin - DIP with a response time of 1.3 μsec. The frequency / voltage converter is a National Semiconductor, type LM2917M, 14 pin DIP tachometer chip. The bandwidth of the tachometer circuit is dc to 1 KHz. A circuit diagram for the 1/rev pulse and frequency to voltage conversion is presented in Fig 5.4. A calibration curve for the linear dc output voltage signal is given in Fig 5.3. The 1/rev pulse was also used as an external trigger signal during the initial data acquisition and response investigation phase of the work. A Xantrex triple output laboratory power supply was used to provide the required regulated 5 volt source voltage for the above described tachometer circuit.

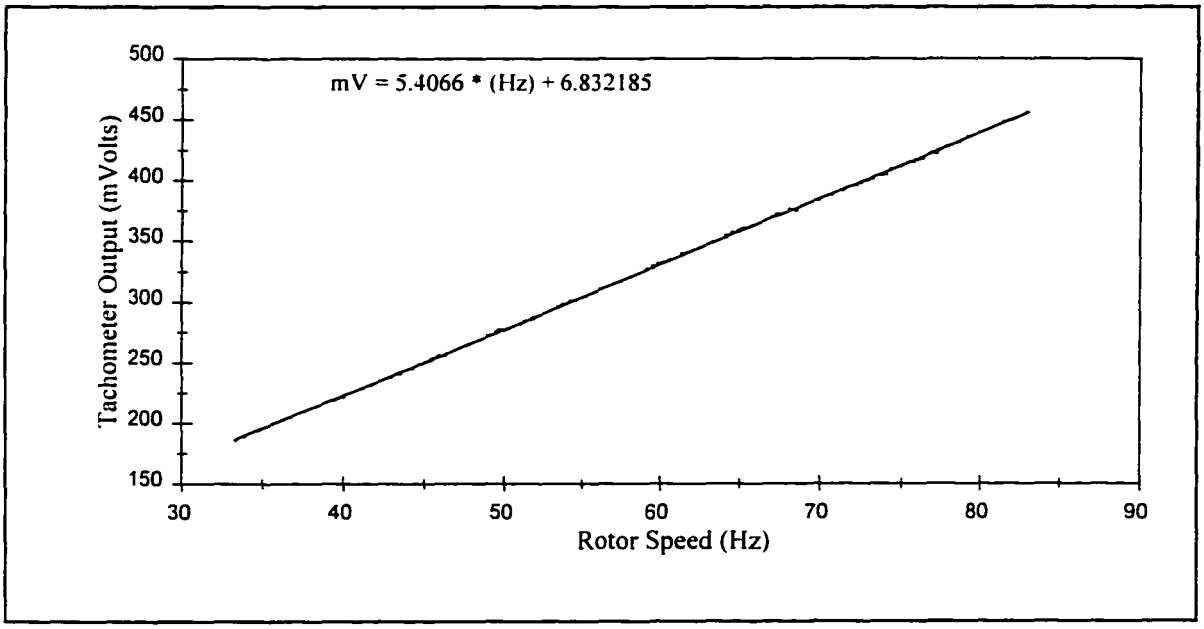


Figure 5.3: Tachometer Calibration

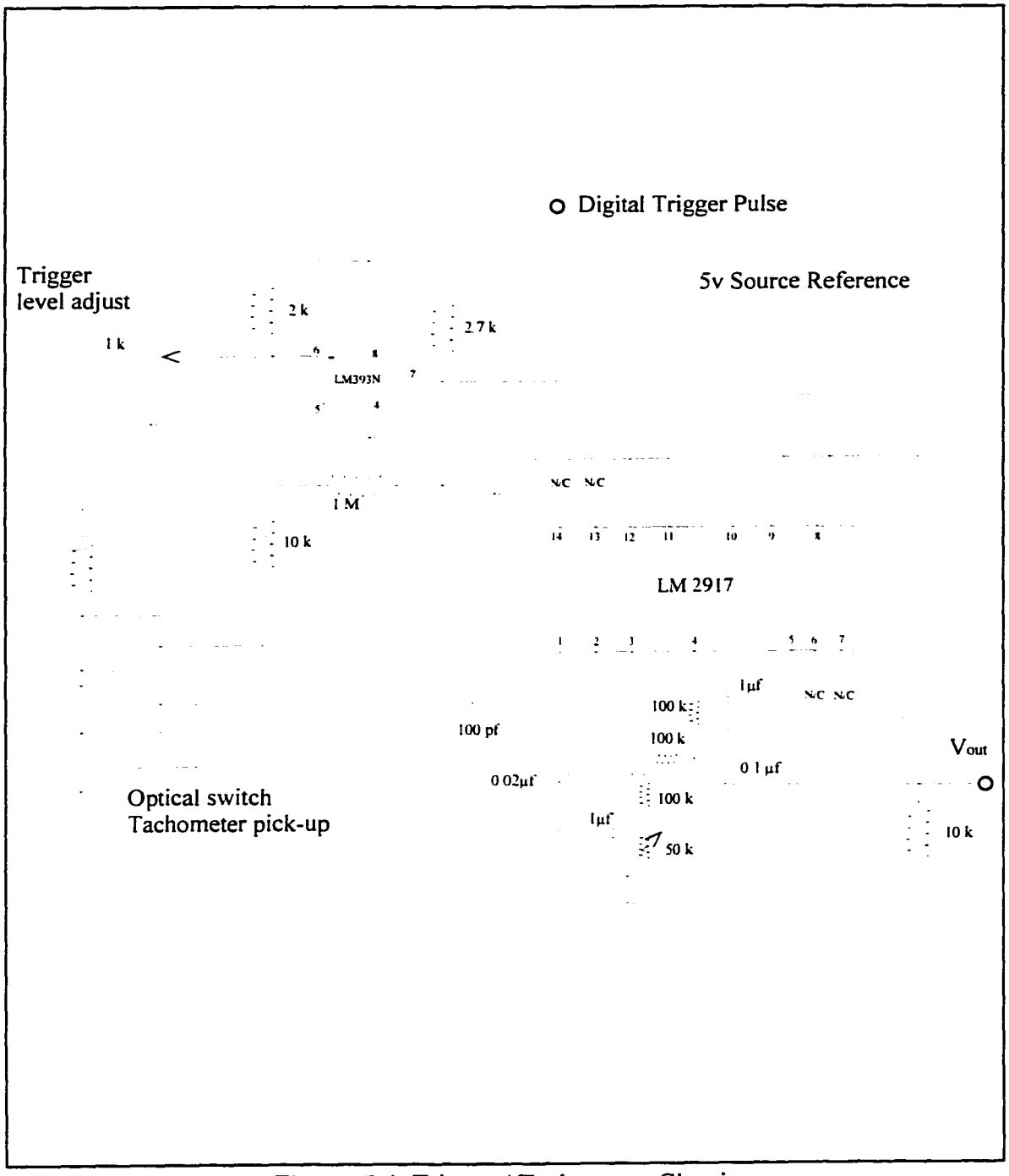


Figure 5.4: Trigger / Tachometer Circuit

5.1.2.3 Torsional Vibration Measurement

Torsional vibration is the angular fluctuation, from constant speed, of a rotating body. To detect this dynamic angular motion, instantaneous speed changes must be measured. For a machine running with no torsional vibration, the speed signal would be a constant dc level. Torsional vibration will cause speed changes reflected as an amplitude modulation of the constant output signal. With constant load conditions, a typical speed transducer output will consist of an average output or dc level representing average machine speed with an additional ac modulation representing the torsional vibration component. Examination of this ac modulation will reveal the amplitude, frequency and phase (if a second reference signal is available) of the torsional velocity variation of the attached component.

The torsional response of the main gear disk at the free end of the gear shaft was monitored using a tacho-generator with the following specification:

Servo-Tek Model# SD740A-2

- output: 7 Vdc/1000 rpm
- linearity: 0.1%
- ripple: 3%
- max rpm: 12,000

The voltage output of the unit was attenuated by a factor of 11 for input to the data acquisition card. FFT examination of the ac portion of the signal will give a good indication of the torsional motion of the gear. A plot of the prototype response, as indicated by this signal, with a free damper as well as the fully locked up damper is presented in Fig 5.5. The information available from this plot is disappointing as the separation of points is excessive. The fundamental torsional lateral frequency is indicated as 67 Hz for the free mode (cf. 64.5 Hz from Table 4.5). In the locked mode there is a

small rise in the 54 Hz area, although not definitive. Another peak at 58 Hz is of unknown origin while the third peak at 69 Hz is attributed to the second frequency in the locked mode (ref Table 4.5). The fourth peak at 77 Hz is the natural frequency of the transducer and mounting. Attempts to refine this response gave inconsistent output readings due to deterioration of the transducer and was therefore abandoned for the optical pick-up tachometer circuit as discussed above.

The original intent was to use this device for the speed signal as well as to provide a means of monitoring the torsional motion at different locations. A disadvantage associated with this type of device is that it must physically attach to the rotor and in the case of the prototype may have influenced the rotor dynamics somewhat.

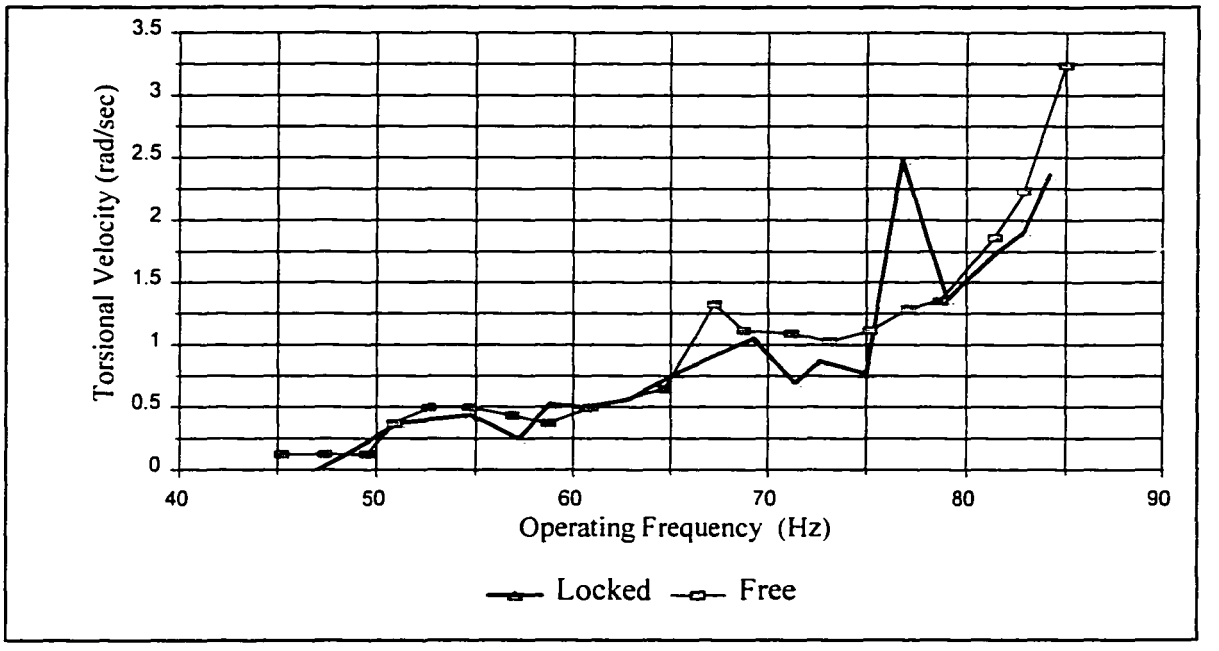


Figure 5.5: Main Gear Torsional Deflection

5.1.3 Data Acquisition

The vibration and speed signals were brought to a desktop computer through analog to digital (A/D) conversion. The lab PC (80286 AT) performs the controller function using the fuzzy logic software developed for the project. Data acquisition was conducted using a Metrabyte Data Acquisition board (DAQ; see Appendix V) together with Quinn Curtis board-specific utility software routines in Turbo Pascal. Software capability was developed to perform both time and frequency domain signal analysis for examination of the prototype response.

The Metrabyte model DAS-16 card is a multi-function high speed analog/digital I/O expansion board for 8088, 80286, 80386 series computers. The card uses a 12 bit successive approximation A/D converter. The A/D conversions are initiated by software command and controlled by an internal programmable interval timer (Intel 8254). The D/A converters are operated with a fixed -5v reference available from the DAS-16 board to give a 0 to +5v output.

For this project the specific board settings were in accordance with Table 5.1.

5.1.4 Control Hardware

The hardware setup for the control system consists of the output of one D/A channel of the Metrabyte DAQ card to a power amplifier supplying the magnetic clutch actuator. The amplifier increases the DAQ card output range of 0 to +5v up to 0 to +22v output signal to the clutch damper.

Table 5.1: Metrabyte Das-16 Data Acquisition Board Settings

gain setting:	+/- 5 volts
DMA level:	3
Unipolar / bipolar config :	Bipolar
Channel config:	8 double ended
Base address:	000:0300
Interrupt level:	4
Board number:	0
Cycle:	0 (single shot)
Mode:	0 (polled mode)
A/D Input Channel selection	
speed	6
vibration	7
D/A Output Channel selection	
control signal (0 - 5 v)	1

5.1.4.1 Magnetic Clutch Damper

The control actuator is in the form of a double ended, magnetically actuated, dry friction clutch located at the free end of the gear or load rotor. The flywheel mass is situated between an inboard and outboard clutch arrangement. Each clutch is rated 5.5 watts at 90 volts dc max. In actuality, a voltage level in excess of 26 volts essentially locks up the additive mass, while a level less than 8 volts leaves the mass free spinning. Even in the free spin state, there is enough sliding friction to bring the mass to the operating speed of

the rotor for a constant speed situation. The clutch is a model Type XBO-4.8G manufactured by the Shinko Electric Company Ltd.

This semi-active type of control system performs the task of dissipating and redistributing the existing energy levels associated with the operating plant. Effectively the control is operated on signal power to the magnetic clutch. For illustration purposes, the power requirement to operate the clutch is evaluated on the basis of a conservative nominal operating supply voltage of 20 volts. This results in a total power absorption of 0.5 W for the dual clutches, representing approximately 0.7% of the drive power capability of the prototype. The full power rating of the prototype drive motor (74.6 W or 0.1 HP) is spent in just overcoming bearing friction and windage losses with the prototype operating near the first fundamental frequency of 65 Hz (ref Table 4.5). (Recall motor no-load top speed is 167 Hz or 10,000 rpm.) For the case of an industrial machine train transmitting significant load, the relative additional power component required to operate the developed control system would be quite small.

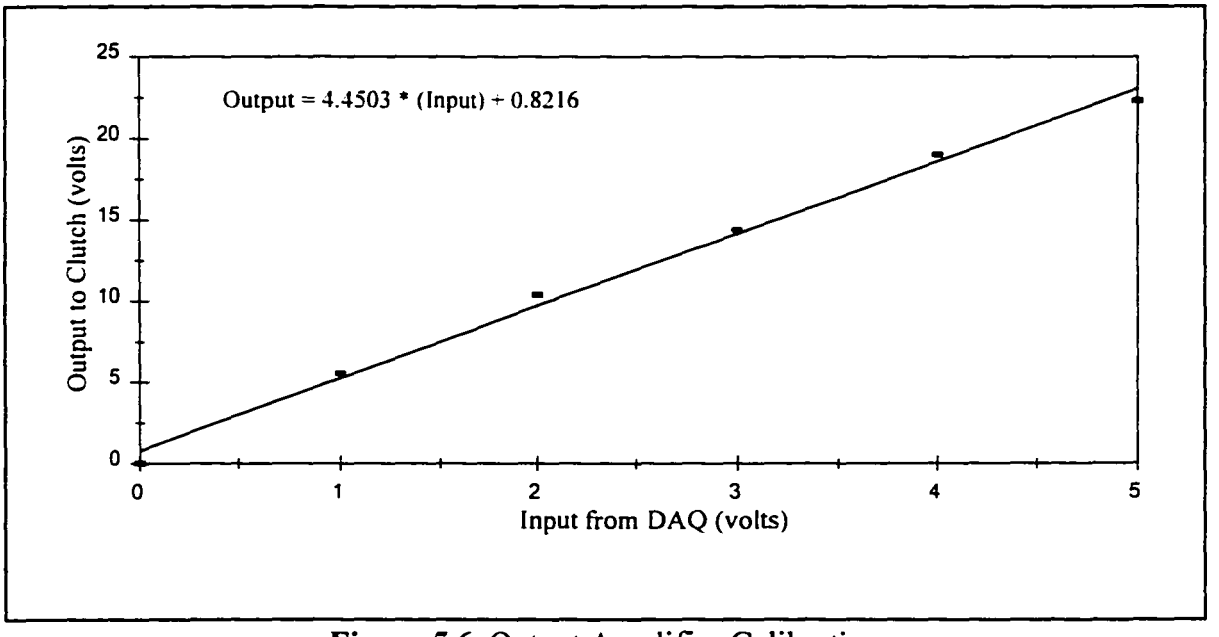


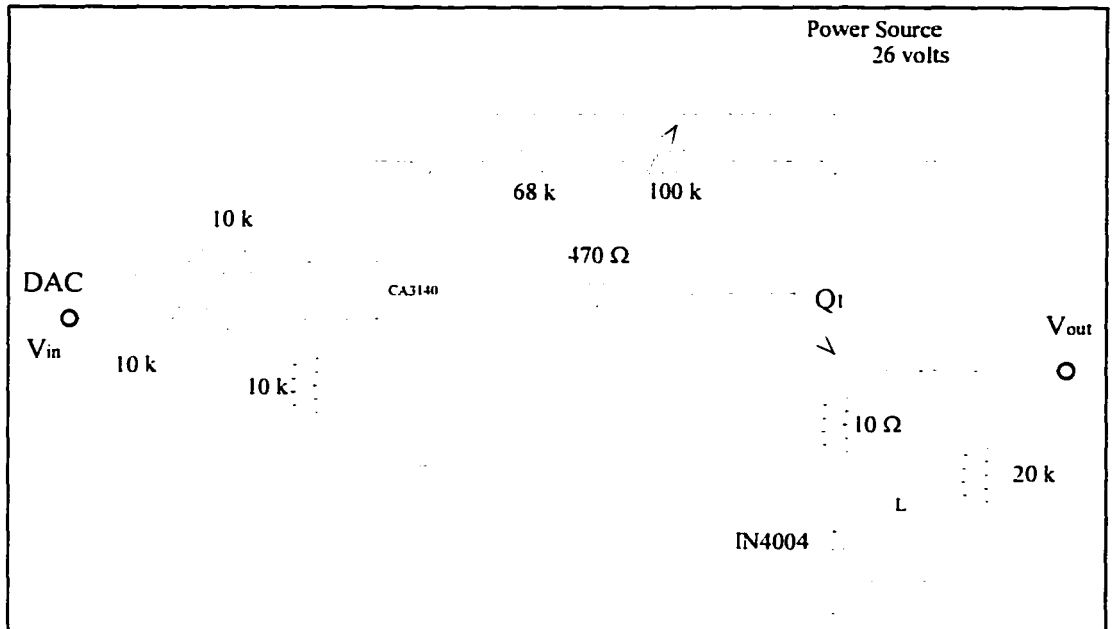
Figure 5.6: Output Amplifier Calibration

5.1.4.2 Amplifier

The analog output of the D/A channels of the data acquisition card has a limited range of 0 to 5 volts. Therefore a proportional amplifier was constructed to deliver 0 to 22 volts to the clutch based on the output value from the data acquisition card. The amplifier circuit uses a CA-3140E op-amp to control the output of the power transistor. This is an 8 pin DIP having a 450 mwatt capability. The amplifier circuit power transistor is a Motorola, type NPN, designated 2N2219-852. The circuit bandwidth is dc to 1 MHZ. A calibration curve for the amplifier is presented in Fig 5.6 with the applicable circuit diagram in Fig 5.7.

The amplifier requires a base power supply of 26 volts to perform the designed function. The 26 volt supply is provided by an HP Harrison 6206B regulated dc power supply rated 0 - 60 volt at 0.5 A or 0 - 30 volt at 1.0 A.

Fig 5.8 presents a composite schematic of the prototype and control setup for this experiment.



Notes:

Q1	medium power transistor, type NPN, with heatsink, designation 2N2219, rated 800 mW
Vin	0 to 5 v (output from data acquisition card D/A channel)
CA3140	8 pin - DIP op amp rated 450 mW
Power	26 v supplied by an HP Harrison power supply #6206B dc power supply rating 0 to 60 v, 0.5 A 0 to 30 v, 1.0 A
L	clutch coil

Figure 5.7: Output Amplifier Circuit

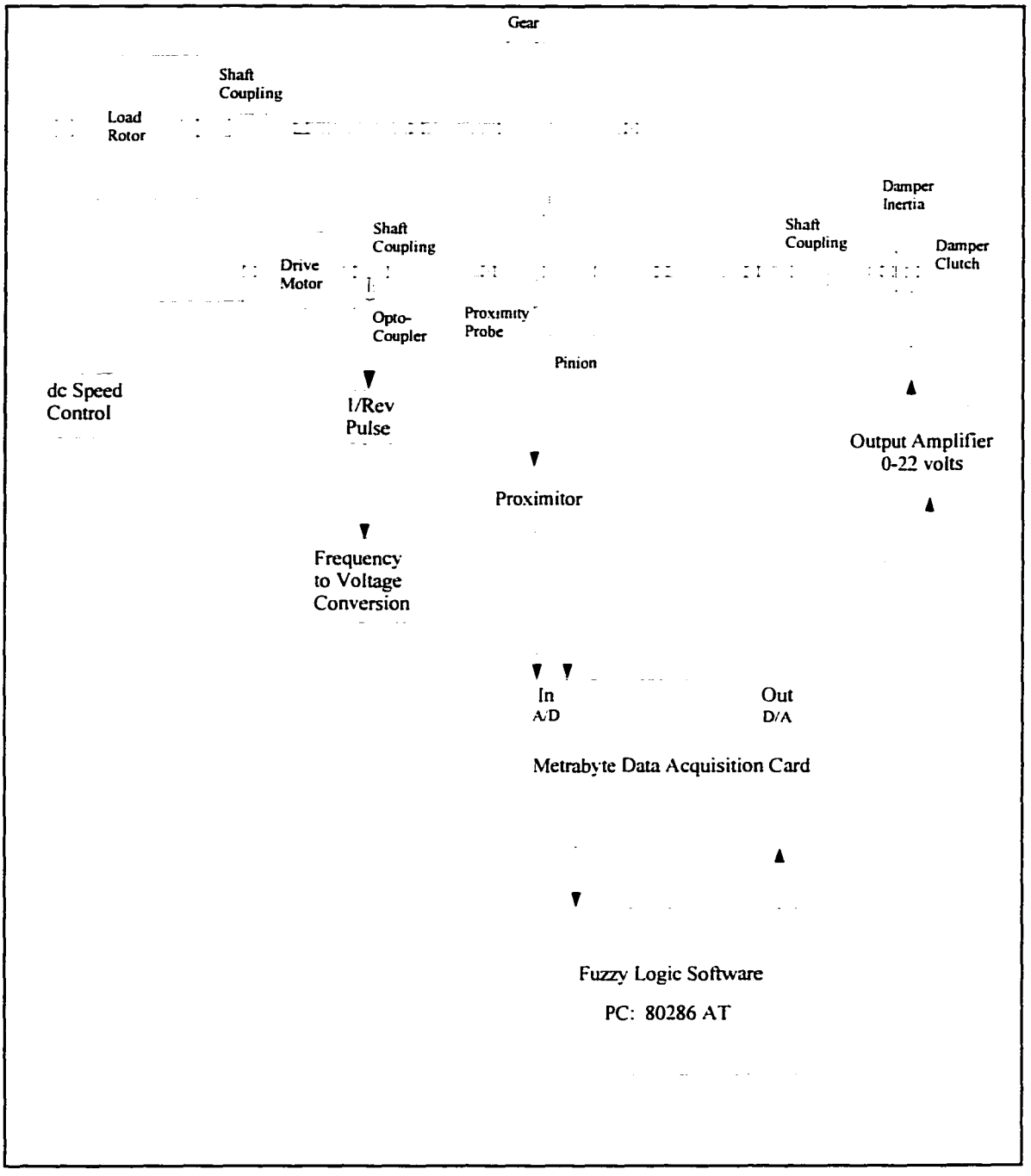


Figure 5.8: Prototype Control Configuration

5.2 Control Development

Active control of large mechanical systems has sparked considerable interest in recent years. There has been a long history of vibration control using passive elements such as mass, springs and dampers. When operating speeds are changing and smooth performance must be maintained over the full range, active modification of the dynamics will be required.

5.2.1 Classical Control Considerations

The control developed in this work is a semi-active control without the ability to input energy, yet has a system modifying characteristic in operation. Therefore actuator function creates some difficulties with the realization of a control using classical or modern control methods as outlined below.

To utilize classical control methods for the solution to this problem, an a-priori knowledge of the relationship between the system response and the transport or operating speed of the prototype will be required [14]. As this information would not generally be available for an industrial application in a quantified fashion for use in the control system, the data would need to be obtained by measurement. This may not always be possible and would be inconvenient in any case.

Secondly, the applicable system parameters of mass, stiffness and damping must be determined for a model of the machine train. These can be evaluated by estimation (calculations), measurements, or by application of system identification techniques. All of these methods are time consuming, and therefore expensive, subject to error, and generally inconvenient. Also, the machine train dynamic parameters for rotating systems

are generally a function of the transport speed, creating another difficulty in obtaining practical values for these parameters [14]. This speed dependancy can give rise to nonlinear components in the total response of the machine train system. Representing the system by a general 2nd order lumped parameter vector matrix equation, assuming now a fully active control system, we have

$$M\ddot{q} + R\dot{q} + Kq = f \quad \ldots\ldots (5.1)$$

where: M = mass matrix
R = Damping matrix
K = Stiffness matrix
q = typical coordinate vector
f = active control force vector

An active control structure for a general rotating system can be depicted as shown in Fig 5.9. The control objective will be to maintain the state at zero (i.e. minimum response) despite any system disturbances. Defining the state vector as

$$x^T = [q^T \dot{q}^T] \quad \ldots\ldots (5.2)$$

allows equation (5-1) to be written as

$$\dot{x} = Ax + Bf \quad \ldots\ldots (5.3)$$

where: $A = \begin{vmatrix} 0 & I \\ -M^{-1}K & -M^{-1}R \end{vmatrix}$ and $B = \begin{vmatrix} 0 \\ M^{-1} \end{vmatrix}$

For the controller structure, as shown in Fig 5.9, the following relationships apply

$$f = T_1 u \quad \ldots\ldots (5.4)$$

$$u = -G x_s \quad \ldots\ldots (5.5)$$

$$x_s = T_2 x \quad \ldots\ldots (5.6)$$

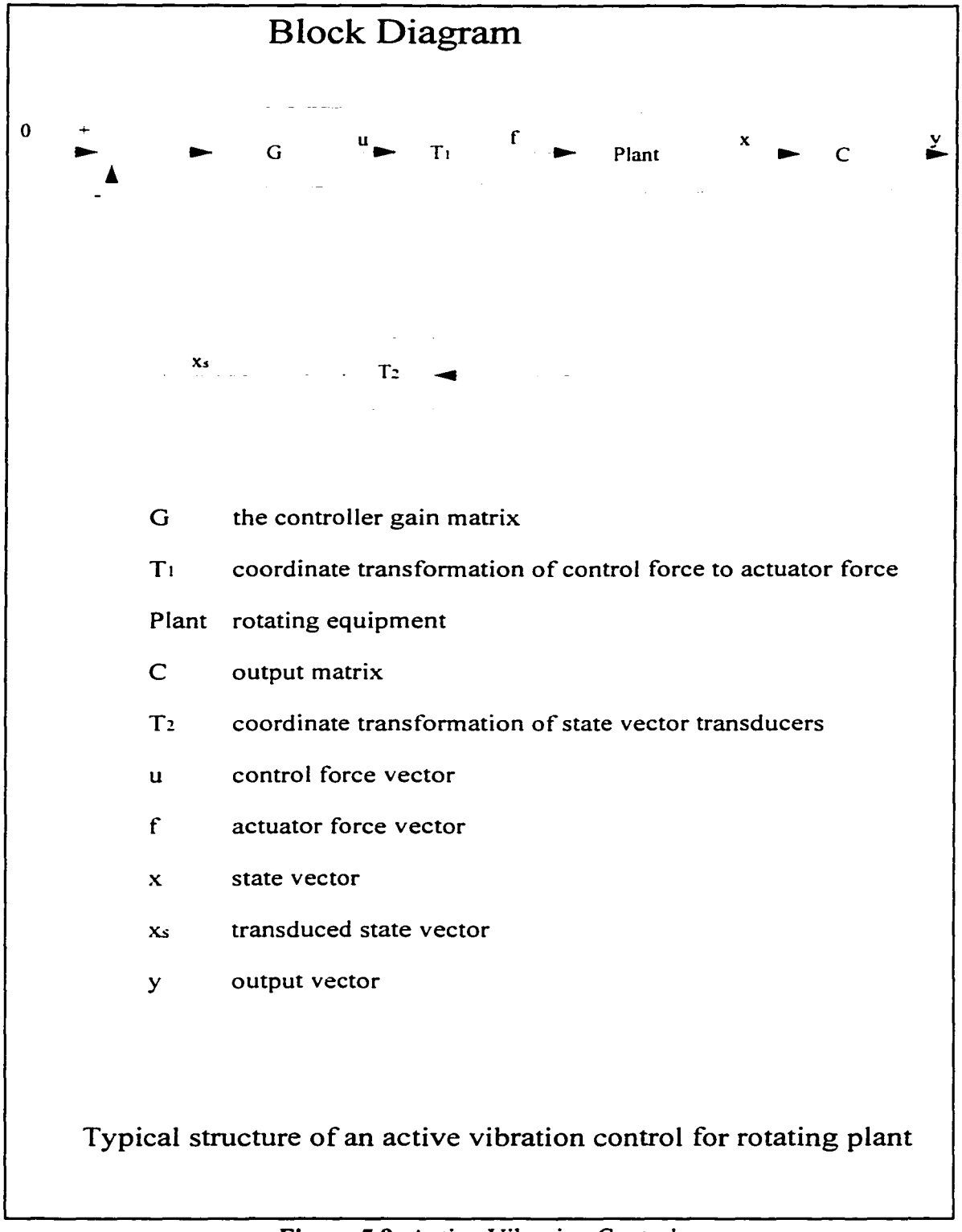


Figure 5.9: Active Vibration Control

where the T_1 and T_2 provide for coordinate transformations for the actuator and sensor systems respectively, required in the practical control implementation. The matrix G is the controller gain matrix. Substituting equations 5-4 to 5-6 into 5-3 gives

$$\dot{x} = (A - B T_1 G T_2) x = A_c x$$

as the closed loop equation. As noted previously [R] and [K], and therefore [A], are transport speed dependent and consequently [G] is transport speed dependent. This implies that the transport speed would need to be constantly measured for input to the controller which makes it an adaptive controller dependent on the plant operating speed.

Also, an assumption is made of complete state vector feedback. It will not be convenient or practical to measure the complete state vector, so a dynamic state observer would be required. The error dynamics between the observer and the plant would be used to generate estimates of the state vector {x} for use in the control system.

A further difficulty associated with the classical methods approach is the approximate nature of the modeling equations (lumped parameter method). Problems arise from the requirement to control an infinitely dimensional system with a finite number of sensors and actuators. The uncontrolled or residual modes of the vibrating plant can lead to problems of observation and control spillover [14]. Problems of this type can cause performance deterioration and lead to instabilities.

For the semi-active system the situation is still further complicated by the constraint of using only one actuator, the nature of which makes the [M] matrix in equation 5-3 also transport speed dependent. As well, for this semi-active system, it is observed that for a fixed operating speed, the response of the control system to increased plant vibration could be to either increase or decrease the damping / inertia effects. Indeed, both directions will be required to effect the control with no way of pre-determining the initial

control action. This fact lends the control system very distinctly to the fuzzy If... Then... rules style of control methods.

The significant complications and inconveniences of applying classical control methods to this problem is likely the main reason this solution has not been developed previously.

5.2.2 Fuzzy Software

The basic control algorithm instituted for the prototype machine train is a realization of a fuzzy logic controller, unique for this application. A fuzzy controller is a model-less paradigm which makes an approach toward state space control using knowledge based rules of operation. When a fuzzy logic control scheme is considered for any plant, some basic assumptions are implied [38]:

a. the plant is both observable and controllable.
b. enough information is available about the system to develop the linguistic descriptors which will form the partitions along the universe of discourse. These descriptors will be used to develop the fuzzy associative matrix (FAM) or rules database.
c. a solution for the control of the plant dynamics exists.
d. stability and optimality are still open issues in fuzzy controller design.

The controller can be manually tuned using a common sense trial and error approach to adjustment of the partitions along the universe of discourse for each input and output variable. Fig 5.10 outlines the universe of discourse for both of the input variables as well as the output variable. It will be noted that an offset zero (ZE) level is chosen as 0.005 volts for input No.1, vibration level. This represents a practical limit to work towards, since striving to achieve a vibration level less than the signal noise floor based

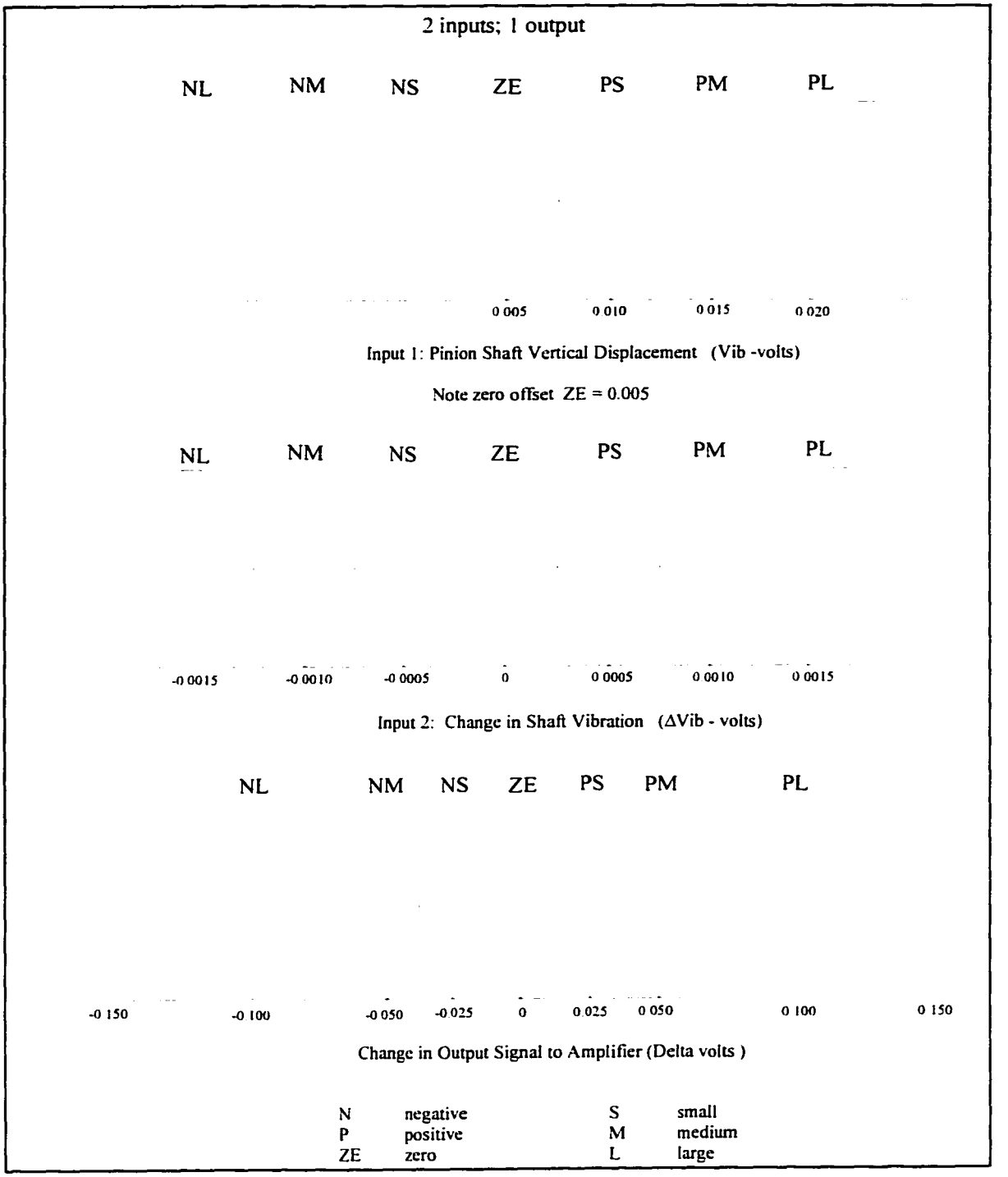


Figure 5.10: Universe of Discourse

on other influences (electrical noise, shaft runout in the probe area, etc...) has the tendency to make the controller somewhat coarse in the actual working range. The fuzzy inferencing procedure developed herein uses the two input variables referred to in Fig 5.10, shaft displacement and change of shaft displacement or velocity. The input variable of transport or machine operating speed was handled in a different manner as described in "Level 1. Approximate Speed Correction" below.

For the experimental application of the prototype plant, the chosen operating range was set arbitrarily at 35 to 70 Hz, specifically selected to include the first significant resonance zone between 60 to 66 Hz. The 70 Hz top speed is a suitable level above the resonance while still allowing adequate data gathering without causing the drive motor of the prototype to overheat excessively.

To characterize the basis for the control regime developed herein, the response of the prototype across a typical operating range, for a free and fully locked damper condition, was obtained using the Metrabyte data acquisition card. Specifically, operating speed and shaft vibration data were collected at various steps in the operating speed range from 30 Hz up to 75 Hz. The pinion shaft vertical displacement signal and the speed signal from the tachometer circuit were collected at a sample rate of 2000 samples per second. A total of 2000 samples for the two signals, or 1000 samples per signal, were collected to give a good definition of the average signal value. The relatively slow collection rate was specifically chosen to give definition of the signal in the lower frequency range up to 250 Hz which is considered to be the significant range for this work.

The discrete values collected for the speed signal were arithmetically averaged for each data point. The vibration reading was also averaged with a subsequent rms value determined for the ac portion of the signal. This procedure entailed subtracting the average value from each discrete value in the digital signal record and summing the

squares of the result. This sum was then divided by the number of discrete points in the signal and a square root performed.

The normal free operation of the prototype crosses a significant resonance at 64.5 Hz. Other minor peaking is indicated within the range from 53 to 56 Hz and also at 47 Hz. With the damper disk locked solid in the magnetic coupling, the prototype pinion shaft major response is shifted down significantly to 53 Hz. These curves are plotted in Fig 5.11 for reference.

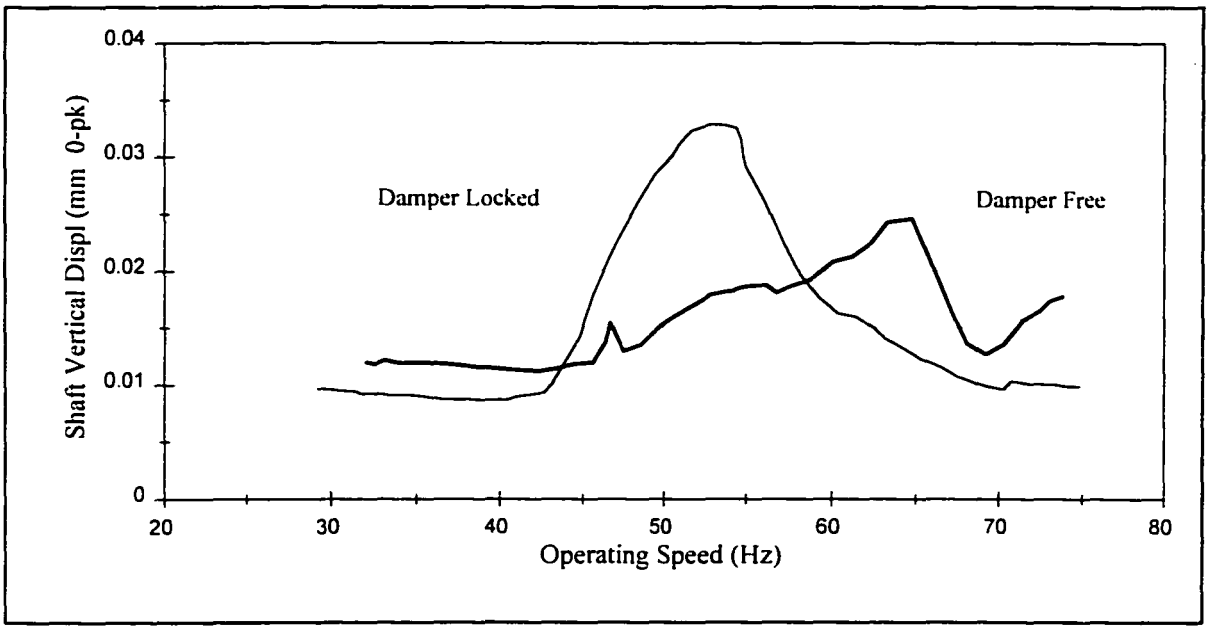


Figure 5.11: Locked vs Free Damper

To further establish the characteristic performance of the plant with the adjustable damper, several runs in the speed range of 30 up to 75 Hz were conducted at various fixed clutch voltage levels between 8 volts and 24 volts. These data are presented in the curves shown in Fig 5.12 through 5.15. Examination of these pinion shaft response curves indicates considerable nonlinearity between the voltage level and the plant

response. To more clearly indicate this nonlinearity of the actuation device, several plots of shaft displacement vs. voltage have been developed from the data in Fig 5.12 to 5.15 and are presented in Fig 5.16. It should be noted that the prototype response at the 24 volt level does not correspond with the fully locked damper response since there is still some slip occurring which precludes the strong amplification in the 50 to 55 Hz range.

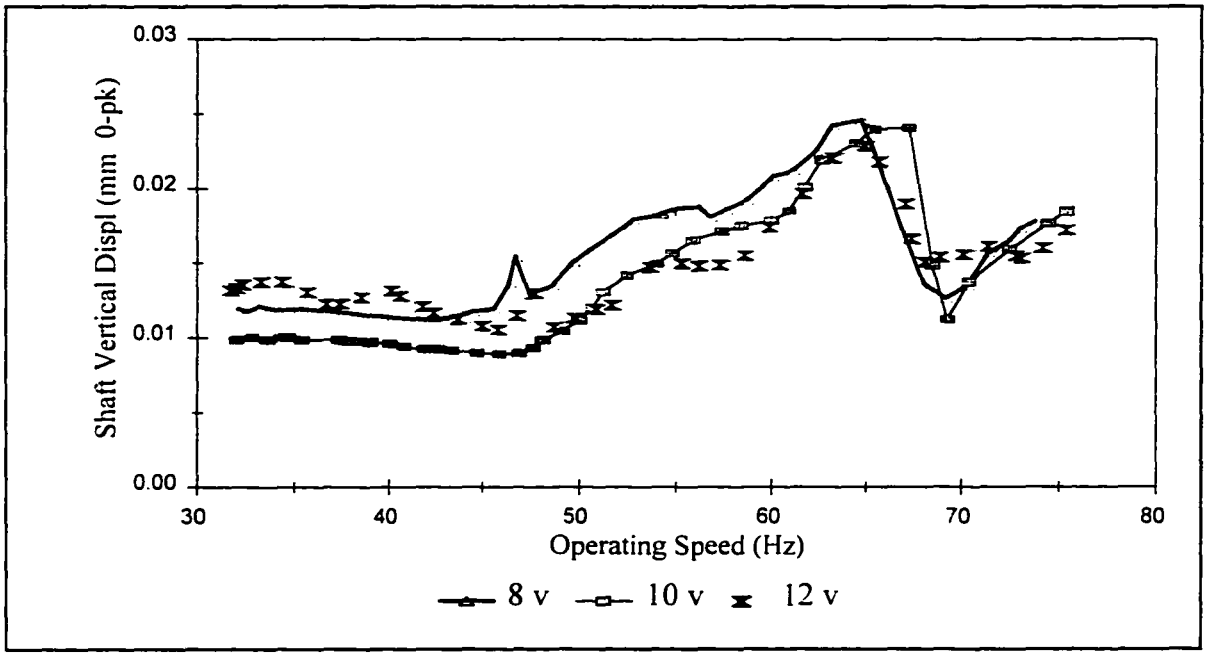


Figure 5.12: Lateral Response at Constant Clutch Voltage

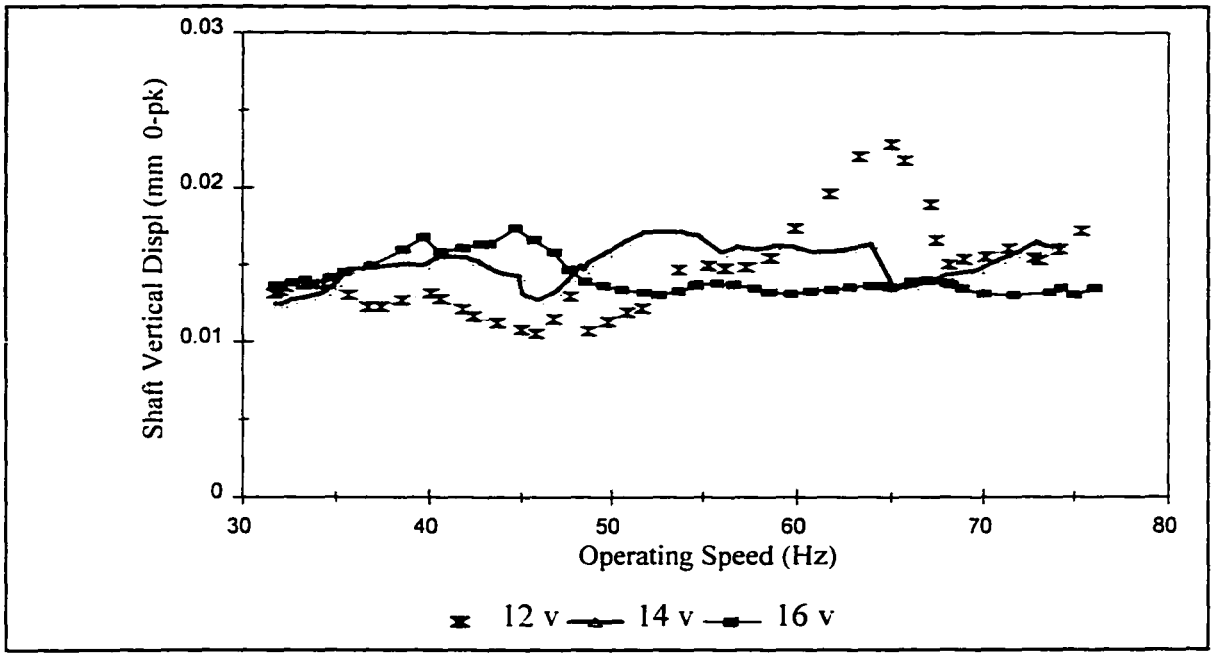


Figure 5.13: Lateral Response at Constant Clutch Voltage

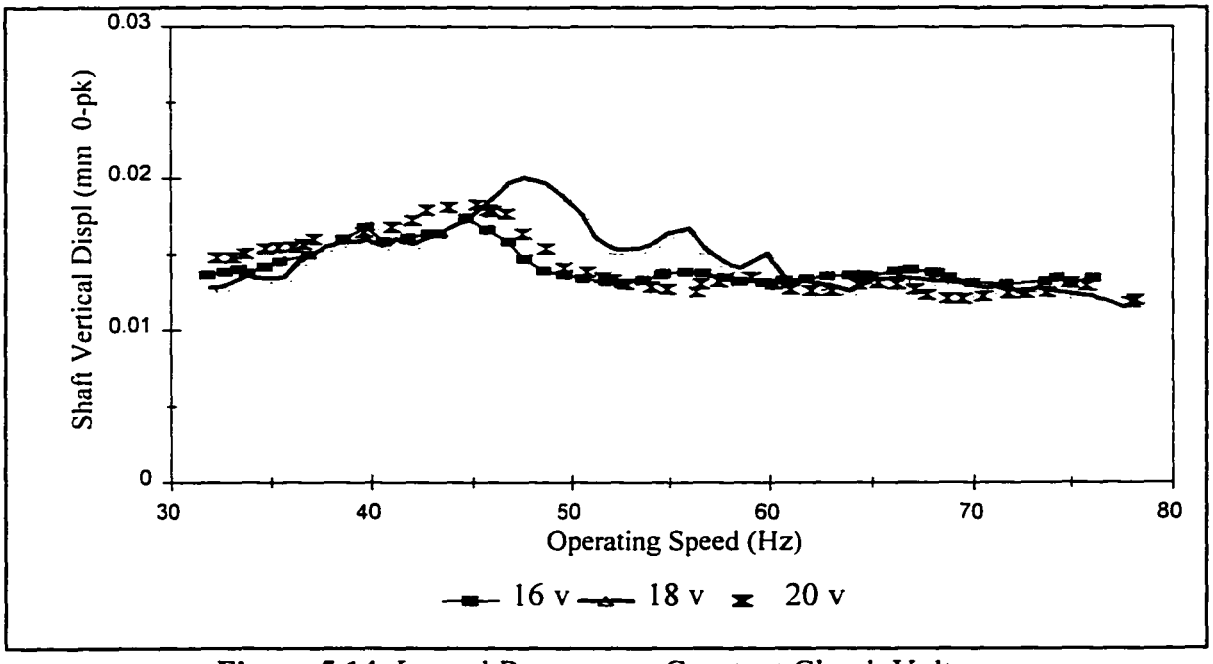


Figure 5.14: Lateral Response at Constant Clutch Voltage

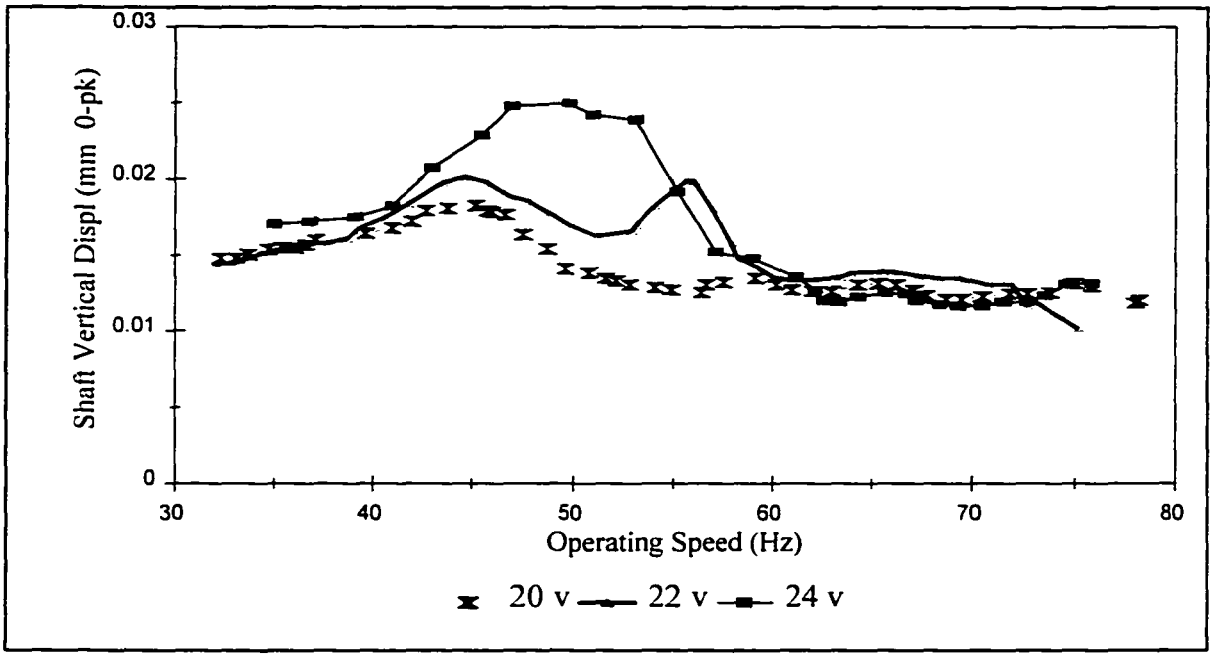


Figure 5.15: Lateral Response at Constant Clutch Voltage

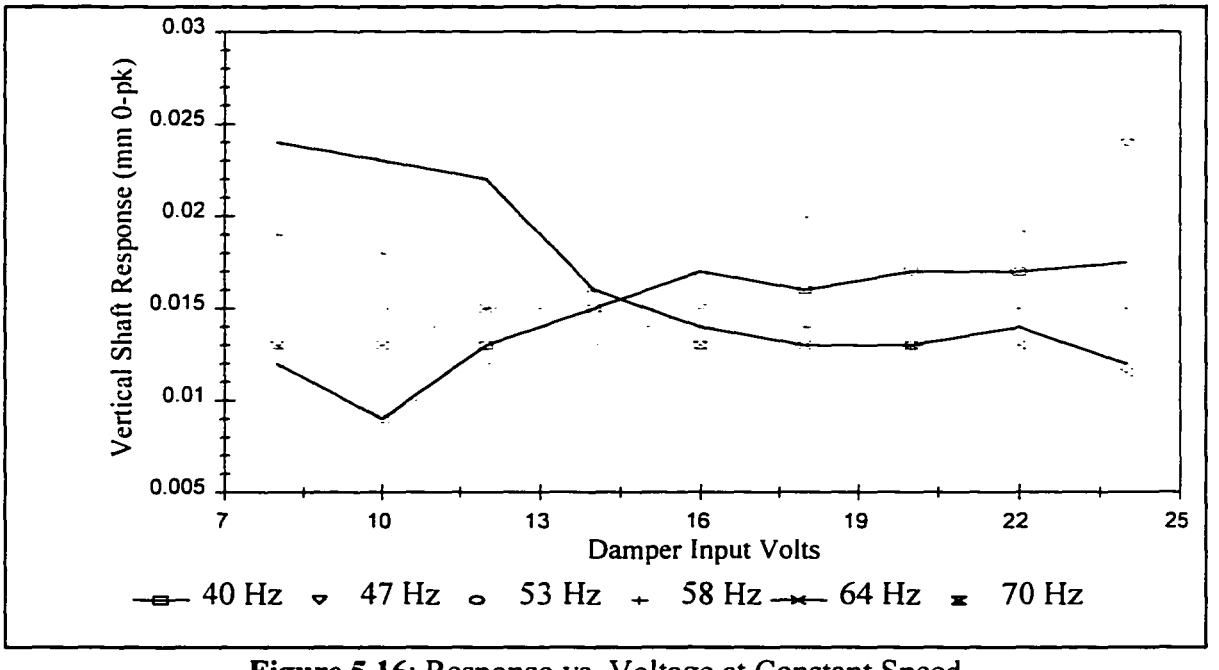


Figure 5.16: Response vs. Voltage at Constant Speed

The controller developed herein has essentially three routines or levels in the determination of the appropriate voltage correction for the output signal to the clutch.

Level 1. Approximate Speed Correction

The initial control attempt was made using change of speed and change of shaft displacement level as the input variables. This gave encouraging results in local speed pockets, however, the control would not respond properly for relatively large changes of speed (> 5 Hz).

In a more effective variation of the control, the fuzzy inferencing was formulated using displacement and change of displacement as the control variables. Examination of a typical application where this control system might be used reveals that operating speed will, for the most part, have constant settings for significant periods of time. Significant in this case will be periods of minutes or hours (i.e. much larger than the control cycle time of approximately 1 second). As such, speed changes should not be included as part of the fuzzy inferencing process. In general, the operating speed of the equipment would be set manually or by a separate speed control system. Variations of this signal within the fuzzy control cycle time would be quite small and of relatively minor influence. However, the overall set point range for the speed is relatively large and therefore a direct or feed forward style of control input correction is required for set point changes. As discussed earlier, the relationship between transport speed and machine train response is rarely, if ever, known in a quantified fashion. However, an approximate relationship can be established in estimating that a high output voltage to the clutch would be required at some frequency above the normal resonance, while a low voltage would be required at some frequency below the resonant speed zone. To allow the control to reset in a qualified fashion to major speed changes, an arbitrary straight line voltage correction function (defined by slope and intercept), spanning the full operating speed range, was

included in the software. Three trial voltage correction functions were attempted. The first function is based on two estimated operating points developed from the following statements. At a low operating speed of the prototype, around 40 Hz, virtually no damper / absorber effect is required. At 70 Hz, a speed above the fundamental free mode resonance of 64.5 Hz, a damper / absorber approaching full lock-up is employed. The first estimated function is summarized in the following table.

Table 5.2: Initial Estimated Voltage Correction Function

Oper Speed Hz	Clutch Voltage	DAQ Voltage	Slope "A"	intercept "B"
40	8	1.6	0.105	-2.59
70	22	4.76		

In this initial estimate, the fuzzy logic control shows distinct improvement over the estimated correction function operating alone (ref Fig 5.17). The straight line function alone produced a stronger voltage than required through most of the speed range from 35 - 66 Hz as indicated in Fig 5.18. Examination of Fig 5.17 and 5.18 indicates that improved response resulted from lower voltage levels produced by the fuzzy logic control in the above noted speed range, as compared with the estimated straight line function. Above this speed range, at 66 to 68 Hz, some marginal improvement is indicated for increased damper voltage (ref Fig 5.18). A new slope for the speed / voltage correction function can now be estimated by a smooth curve drawn through the lower points of the fuzzy logic control response curve.

Each time the logic goes through the speed correction routine, with the speed difference exceeding 2 Hz, a speed reference is updated to the most recently measured value. After

each data collection event, the difference between the measured speed and the speed reference is examined. If the difference exceeds 2 Hz, the software resets the output voltage in accordance with the estimated correction function producing, in this case, the higher vibration at the above noted points as indicated in Fig 5.17. It is also observed in Fig 5.17 that the fuzzy logic does indeed iterate to reduce the measured lateral vibration.

A second trial straight line speed / voltage correction function was then incorporated in the software. The second function had reduced slope as defined by the slope and intercept points given in the following table.

Table 5.3: Second Estimated Voltage Correction Function

Oper Speed Hz	Clutch Voltage	DAQ Voltage	Slope "A"	intercept "B"
40	8	1.6	0.079	-1.56
80	22	4.76		

The prototype response using this function is presented in Fig 5.19. This indicates that better agreement is achieved in the lower speed range between 35 and 58 Hz. Again, in the range of 60 to 65 Hz some response improvement occurs from a lower voltage than provided by the estimated voltage correction function for this trial (ref Fig 5.20).

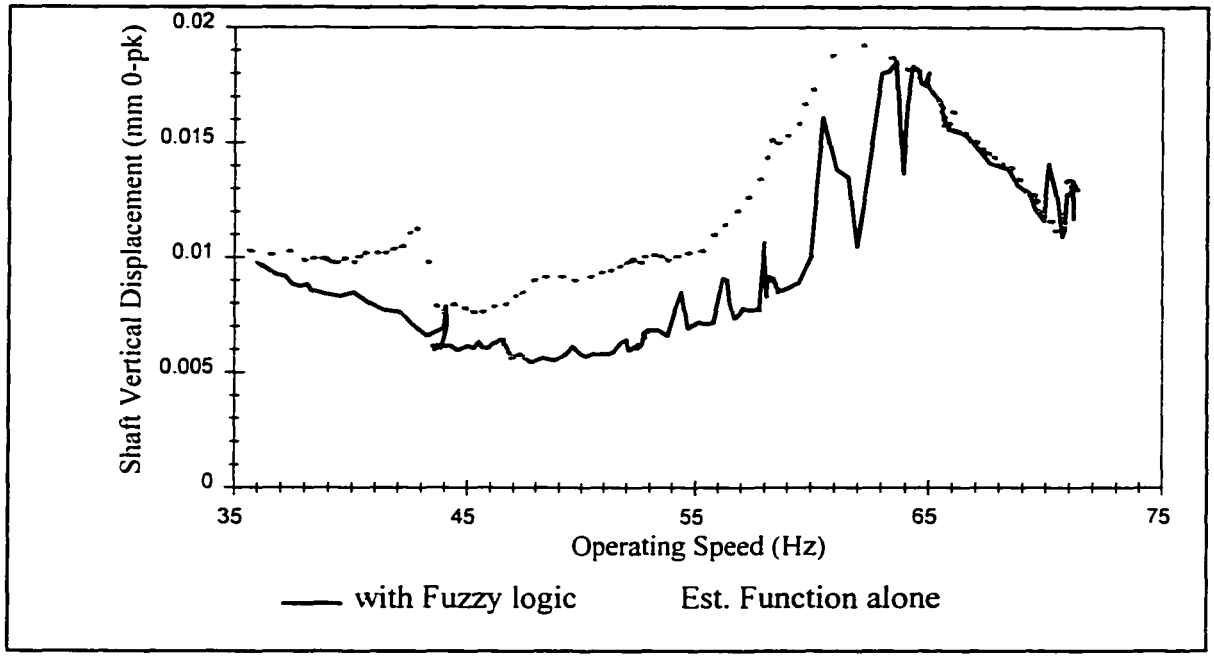


Figure 5.17: Lateral Response with Initial Estimated Function

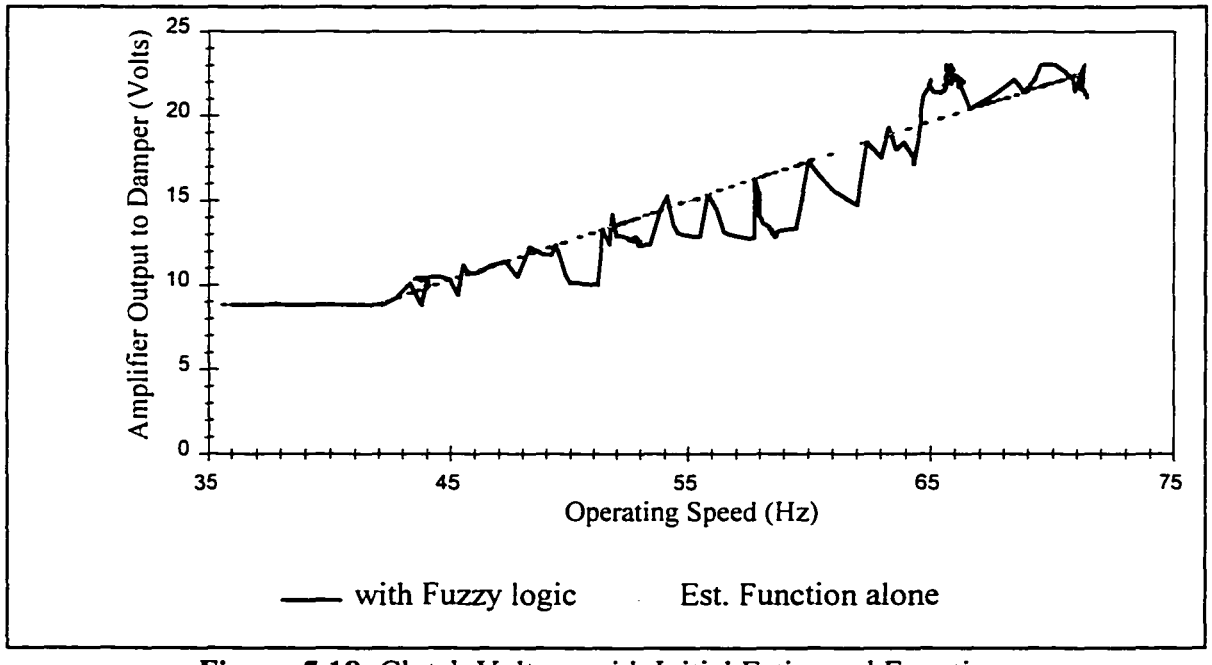


Figure 5.18: Clutch Voltage with Initial Estimated Function

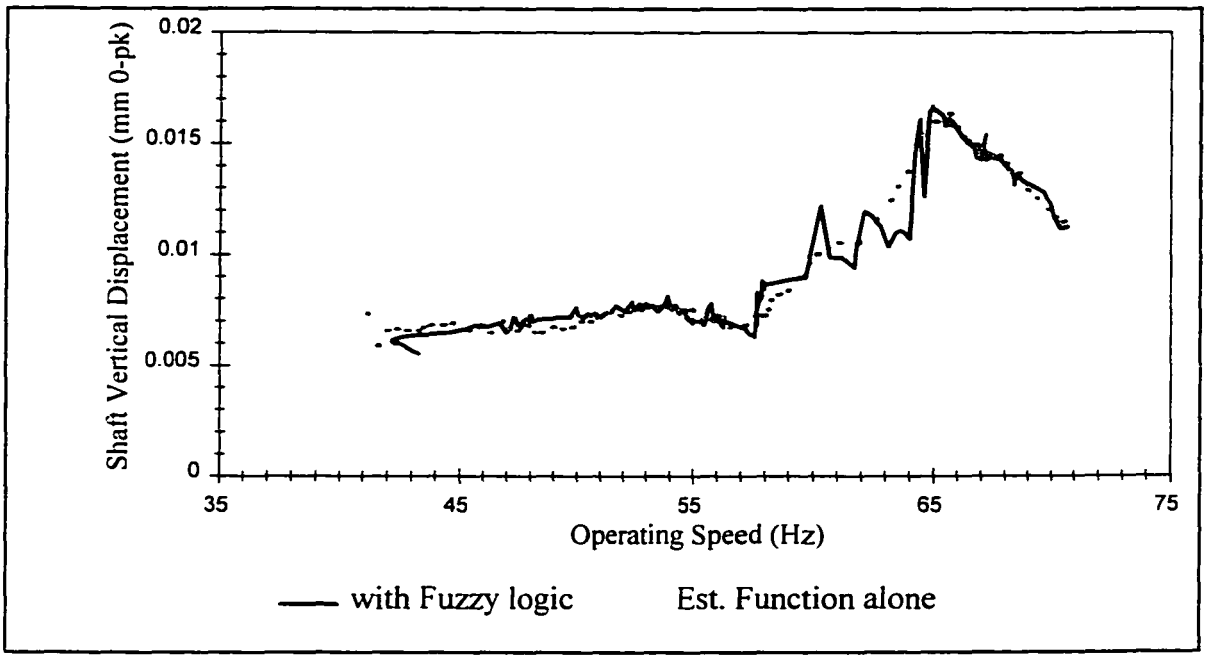


Figure 5.19: Lateral Response with Second Estimated Function

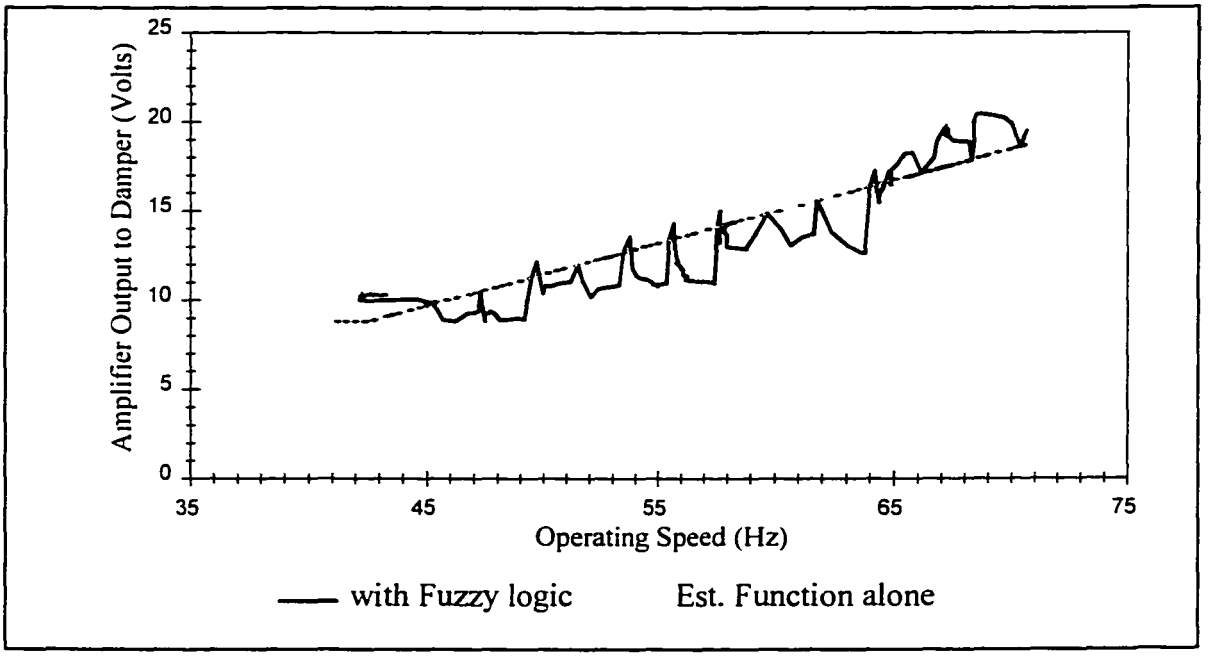


Figure 5.20: Clutch Voltage with Second Estimated Function

A third trial voltage correction function of still lower slope, based on the estimated slope and intercept points as given in table 5.4, was then incorporated in the software.

Table 5.4: Third Estimated Voltage Correction Function

Oper Speed Hz	Clutch Voltage	DAQ Voltage	Slope "A"	intercept "B"
40	8	1.6	0.04	0
80	15	3.2		

The prototype response for an initial run using the third estimated voltage correction function is shown in Fig 5.21. This shows close agreement across virtually the entire speed range, with a slight anomaly at the low speed end between 35 and 40 Hz. This likely results from changing lubrication conditions in the sleeve bearings causing some light load, low speed instability. For an industrial machine train with normal loading and constant lubrication supply, this anomaly should not occur.

In a second run with this function (Fig 5.23), the same characteristic response in the 35 to 40 Hz range is indicated. However, some improvement is noted between 44 and 54 Hz with a slightly increased output voltage (see Fig 5.24). Also, for the range 57 to 66 Hz a small increase in the shaft response (typically 0.002 mm) is noted for approximately the same level of output voltage. Some of these smaller changes may result from the varying oil film conditions in the sleeve bearings. In any case, the improvement over the free damper condition is significant not only in the area of resonance, but for the entire operating range (ref Fig 5.29). It should be noted that the looping shown in Fig 5.21 to 5.24 occurred as a result of allowing the prototype speed to dwell in the area of free mode

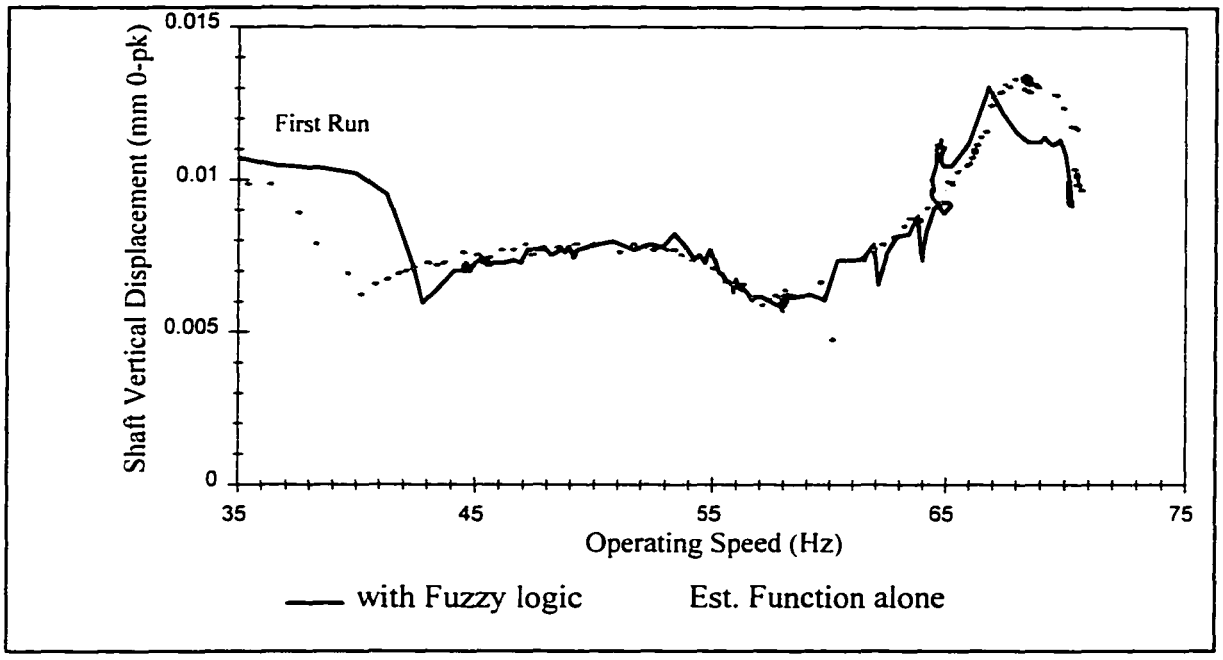


Figure 5.21: Lateral Response with Third Estimated Function (i)

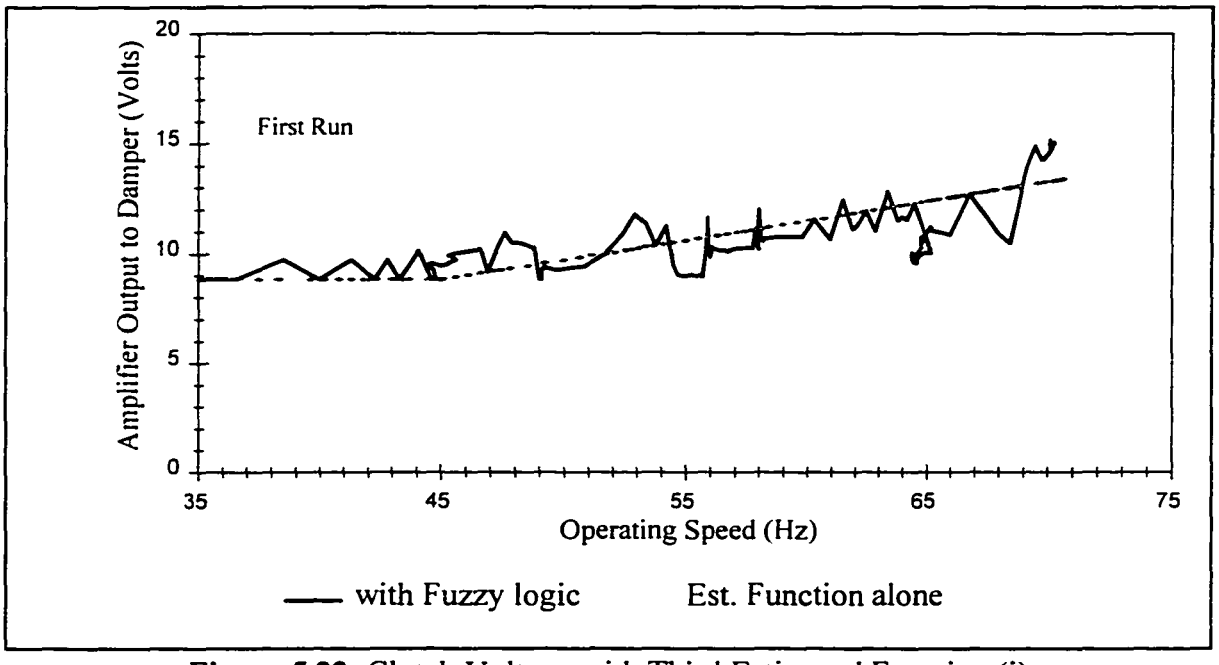


Figure 5.22: Clutch Voltage with Third Estimated Function (i)

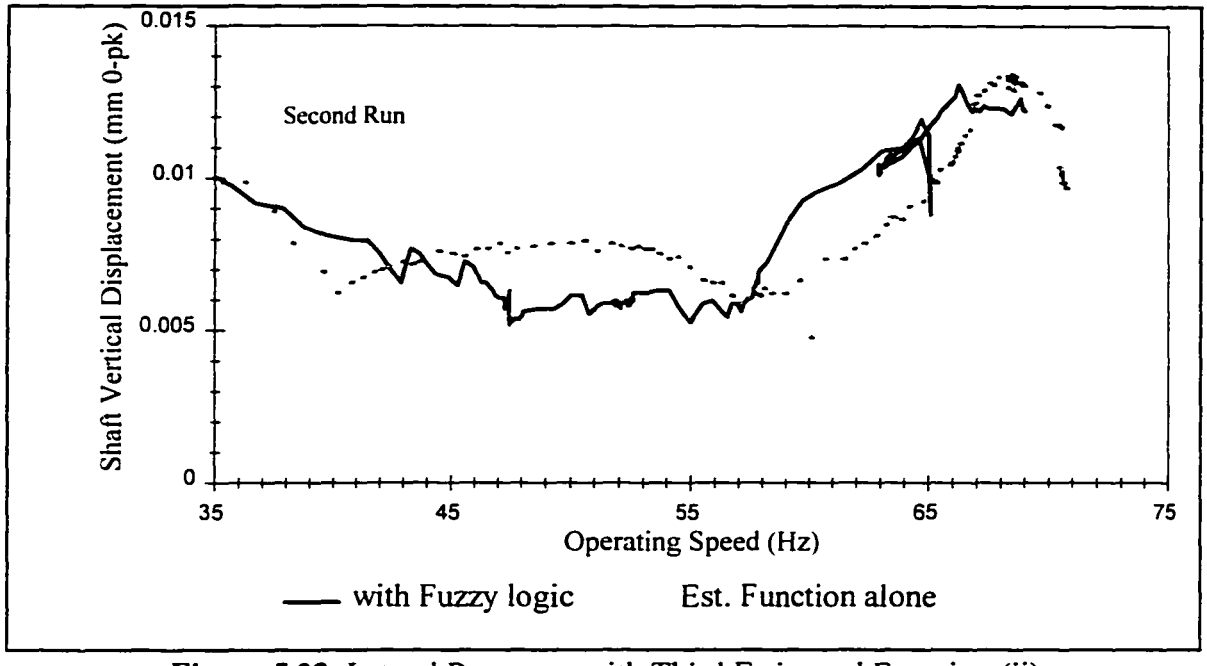


Figure 5.23: Lateral Response with Third Estimated Function (ii)

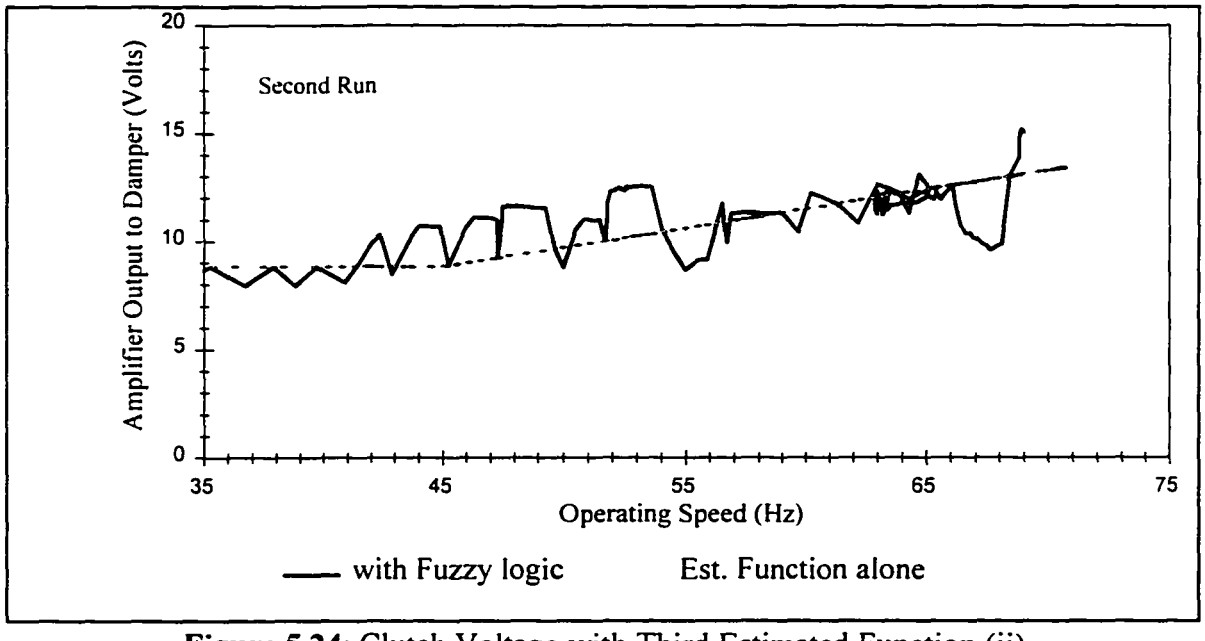


Figure 5.24: Clutch Voltage with Third Estimated Function (ii)

resonance. During this time period, the speed was allowed to fall back through the resonance zone before proceeding to the full speed of 70 Hz.

The use of a single straight line voltage correction of low slope provides some uncertainty for the approach to 70 Hz. In the speed range 63 to 66 Hz, the voltage is at a relatively high level with an increasing trend with speed. As the plant operating speed approaches 67 to 68 Hz, the better running condition is found at a lower voltage level to avoid any amplification from the second frequency (locked mode 3, Table 4.5) associated with the locked damper condition. At the upper speeds of 69 to 70 Hz either a low output voltage (free damper) or a high output voltage (damper locked) will give acceptable results (ref Fig 5.11). For both of these runs at the 70 Hz speed, the fuzzy logic favors the higher voltage (ref Fig 5.22 and 5.24) which is indicated to be the least response option (ref Fig 5.21 and 5.23). Examination of output voltage patterns for both final runs in Fig 5.22 and 5.24, shows a distinct pattern of voltage reduction through 67 to 68 Hz with subsequent voltage rise from 69 to 70 Hz.

The third estimated voltage correction function appears to come fairly close to the optimum function which allows the fuzzy inferencing software to work effectively across the complete speed range to find a practical estimate of the true function as it operates.

Level 2. Pre-Minimization

As the estimated function introduced in Level 1 is only approximate, the pre-minimization routine was developed to establish a more positive approach to the local minimum on a wider scale compared with the fuzzy inferencing procedure as described in Level 3, following. At each intermediate operating speed between 35 Hz and 70 Hz, there exists an optimum damping value which will result in a shaft displacement minimum. Because of the approximation of the initial function, the possibility exists for

the approach to minimum shaft displacement to be from a higher or lower than optimum value of damping as provided by the clutch. This pre-minimize routine initially outputs a significant fixed voltage change of 0.2 volts and examines the response to determine whether an improvement has been effected. Fig 5.25 illustrates the several scenarios associated with this three iteration procedure.

The vibration level entering this procedure is noted as V_0 and the subsequent vibration level after one iteration through the procedure as V_1, etc. Then, if the shaft vibration has been reduced (i.e. $V_1 < V_0$) (Fig 5.25a & b), the output is repeated and examined again. If the second step results in an improvement (i.e. $V_2 < V_1$) (Fig 5.25a), a third step is made with an output value adjusted by a slope ratio from the first and second steps. The slope ratio (SR) is defined as follows:

$$SR = (s_1 \pm s_2) / s_1 \quad \ldots\ldots (5.1)$$

where $s_1 = V_1 - V_0$ ..... (5.2)

$s_2 = V_2 - V_1$ ..... (5.3)

A third step voltage output value is then defined as

$$\text{Output (volts)} = 0.10 * SR \quad \ldots\ldots (5.4)$$

If $V_2 > V_1$ (Fig 5.25b) the slope adjusted output value is multiplied by N = -1.

If no improvement resulted from the first step (i.e. $V_1 > V_0$) (Fig 5.25c, d & e), the second step output is doubled to 0.4 volts and multiplied by N = -1. This double step can result in three possible outcomes. In the first case illustrated in Fig 5.25c, the second step vibration level exceeds the first step vibration level (i.e. $V_2 > V_1$), and an adjusted output voltage signal of (0.2 + 0.1*SR) volts is sent to the amplifier with the multiplier N = 1. For the cases 'c', 'd', and 'e' from Fig 5.25, s_2 is now defined as

$$s_2 = (V_2 - V_0) \quad \ldots\ldots\ldots\ldots\ldots\ldots\ldots\ldots\ldots\ldots\ldots\ldots\ldots\ldots\ldots\ldots \quad (5.5)$$

For the next case (Fig 5.25d), the vibration level for the second step, V_2, falls between the initial vibration level, V_0, and the first step level, V_1, (i.e. $V_0 < V_2 < V_1$). For this situation, a slope adjusted output signal of (0.1* SR) volts is made and the multiplier N is maintained at +1. In the third situation (Fig 5.25e), the second step vibration level falls below the initial level (i.e. $V_2 < V_0$). In this case, the output signal is (0.1*SR) volts with N = -1. In any case, after three steps in this routine, the control is passed to the fuzzy inferencing procedure for local minimization of the shaft vibration.

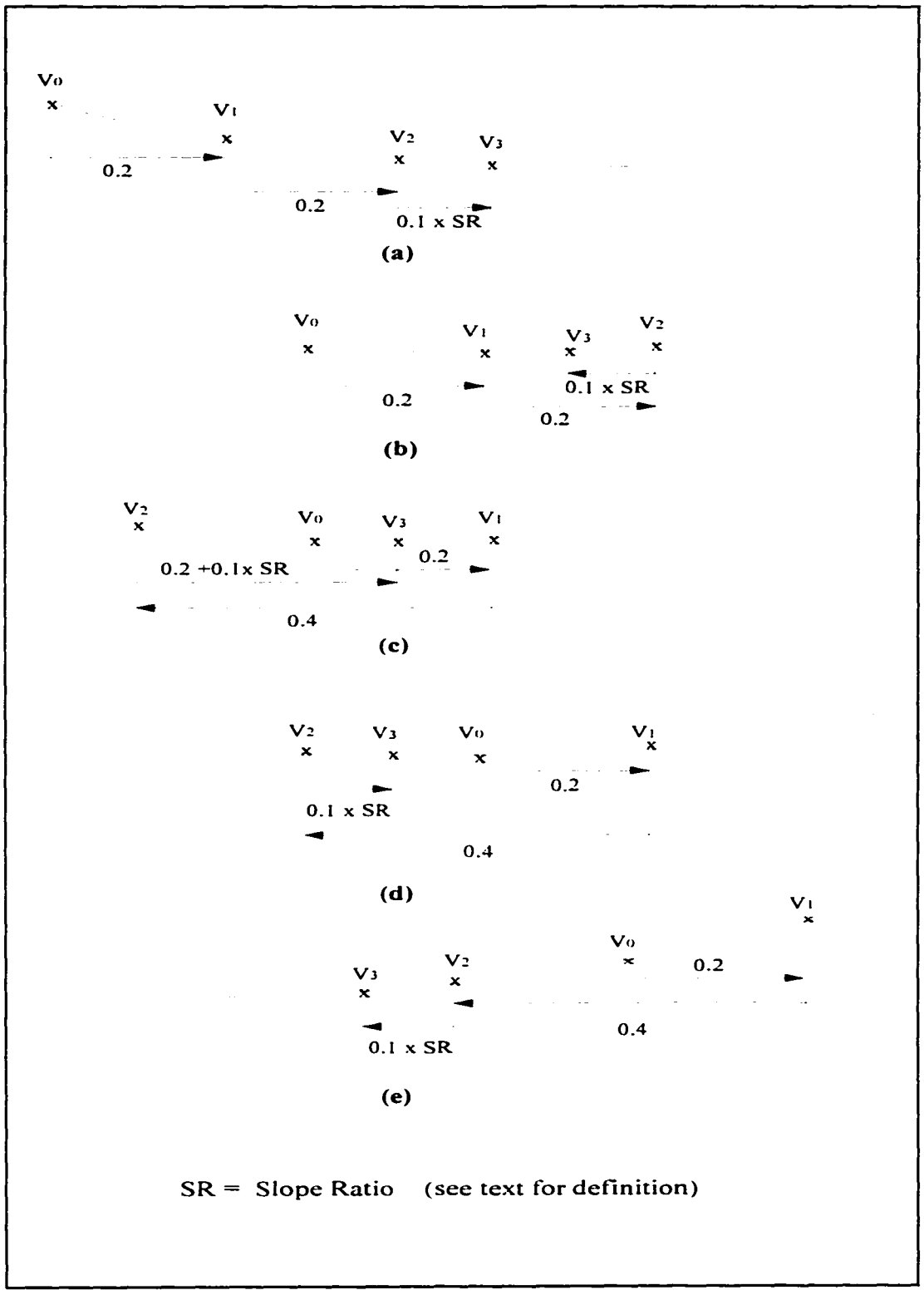


Figure 5.25: Pre-Minimize Procedure

Level 3. Minimization Through Fuzzy Inferencing

This portion of the control algorithm contains the fuzzy logic and inferencing procedure. The crisp input values of shaft displacement level, and change of shaft displacement level (velocity), are fuzzified into appropriate membership functions with the associated membership values. This is based on the defined input membership functions on each respective universe of discourse as presented in Fig 5.10. The inferencing procedure utilizes the fuzzy associated matrix or rules database, as given in Table 8, to determine the appropriate output membership functions and membership values for each combination of input values in the matrix. For the membership functions used herein, the four possible combinations of the two input functions results in four output membership functions with associated memberships. These are combined in a centroidal method of defuzzification to determine the appropriate crisp output correction voltage.

It should be noted that for this control, which is semi-active, an effective method of obtaining action in two directions can be achieved by simply reversing the FAM (i.e. multiplying by N = -1). Whenever the vibration trend from the moving average calculation and the change of vibration level falls into the positive / positive range of the input universes of discourse, the minimum output region has been passed. Multiplying the FAM by N = -1 reverses the direction of the corrective output signal effectively providing a control which is able to approach the minimum vibration response operation region from both directions.

Table 5.5: Fuzzy Associative Matrix (FAM)

Rules Database

The following fuzzy associative or rule based matrix was developed from a basic knowledge of the general effect of a torsional vibration damper / absorber as the only requirement. The format is that of a basic state variable control applied to the displacement parameter representing the pinion shaft vertical vibration.

		Vib			
		ZE	PS	PM	PL
ΔVib	NL	PS	PM	PL	PL
	NM	PS	PM	PL	PL
	NS	ZE	PS	PM	PL
	ZE	ZE	NS	NM	NL
	PS	ZE	NS	NM	NL
	PM	NS	NS	NM	NL
	PL	NS	NM	NL	NL

A flow diagram for the fuzzy control program developed for this work is given in Fig 5.26. The program "FuzzyControl" is listed in Appendix III. The membership function partitions on the universe of discourse can be input manually or the information may be read directly from a file. A data input program "Fuzzy.mod" for definition of the membership functions on the universe of discourse is also listed in the appendix.

The fuzzy logic routine estimates the output voltage values for each speed setting providing the machine train response to the active damper / absorber device is relatively smooth and the output voltage corrections are not excessive (which may cause instability) but large enough to overcome local minima. If the output corrections are too large, an unstable response may result as indicated in Fig 5.27. In this case, the speed of the prototype was increased to just beyond 59 Hz, held constant, and then allowed to fall back somewhat to around 58.6 Hz. Further voltage increases then occurred, up to 19-20 volts, ostensibly causing a back and forth action across a minimum which resulted in the corresponding and unresolved increase in the prototype response. As a comparison, referring to Fig 5.21 for the same type operational mode (dwell and fall back in speed) at around 64 - 65 Hz, a slight increase in the rotor response was resolved adequately by the fuzzy logic with suitably sized output corrections.

On the other hand, if the output corrections are too small, the fuzzy inferencing process may not be capable of negotiating local minima in the plant response curve. Fig 5.28 shows a virtually constant output voltage against a continuously rising response characteristic, indicating an inadequate control function. Also for a control with inadequate output corrections and with prototype operational speed changes of less than 2 Hz, the inferencing process may still allow the vibration level to rise while searching for the local minimum. Optimum selection of the appropriate membership function support sizing (ref Fig 3.3) along the universe of discourse is significant, since too small a correction may get hung up while too large a correction may lead to instability.

This solution was developed for the prototype in a trial and error fashion. Incorporation of "learning" in the software could provide for optimization of support size during operation.

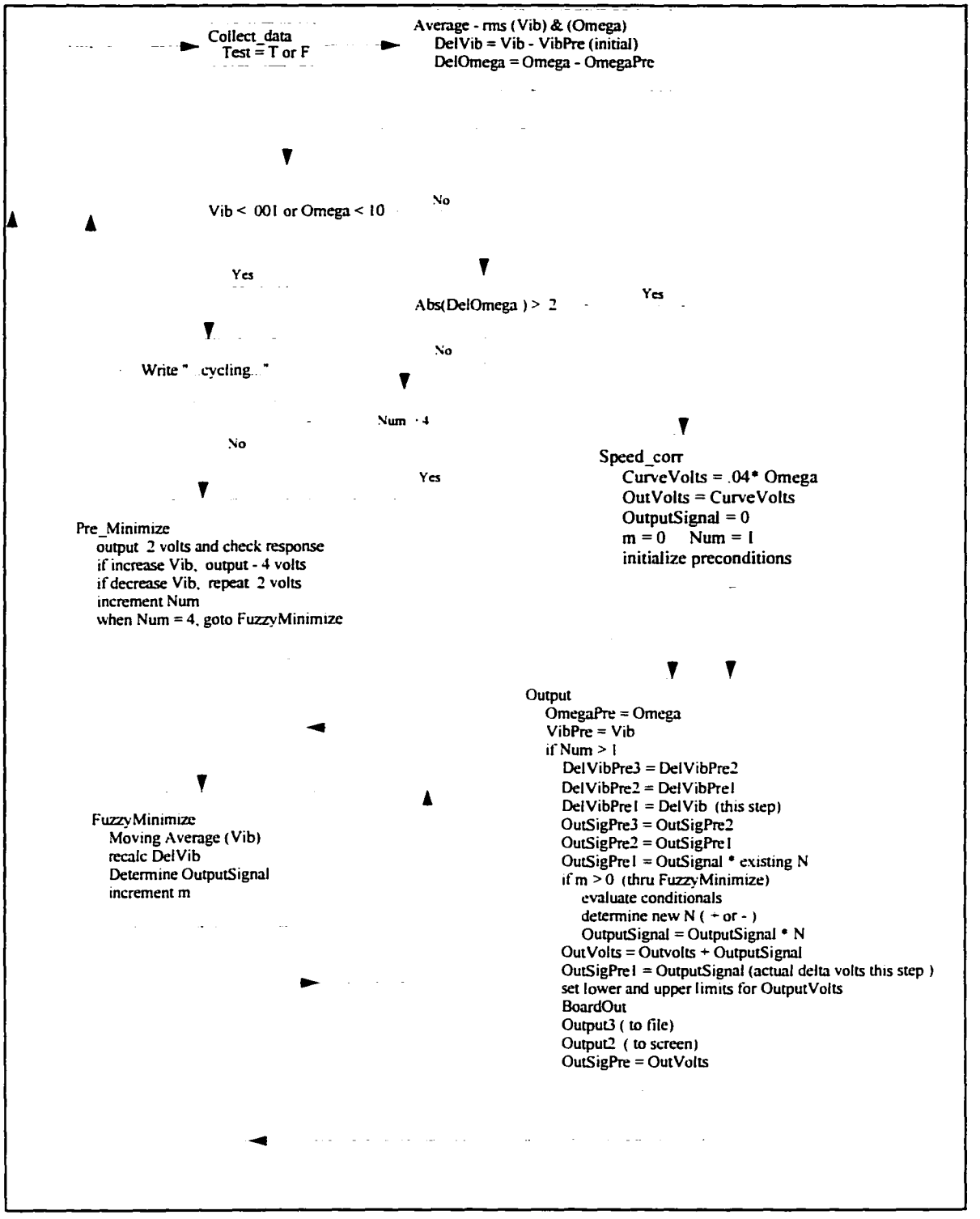


Figure 5.26: Fuzzy Control Flow Diagram

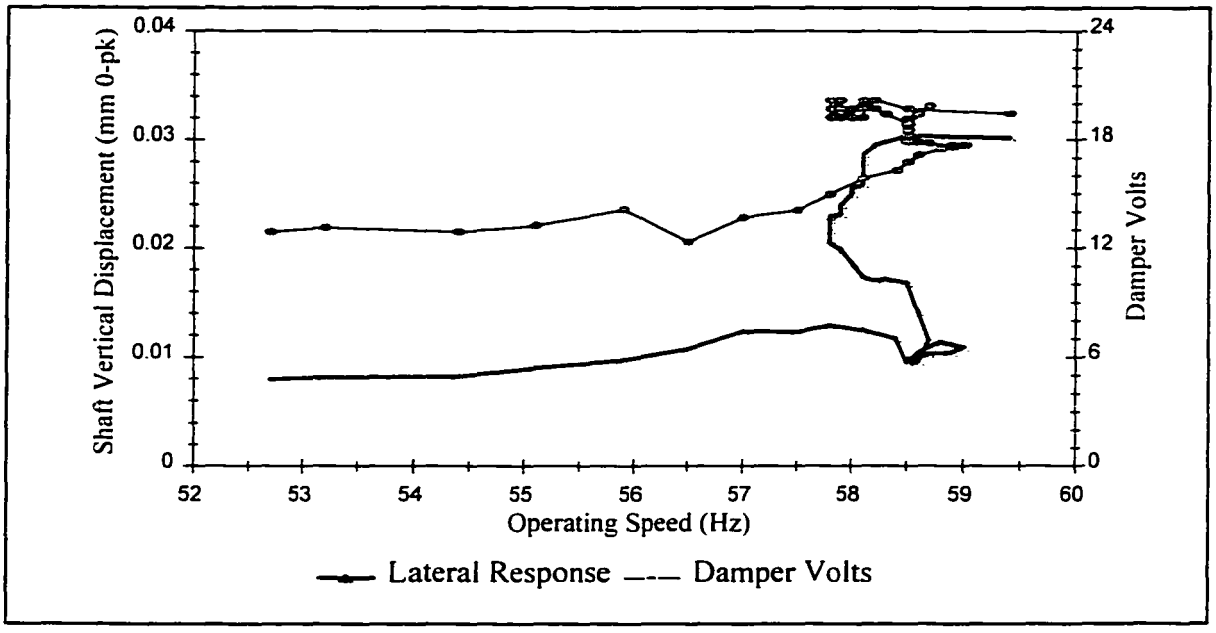


Figure 5.27: Instability From Over-Correction

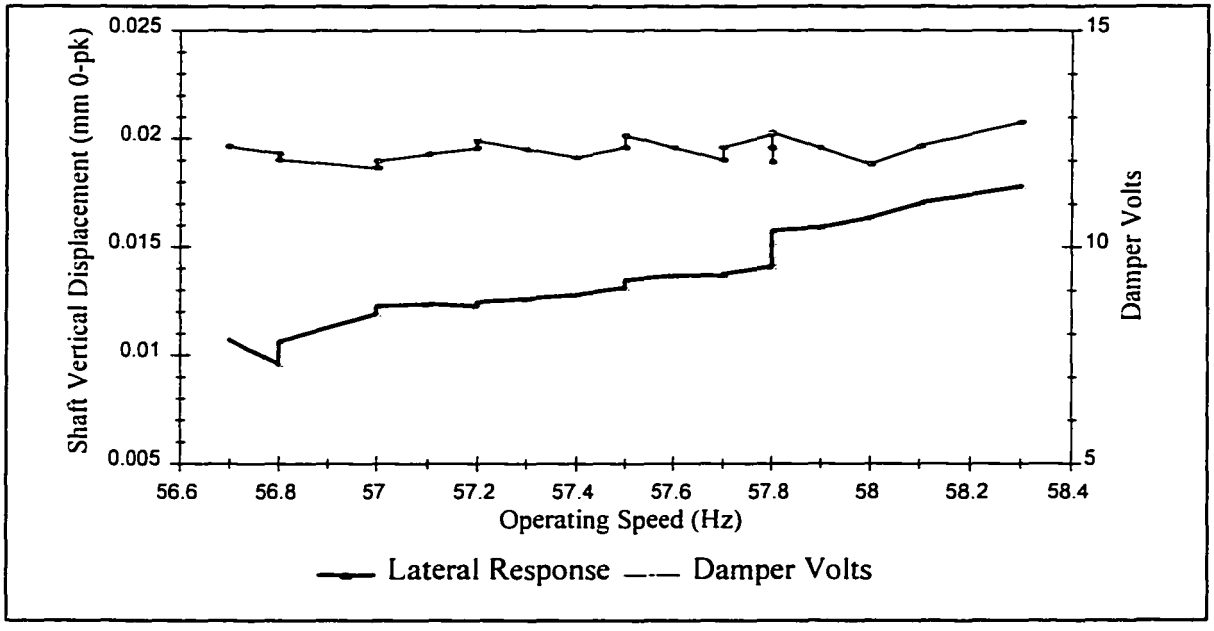


Figure 5.28: Ineffective Under-Correction

5.3 Final Result

With the three level controller, as developed for the prototype in the previous section, incorporated in the control software an optimum damping effect plus mass addition influence is automatically incorporated for the plant operation. For operation at fixed speed (i.e. speed variations < 2 Hz) the fuzzy logic inferencing function determines the output voltage to the clutch to maintain a minimum vibration response. For speed changes in excess of 2 Hz the control recycles to the speed correction function and through the pre-minimize search procedure prior to settling in the fuzzy logic procedure once again.

The measured effect is to attenuate the coupled lateral vibration as monitored at the pinion shaft. Pinion shaft response curves with the controller operational are re-plotted in Fig 5.29 against the original response measured for the free and fully locked clutch modes (ref Fig 5.11). For both runs using the developed controller, the response across the speed range has been significantly reduced by the damper / absorber influence. It will be noted, however, that some minor differences exist between the two controlled runs. These differences are attributed to nonlinearity of the clutch operation with respect to the dry friction plates, as well as changing lubrication conditions through the run as previously stated. This is a trial and error development and no attempt has been made to optimize the fuzzy logic, which may also contribute to minor differences in the response characteristic.

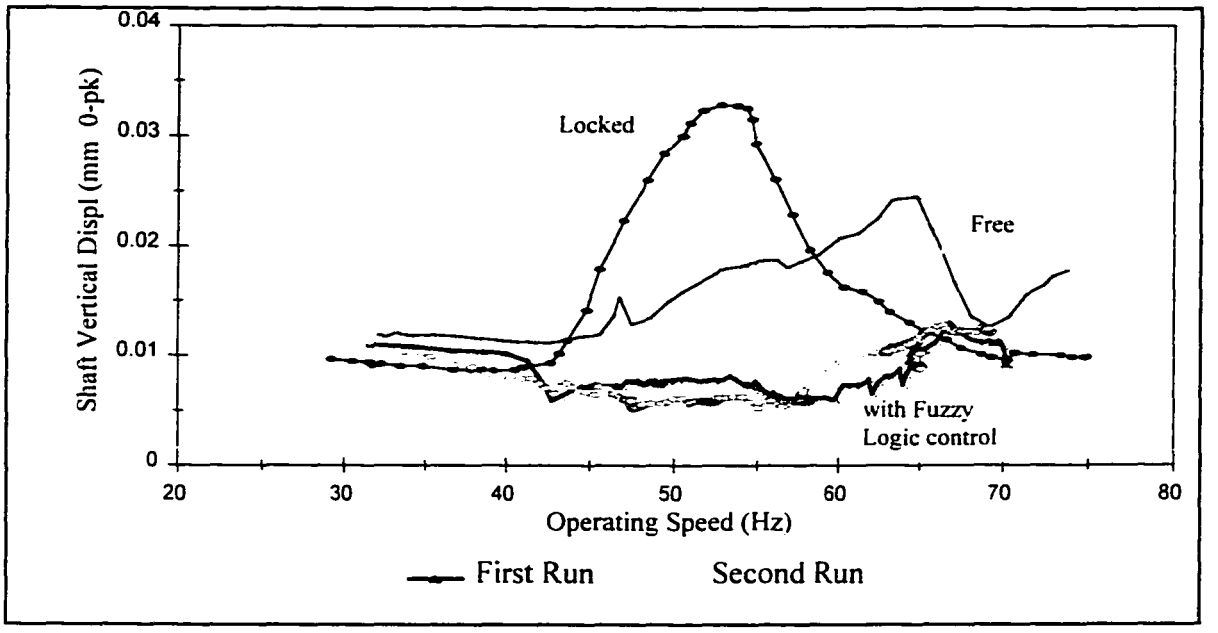


Figure 5.29: Lateral Response with Active Fuzzy Control

Chapter 6

Discussion of Results

6.1 Prototype

The prototype was constructed to provide a realistic example of the torsional lateral coupling experienced in real machine trains having offset gears (ref Fig. 4.2). Tables 4.2, 4.3 and 4.4 give the associated physical properties of the prototype machine train. The natural frequencies of the system are presented in Table 4.5.

The lateral motion of the prototype is in the form of pinion shaft bending. In a real machine, the more likely cause would be due to bearing housing flexibility resulting from its construction and integration into the casing of the gearbox. Most gearbox shafting is constructed with significant stiffness against bending.

The control methodology is based in fuzzy set theory. The rules database is developed from an attempt to model how an experienced human operator would effect the control if he were able to modify the damping force while observing the system response. The control matrix is based on a set of basic common sense rules seeking to minimize the system response by incrementally adjusting the damping torque.

The implemented control actuator device for the prototype is constructed using a coulomb friction type adjustable magnetic clutch. Even though the effect of this device is nonlinear as may be readily noted from the constant clutch voltage curves shown in Fig 5.12 to 5.16, the fuzzy logic methodology can work around this difficulty. Nonlinearities will be present in the clutch damper because of the nature of dry surface sliding friction, the effects of increased temperature with usage, and also any contaminants which may be introduced to the sliding surfaces as they are exposed to the lab atmosphere.

The preferred device at the onset of the experimental stage was a non-contact magnetic coupling which would provide the damping torque between the main prototype and the additional inertia strictly by magnetic field effects. The operation of such a coupling design is expected to make a closer approach to linearity and be more repeatable than the device used in the prototype. Nevertheless, nonlinearities from hysteresis effects would still have to be taken into consideration. The cost of a magnetic coupling, however, was prohibitive and a more economical prototype device was selected for the experimental work. Two positive effects resulted from this selection. Firstly, the principle of reducing the lateral vibration using a variable torsional damper / absorber is successfully illustrated using the selected device and the general concept is a feasible solution for industry. Secondly, the fuzzy logic paradigm for control works well with the selected actuator even with the inherent nonlinearities associated with a Coulomb friction design.

The magnetic clamping force in the prototype damper device is varied in an attempt to seek a minimum response of the pinion shaft vibration across the full speed range of the plant. The control is nonlinear as the changing damping factor results in two interacting effects:

i) nonlinear damping of the unwanted torsional vibrations

ii) modification of the mass elastic properties of the prototype.

The second effect is demonstrably evident in the shift of the peak response when operating with the added inertia disk in the free state compared with the disk fully locked-up (ref Fig 5.11). A third effect, of increased torsional stability, can have a significant influence when the machine train is operated with automatic speed control. This is discussed in further detail in Chapter 7, Conclusions and Recommendations, following.

The frequency spectrum of the prototype drive motor torque contains strong 60 Hz and 120 Hz components. This provides many excitation frequencies associated with the changing speed due to the well known phenomenon of sum and difference frequencies. This phenomenon virtually ensures that the response of the system at any speed cannot be regarded as, or simplified to, the response of a SDOF system. The response of the system will be the summation of the individual responses of the various active driving frequencies which are generated through the interaction of the particular operating frequency and the above noted fixed frequencies [40]. These exciting frequencies may originate directly with running speed or its harmonics and in combination with other frequency drivers inherent in the plant system. As the driving frequencies change with speed, the mode summation will have changing components due to changing modal participation in the response. This means that the effective modal mass will change with speed. Therefore the optimum damping coefficient will also change with speed.

Vibration difficulties occur when, as a result of varying speed, the characteristic exciting frequencies associated with the driven plant coincide with the structural natural frequencies based on the inherent plant dynamic properties of mass and stiffness. The interference diagram, illustrated in Fig 6.1 for the free damper condition, shows the crossing of the 1x operating frequency with the first natural frequency of 64.5 Hz (mode 2 Table 4.5). A similar diagram is presented in Fig 6.2 for the locked damper condition. These two figures illustrate the frequency shift caused by the increased mass effect, with the 1x crossing in Fig 6.2 now occurring at 53.8 Hz. It is also evident for the locked

damper condition, that a second natural frequency exists in the operating range at 67.9 Hz, which is successfully negotiated by the control system (ref Fig 5.29).

For the locked damper condition, the measured prototype peak response occurs at an approximate lower frequency of 53 Hz. This also occurs with greater amplitude compared with the free damper response at 64.5 Hz (ref Fig 5.11). This is attributed to new excitation frequencies resulting from the well known phenomenon of sum and difference frequencies [40] which describes the interaction of fixed and varying excitation frequencies. The strong 60 Hz component in the torque output of the drive motor combines with the operating frequency to form new excitation frequencies. This phenomenon creates exciting frequencies at several locations throughout the operating range. In the case of operation at the 53 Hz resonance point, a combination occurs according to the following formula [40]

$$F_{ex} = F_a \pm 2*(F_a - F_b) \quad \ldots\ldots\ldots\ldots\ldots\ldots\ldots\ldots \quad (6.1)$$

where: F_a is the varying frequency = 53 Hz

F_b is the fixed frequency = 60 Hz

F_{ex} is the combined exciting frequency

to give a resulting 67 Hz exciting frequency (using the negative sign). Fig 6.3 illustrates some of the spray of exciting frequencies associated with the interacting sum and difference combinations effective in the prototype plant. A similar spray of exciting frequencies is in effect at each harmonic level. The plant response at the modified lower frequency is then a combination of the first and second modes being excited simultaneously. Specifically, with reference to Fig 6.3, it can be observed that operation of the prototype at 53 Hz provides an excitation of the fundamental at 53.8 Hz, by the 1/rev drive frequency, as well as the excitation of the second mode at 67.9 Hz, by the combined exciting frequency of 67 Hz as calculated above.

In the initial stages of the work, an alternative control concept of implementing a direct counter torque against the torsional motion in place of the controllable damper was considered. This would require a torque actuator with a response time (t < 10 msec) faster than is currently available commercially, and was therefore abandoned. Furthermore, if such a device were available it would require significantly more power than the control system developed herein.

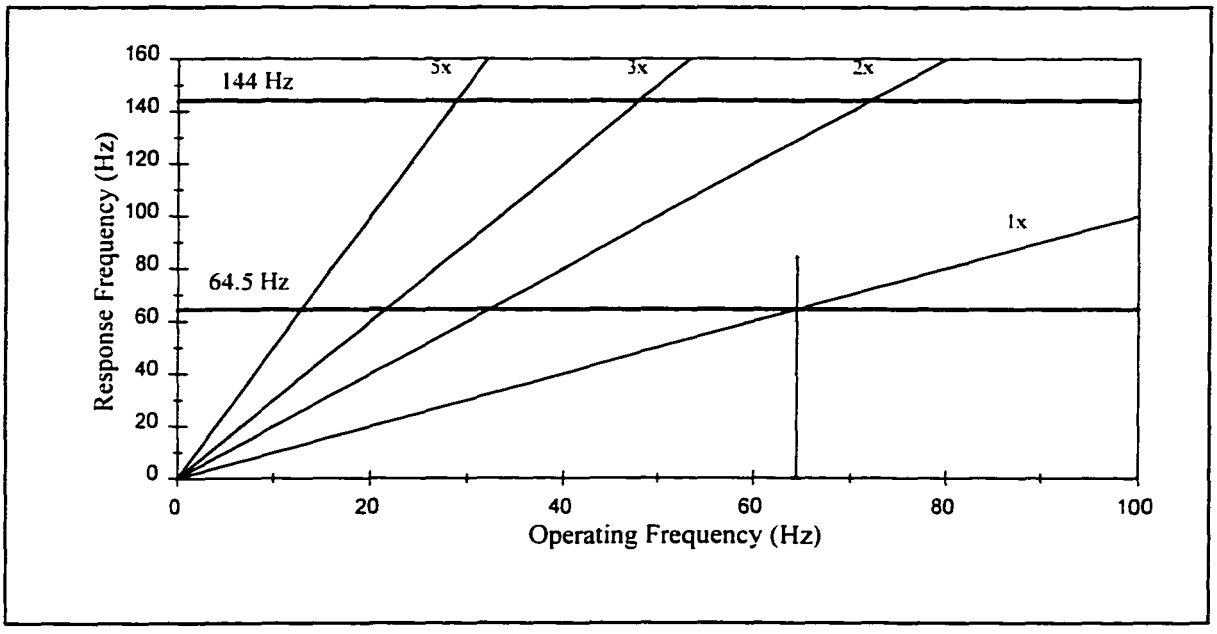


Figure 6.1: Interference Diagram for Free Damper

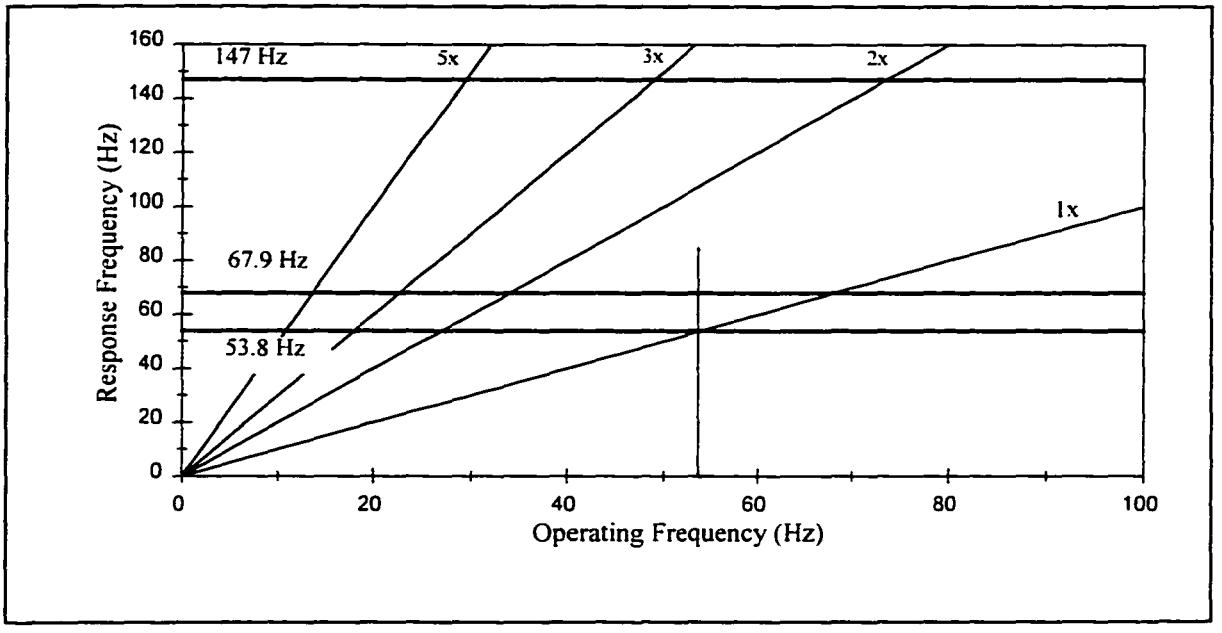


Figure 6.2: Interference Diagram Locked Damper

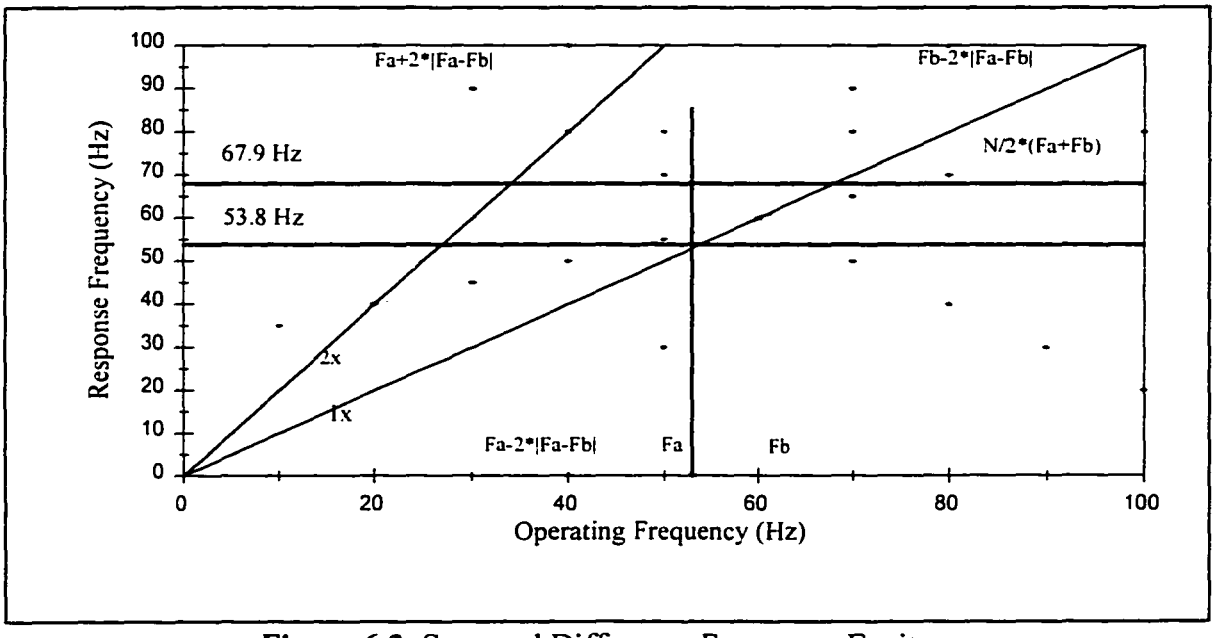


Figure 6.3: Sum and Difference Frequency Exciters

6.2 Computer Simulation

The rotor prototype utilized for this exercise is illustrated in Fig 4.2. The torsional lateral mode shapes identified by finite element analysis (Cosmos/M program) are presented in Appendix IV. These are confirmed with results from Matlab; Table 4.5 gives the comparison of natural frequencies from these two approaches.

The mode shape plots and tabulated data in Appendix IV describe the first two significant modes (modes 2 and 3, Table 4.5) of the rotor in the free damper condition as well as the first three significant modes (modes 2, 3 and 4) for the rotor in the locked damper condition. This mode shape information indicates clearly (see Appendix IV) the interaction between the torsional and lateral regimes across the operation speed range of a typical offset geared machine train arrangement.

To provide some dimension to the severity of the applicable motions, a set of computer simulations were performed using the prototype mathematical model with the Matlab / Simulink program. The various rotor states from a free damper to a fully locked-up damper were investigated. At clutch / damper voltages of less than 8 volts, the additive mass is considered to be free spinning (i.e. no added mass). At voltages greater than 24 volts the additive mass is approaching lock-up with no further significant improvement in vibration level evidenced from further increases (ref Fig 5.15). For each intermediate voltage between 8 and 24 volts, there will be a portion of the additive inertia which can be considered as attached to the rotor, with the remainder of the inertia considered as slipping. The amount of "attached" inertia will be related directly to the acceleration level of the damper inertia disk at the point of slip initiation. As the voltage is increased so is the clutch clamping force and, consequently, the acceleration level at the point of slip initiation, resulting in an increased effective inertia addition. The torque level in the connecting shaft will be a function of the acceleration of the "attached" inertia and the

damping associated with the slipping inertia (refer to the bondgraph diagram in Fig 4.3). For intermediate voltage levels (8 - 24v), the simulation assumes a linear distribution of the fixed and slipping inertia in accordance with the following relationships (ref Fig 4.3):

I_{13} = fixed clutch rotor Inertia + (SIR) x damper disk Inertia ..... (6.2)

I_{15} = damper disk Inertia (1 - SIR) ..... (6.3)

where: SIR = slip inertia ratio

I_{13} = Inertia assumed attached to the main rotor

I_{15} = slipping Inertia

To determine appropriate values of damping for both free and locked conditions, a slip resistance was inserted in the bondgraph in parallel with I_{13} . A full inertia value of 0.00065 kg m^2 (see Table 4.4) was used for I_{13}. For these computer runs the value of I_{15} was set to zero with R_{25} set to a large value (20,000 Nm-sec/rad). Through a number of trial simulations, a damping value (slip resistance) of 2000 Nm-sec/rad was determined as representing the high output voltage level of 24 volts (i.e. locked condition response) while a minimum slip resistance of 0.0003 Nm-sec/rad was determined to adequately represent the 8 volt level (i.e. free condition response). These approximate relationships were used in computer simulations across the voltage range from 8 to 24 volts. The damping values applicable at intermediate voltages were estimated using a cubic spline interpolation for an assumed exponential damping distribution of the 16 integer voltage steps between 8 and 24 volts. This distribution is presented in Table 6.1. together with the estimated linear distribution of slip inertia ratio (SIR) with voltage.

Fig 6.4 presents the results of simulation runs at an operating frequency of 64.5 Hz. The measured shaft excursion of the prototype was used as a guide for determining the strength of the 1x forcing function used in the simulations. This forcing function would

typically result from dynamic unbalance of the rotating elements. The maximum shaft twist experienced by the load shaft in the free damper condition was determined to be 0.04 radians, 0-pk (ref Fig 6.4). This translates to a shaft stress of 34 MPa (4950 psi). The vibratory stress would be additive to any steady load stress which may be active in the normal operation of the machine.

Table 6.1: Damping and Inertia Distribution with Voltage

Voltage	Damping, R_{25} (Nm-sec/rad)	Slip Inertia Ratio (SIR)
8	0.0003	0.001
9	0.0008	0.063
10	0.0021	0.125
11	0.0057	0.188
12	0.0152	0.25
13	0.0407	0.313
14	0.1087	0.375
15	0.2902	0.438
16	0.775	0.500
17	2.07	0.563
18	5.52	0.623
19	14.8	0.688
20	39.3	0.750
21	105	0.813
22	281	0.876
23	750	0.938
24	2000	0.999

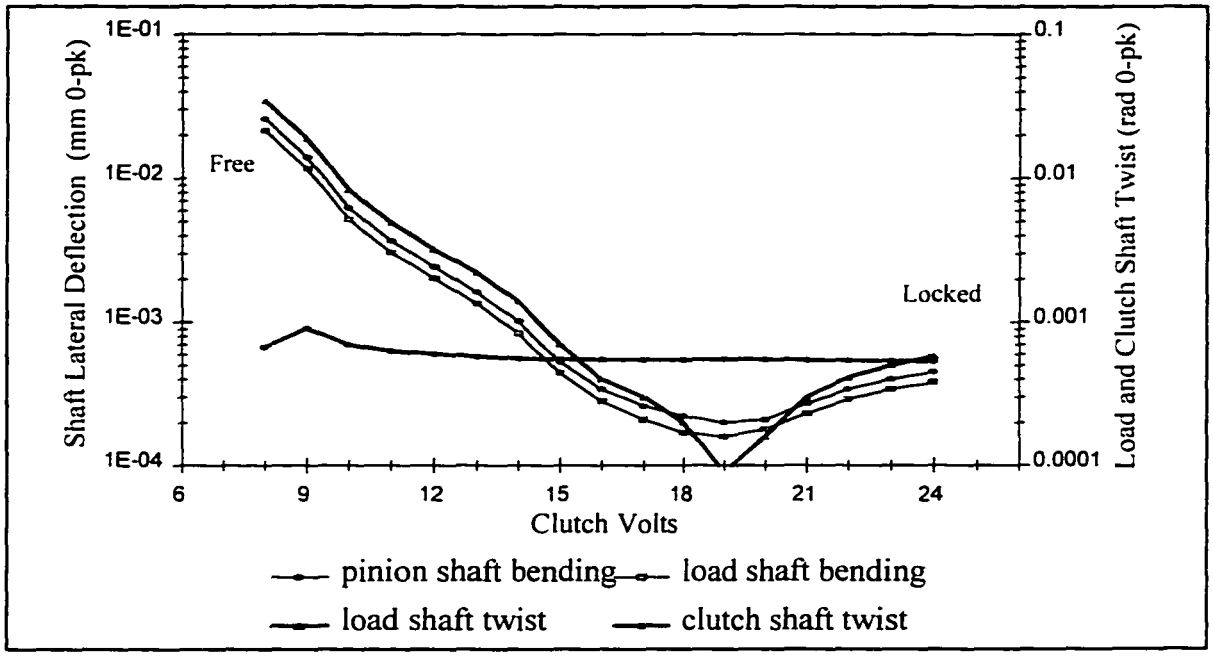


Figure 6.4: Rotor Response Simulation (64.5 Hz)

For a typical shaft material of 4140 steel, with ultimate stress of 620 MPa (90.000 psi), the military standard Mil-167 suggests a maximum nominal torsional stress of $S_{ult}/25$, or 24.8 MPa (3600 psi). The recommended allowable vibratory stress is ¼ of this value or 6.2 MPa (900 psi) pk-pk. Continuous operation at the vibratory stress level indicated above would certainly result in premature failure of the machine in torsion.

The radial displacement of the pinion shaft at resonance, with a free damper condition, from Fig 6.4 is 30 μm. At 64.5 Hz this represents a velocity of 12 mm/s which based on the 'fuzzy' IRD General Machinery Vibration Severity Chart corresponds to the linguistic descriptor of "Rough". Operation at this speed with the indicated response levels would obviously require some modification to ensure longevity of the machine.

At the other end of the spectrum for the nearly locked damper, the computer simulations indicate that the load shaft twist as well as the pinion shaft excursion has been reduced by

a factor of 65 (ref Fig 6.4). It will be observed also that the fully locked damper does not represent the minimum response state. Indeed, operation at some intermediate level of damping gives improved performance. From the prototype experimental runs, the measured improvement factor on the shaft vibration is between 2 and 3 because of other running influences (misalignment, bearing motion, shaft runout, etc.) which mask the torsional and bending information by establishing a significant signal noise floor level. However, the actual improvement factor in the torsional and bending motions alone will be considerably higher, more in line with the computer simulation numbers.

A similar pattern is evident for simulations at an operating frequency corresponding to the locked damper resonant frequency of 53 Hz as presented in Fig 6.5. To allow the computer simulated response to match the previously noted increased amplitude for this resonant condition, a second forcing function at the 67.9 Hz frequency was introduced with adequate excitation amplitude to produce a similar increased response as exhibited by the prototype plant. The maximum simulated clutch shaft twist, from Fig 6.5, is indicated as 0.1 radians 0-pk. This corresponds to a shaft stress of 150 MPa (21,750 psi). As the damper inertia is released toward the free condition, the shaft twist is reduced by a significant factor due to the move away from resonance. Comparing the free condition response to the locked response, the pinion and gear shaft excursions are reduced by a factor of 23. In this case as well, the peak improvement occurs at some intermediate level of damping and not with either of the extremes. Some appreciable amount of torsional damping improves the vibration response of the rotor.

In addition a composite simulation including the developed fuzzy control with the prototype mathematical model was performed in Matlab. This was done to investigate the general torsional response and ensure the successful negotiation of the identified resonance zones without adverse effects. The main area of concern is the rotor shaft torsional response, in the general case, since the control is based specifically on the lateral response without specific measurement of torsional excursions. In particular, this

investigation addresses mode 3 (67.9 Hz Table 4.5) for the locked damper, which is essentially a torsional mode with small lateral participation.

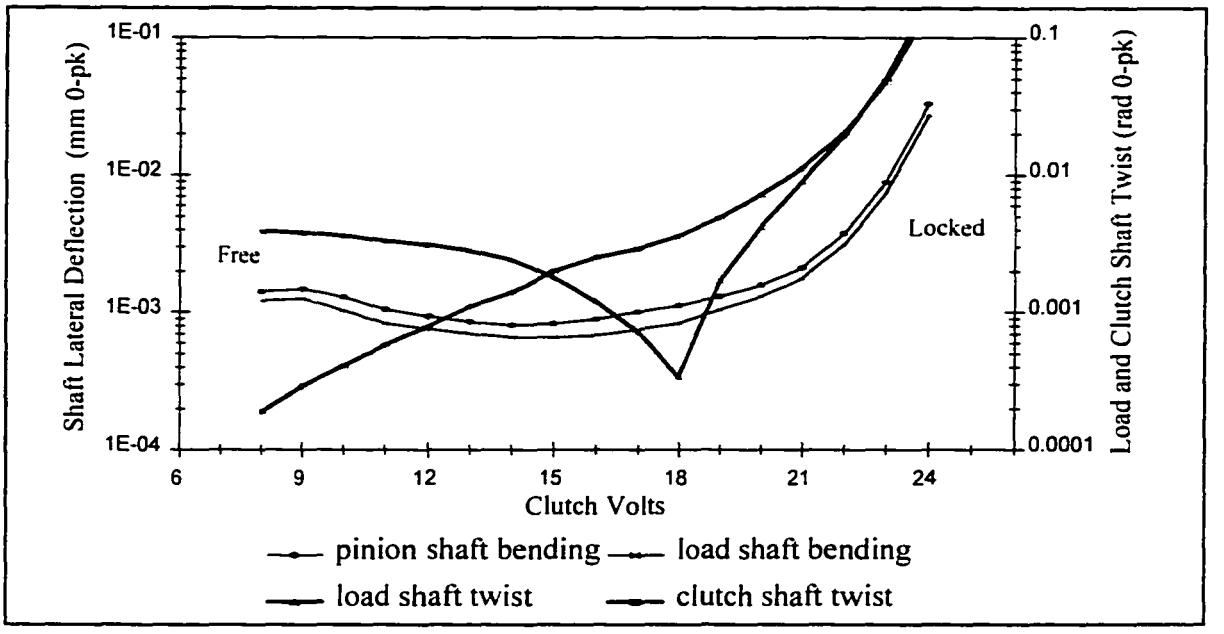


Figure 6.5: Rotor Response Simulation (53.8 Hz)

The development of the full simulation was conducted in a somewhat piecewise fashion. Control updates to the plant are executed at approximately once per second, and each update reconstructs the system [A] matrix. The flow of the simulation is such that the dynamic model is allowed to run for 0.5 s whereupon data is acquired from the plant. Specifically, the acquired control input variable represents the lateral response of the pinion shaft. An rms value of the variable is then determined based on the data from this 0.5 s simulation. This new value is compared with the most recent previously acquired value and is presented to the developed controller as shaft displacement and change of shaft displacement for determination of the required output correction. A further 0.5 s simulation is then performed prior to sending the control correction signal to the model of

the plant. After the control signal is sent, another 0.5 s simulation of the model is run prior to collecting data for the next correction step.

In the charts shown, the simulation in each case is initiated with a free damper condition. The control is initiated with the first level of control at the 1.5 s mark. Note that the additional forcing function is included for the 53 Hz simulation as previously discussed. The dramatic effect of the control parallels the response measured for the prototype experiments (ref Fig 5.29) and confirms the effective control of both the torsional and lateral vibration response across the desired speed range.

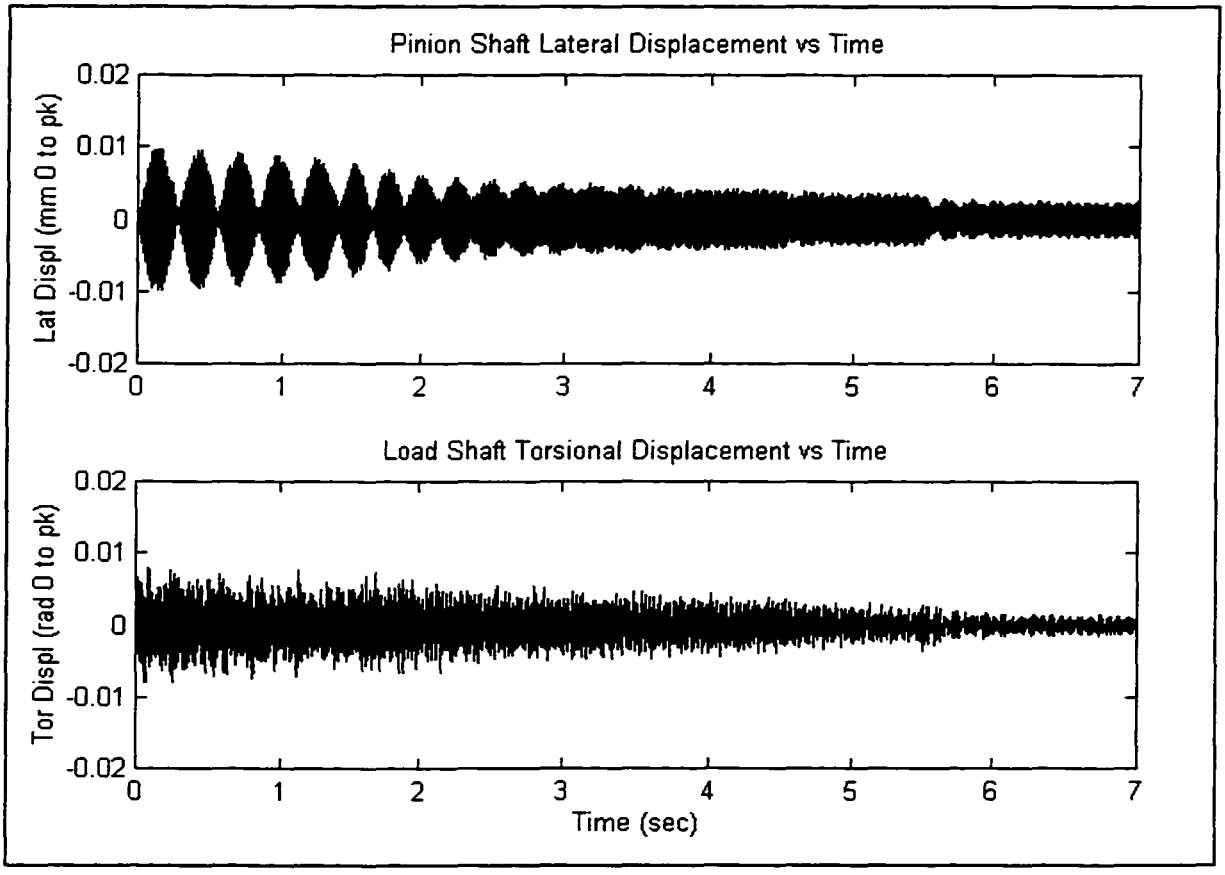


Figure 6.6: Composite Simulation Response (53 Hz)

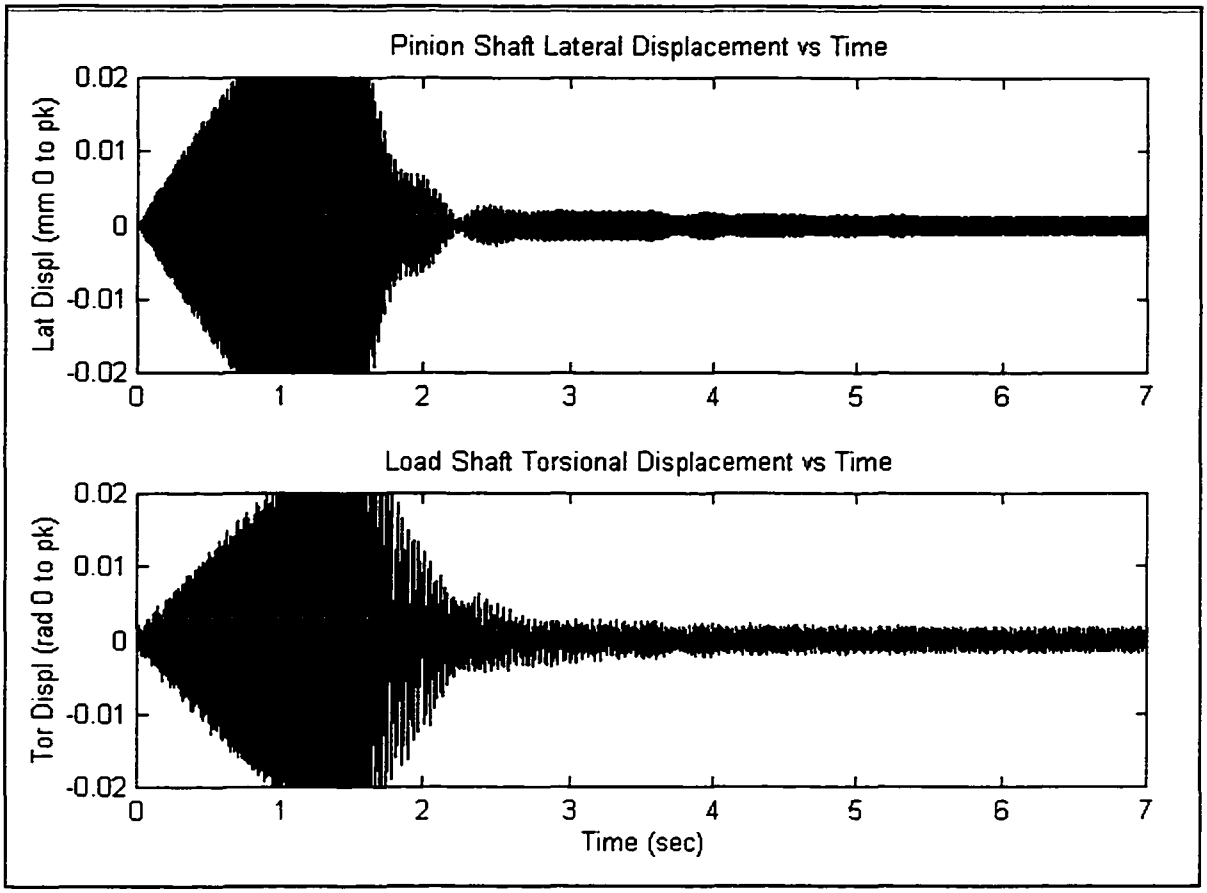


Figure 6.7: Composite Simulation Response (64.5 Hz)

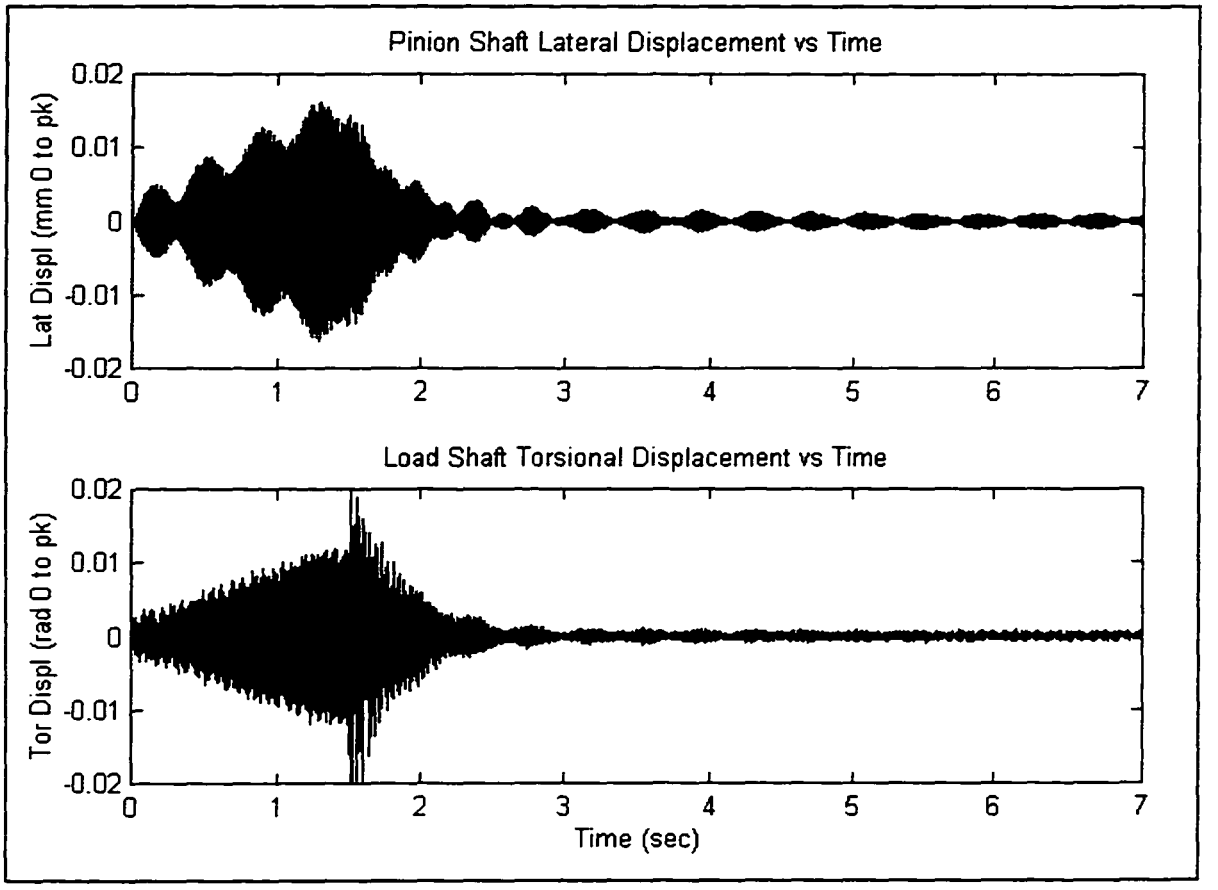


Figure 6.8: Composite Simulation Response (67 Hz)

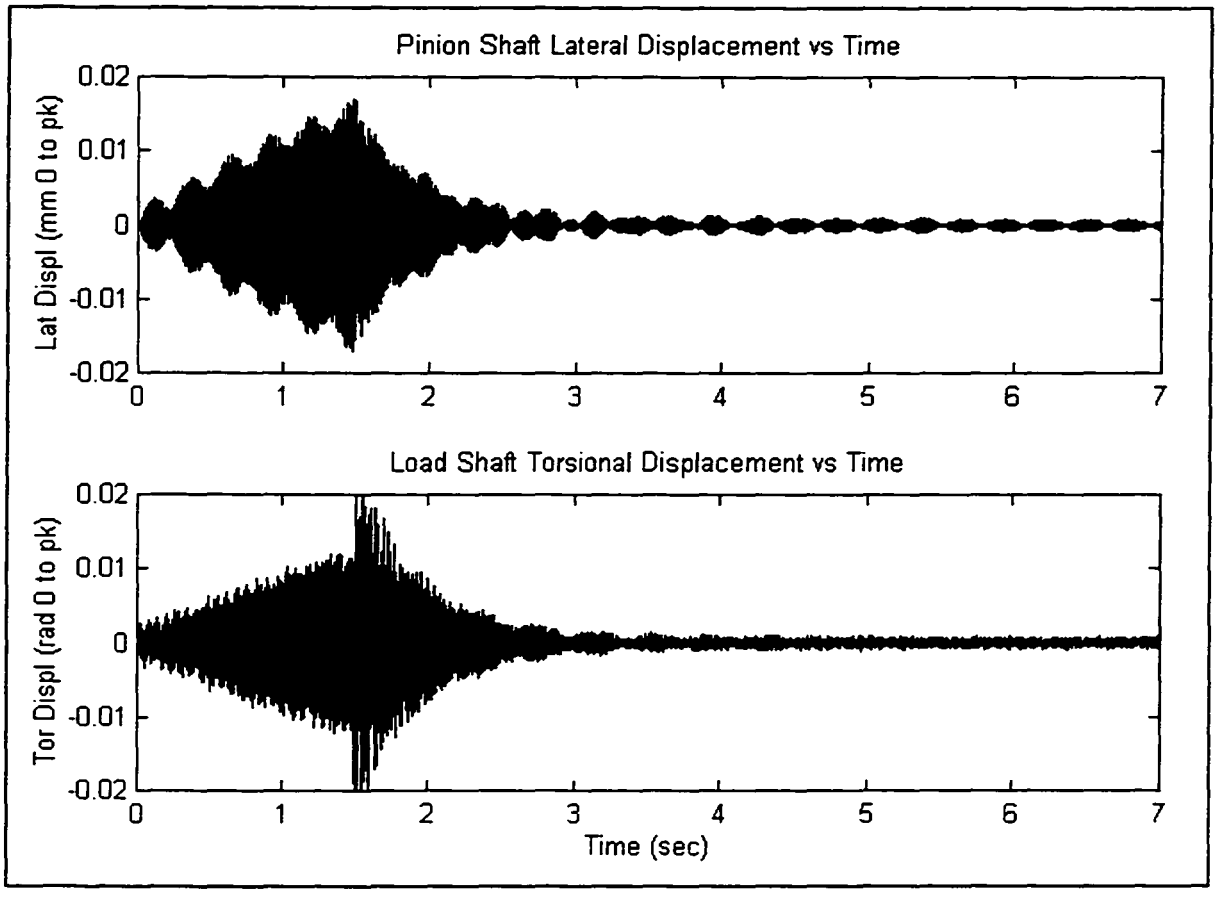


Figure 6.9: Composite Simulation Response (68 Hz)

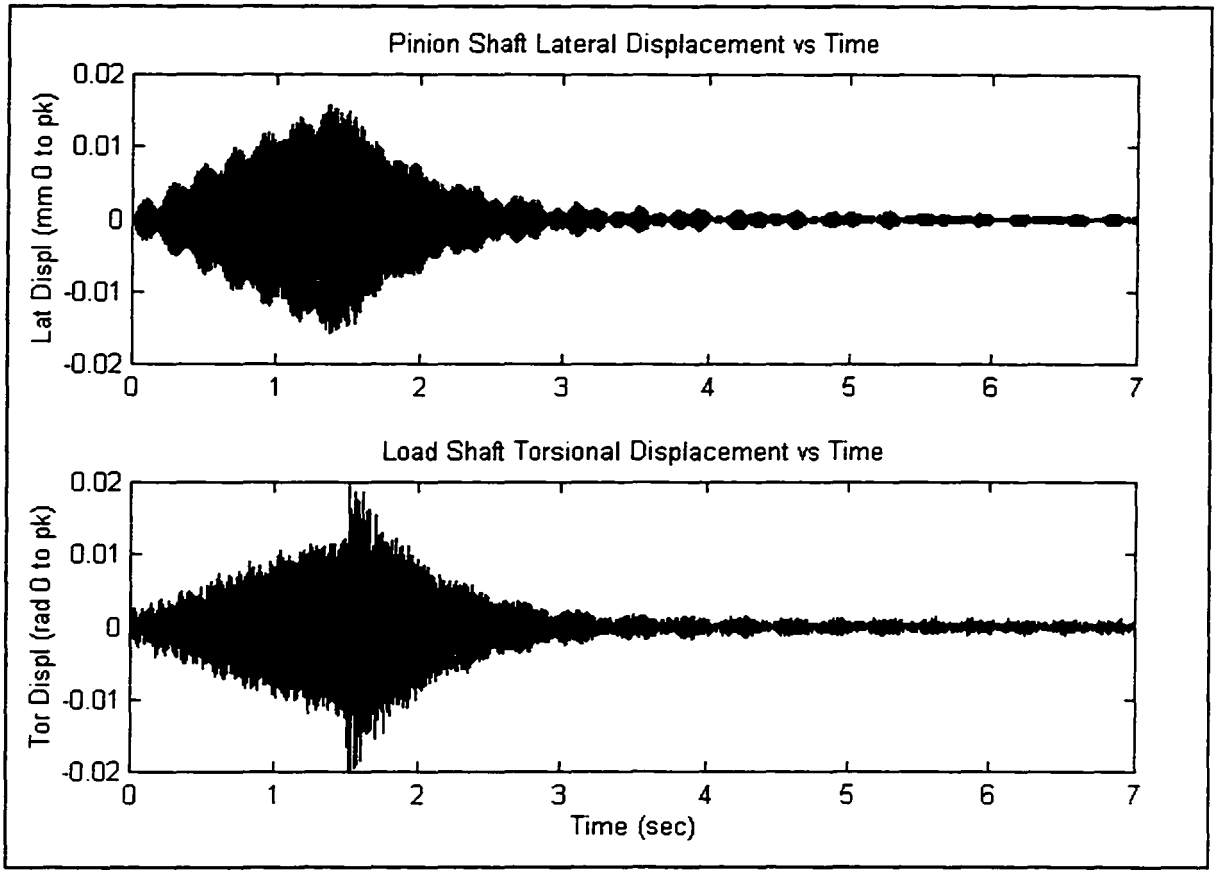


Figure 6.10: Composite Simulation Response (69 Hz)

6.3 Relevance to a Real Machine Train

Resonance is still prominent on the list of machine vibration symptoms to be treated in the design stage or with system modifications after installation. While it is a product of the system design, i.e. mass-stiffness-damping properties, resonance may be excited by any of several forcing functions active in an operating machine train. The likelihood of exciting a resonance is significantly increased when the machine is required to operate across a speed range.

Demanded precision in engineered products leads directly to added cost and extended lead times. Precision of the input information of a model gives precision to the output. However, the output is only as precisely correct as the reliability of the precision of the input. Unknown factors and nonlinearities associated with input quantities will necessarily render the precision of the output to be invalid or at least sub-optimal. The input information is not always determinate. For instance, what is the torsional stiffness of a multistage pump shaft or an induction motor shaft? If three built-up units are measured, three different results will likely occur with the variations exceeding the precision of each individual measurement. Normally, measurements of such quantities would not be available and at best an estimation of the value would be made based on fundamental theory and experience. Likewise, the estimation of mass and its distribution in a lumped parameter model is subject to uncertainty. Rarely will an industrial problem afford the time and expense of a calculation procedure which will improve the quantification of input information to allow optimum damping values to be determined. Also, for the offset geared machine train, it appears certain that the optimum damping at one speed will be not remain optimum across the full speed range of operation.

Active vibration control systems are generally considered for applications where passive systems fail to provide the required performance, or where operating conditions vary

significantly requiring frequent variations in the control forces. Passive control can only react to localized variables, whereas active / semi-active controls can be tailored based on variables read from remote locations.

Every complex machine train will have many natural frequencies and mode shapes associated with it. The response at any speed will be the sum of all applicable modal responses for the system. In a completely linear system the modal participation would also be expected to be linear for a single forcing function at the operating speed. Real machines are never completely linear and forcing functions are rarely single toned and operating alone. Usually there will be a number of forcing functions with possibly one being dominant. Therefore the modal summation or system response will be different at each speed. Nonlinearities in the system will tend to exaggerate this effect. If all the mass elastic properties are known it is possible to select a damper device which is optimum for one speed. This will however not be optimum for all speeds.

The controllable damper provides the opportunity of having optimum damping at all operating speeds as it relates to the measured variable. The control of such a device is not conducive to classical control methods due to the normal nonlinearities in complex machine trains as well as in the control actuating device itself. Further complicating the situation is the modification of effective mass properties of the system by the control action of the actuator as well as the transport speed dependency of the plant dynamic properties.

Chapter 7

Conclusions and Recommendations

This work confirms the effect of the addition of a variable torsional damper / absorber on the combined torsional lateral response of a machine train plant. The application portion of this thesis outlines the basics of a bondgraph model which simulates the combined response of an offset shaft geared machine train (ref Fig 1.1). The preliminary results of the computer simulation, as well as the prototype experiments, indicate that indeed the desired effects are made on the gearbox shafting lateral and torsional vibration modes of the composite machine train.

The torsional damper is not a typical solution applied to industrial machine train resonance problems. However, in the form presented herein with fuzzy logic control, it does offer a solution for machine trains having a set of offset gears which exhibit excessive lateral response at some speeds within the desired operating range. The lateral response of the plant is coupled with the torsional regime and application of the technology developed herein offers a viable solution for this operation predicament.

The fuzzy logic controller is a model-less paradigm offering a corrective control input based on the selectively monitored state response of the plant. This renders the controller inherently responsive to nonlinear plant or actuator components. The corrective input can

be directed at the specific troublesome area by placement of a suitable transducer to report vibration level and allow the appropriate correction via the programmed controller. If more than one location is involved, this can be accommodated by examining the several appropriate signals and having the control system operate with respect to the highest relative value.

In the development of the control for the prototype plant, the method of establishing the speed correction approximating function slope was by trial and error. This could be approached in an industrial application by sequencing the machine through a number of steps in the speed range while adjusting the effective damper voltage to achieve the minimum response. This information would allow estimation of an appropriate function which would very closely approach the optimum function. However, the elegant method will be to have the software continuously update the function estimate as it finds a minimum response for any set speed in the range of interest This will allow the control to self adjust for any outside disturbances as well as characteristic changes which may occur over the life of the machine.

Within the fuzzy inferencing procedure, the choice of normalized triangular membership functions with symmetric overlap was made for programming convenience. A multitude of choices for membership functions are available and could be investigated for improved suitability for this problem. The developed fuzzy controller represents a first generation or non-adaptive type of controller. The next generation in the development will be to incorporate a learning or self-modifying function to tune the fuzzy matrix, or the membership function partitions to be more effective with each step.

Several possible paths could be investigated for an effective adaptive function. Weights may be applied to the various rules in the database on the basis of an error factor determined from the ratio of the actual system output to the correct system output. In this case again, the correct system output may need to be arbitrarily selected as a reasonably

attainable acceptable vibration level. The weighting would apply only to those rules fired in the inferencing process for the most recent step.

Alternatively, some method of adjusting the support sizing of the membership functions could be incorporated based on smoothness of measured system response. This could be accomplished by comparing the actual response measurement to the predicted response from the running average. If the measured value is above the predicted value, then the membership function support would be reduced and vice versa. This method could be applied to the input or the output universe of discourse. It could be applied to all of the membership functions as a whole or just to those involved in the most recent inference step.

The recommended physical location of the damper will usually be at the blank end of the high speed shaft of the gear box to obtain maximum effect of the additive mass for the significant excited modes of the machine train. An outboard location might well be quite effective for the lowest mode, but may not allow effective influence over higher modes which may be excited throughout the speed range.

As alluded to in Chapter 6, a consequential effect of adding a torsional damper to a system is that of increased torsional stability. This may have very significant effects when the system is operated under automatic speed control. Usually, an automatic speed control uses a feedback tachometer signal for comparison with a preset value with the error signal sent to the output torque device, engine or electric motor. Stability of such control systems can be a significant problem where torsional variation in the feedback signal is a significant factor. Normally, the solution for torsional stability is to limit the gain of the control system which leads to an actual output speed less than the desired speed. Application of a variable damper system would reduce torsional variations thus enhancing the stability of the speed control system. This was observed first hand on the prototype. The speed control for this device is a simple rheostat in an open loop system.

This makes it very sensitive to the changing light load condition of the operating prototype machine. Selection of a specific operating speed for this device is difficult in any case, but is considerably improved when the damper is active. The fuzzy logic controlled torsional damper could find application in helicopter drive trains where it would provide the triple function of attenuation of torsional response as well as lateral coupled gearbox response while enhancing the torsional stability of the applied speed control.

The following recommendations are given as the perceived direction which further work along the vein of this study could proceed:

1) develop within the software the ability to update automatically as the fuzzy logic estimates the optimum function relating the clutch volts to plant operating speed.

2) develop a learning capability within the control software to allow self modification of the partitions along the universe of discourse. This may be applied to individual partitioning or the complete set as a whole.

3) incorporate a purely magnetic clutch in the prototype system to allow evaluation of the system response with viscous damping compared to Coulomb damping. Determination of the more mechanically effective type of damping device, together with a relative cost analysis of each design, would help in the more feasible application of a damping device to a real machine train.

4) seek a field example where application of a fuzzy logic controlled damper / absorber device may be employed for further investigation and enhancements of the concept.

REFERENCES

[1] Future Directions of Coordinated Performance Optimization; Electrical Equipment News; October 1992

[2] Lewis, F.M.: Torsional Vibration in Reciprocating Machines; Shock and Vibration Handbook; Second Edition; McGraw Hill; 1976

[3] Ormandroyd, J.; and Den Hartog, J.P.: The Theory of the Dynamic Vibration Absorber; ASME Transactions, Vol 49-50;1927-28

[4] Den Hartog, J.P.; and Ormandroyd, J.:Torsional Vibration Dampers; ASME Transactions, Vol 52; 1930

[5] Brock, J.: A Note on the Damped Vibration Absorber; Journal of Applied Mechanics, Vol 13 No.3; September 1946

[6] Brock, J.: Theory of the Damped Vibration Absorber for Inertial Disturbance; Journal of Applied Mechanics, Vol 16 NO.1; March 1949

[7] Lewis, F.M.: The Extended Theory of the Viscous Vibration Damper; Journal of Applied Mechanics, Vol 22 NO.3; September 1955

[8] Szenasi, F.R.; and Blodgett, L.E.: Isolation of Torsional Vibration in Rotating Machinery; National Conference on Power Transmission 1975

[9] Wachel, J.D.; and Szenasi, F.R.: Field Verification of Torsional-Lateral Coupling Effects on Rotor Instabilities in Centrifugal Compressors; NASA Publication No. 2147; 1980

[10] Iannuzzelli, R.J.; and Elward, R.M.: Torsional Lateral Coupling in Geared Rotors; ASME No. 84-GT-71; 1984

[11] Simmons, H.R.; and Smalley, A.J.: Lateral Gear Shaft Dynamics Control Torsional Stresses in Turbine Driven Compressor Train; ASME No. 84-GT-28; 1984

[12] Schwibinger, P.; and Nordmann, R.: The Influence of Torsional-Lateral Coupling on the Stability Behavior of Geared Rotor Systems; Proc. of the Fourth Workshop on Rotor Dynamic Instability Problems in High Performance Turbomachinery; Texas A&M University; June 1986

[13] Stanway, R., and Burrows, C.R.: Active Vibration Control of a Flexible Rotor on Flexibly Mounted Journal Bearings; Journal of Dynamic Systems, Measurement and Control; Vol 103, No. 4, 1984

[14] Ulsoy, A.G.: Vibration Control in Rotating or Translating Elastic Systems; Journal of Dynamic Systems, Measurement and Control; Vol 106, No. 1, 1984

[15] Firoozian, R., and Stanway, R.: Modeling and Control of Turbomachinery Vibrations; ASME Journal of Vibration, Acoustics, Stress and Reliability in Design; October, 1988.

[16] Raju, P.K., and Sun, S.P.: Modal Control of a Flexible Beam with Multiple Sensors and Actuators; ASME Conference of Mechanical Vibration and Noise, 1991.

[17] Ulbrich, H.: Control of Flexible Rotors By Active Elements; ASME Conference of Mechanical Vibration and Noise, 1991.

[18] Burdess, J.S. and Metcalfe, A.V.: Active Control of Forced Harmonic Vibration in Finite Degree of Freedom Structures with Negligible Damping; Journal of Sound and Vibration, 1983, 93(3), Academic Press.

[19] Burdess, J.S. and Metcalfe, A.V.: The Active Control of Forced Vibration provided by Arbitrary Disturbances; ASME Journal of Vibration, Acoustics, Stress, and Reliability in Design, January 1985, vol 107

[20] Metcalfe, A.V., and Burdess, J.S.: Experimental Evaluation of Wide Band Active Vibration Controllers; ASME Conference of Mechanical Vibration and Noise, 1991.

[21] Maday, C.J., and Johnson, N.H.: A Decentralized Non-Collocated Active Control Algorithm; ASME Conference of Mechanical Vibration and Noise, 1991

[22] Zhu, W., Castelazo, I., and Nelson, H.D.: An Active Optimal Control Strategy of Rotor Vibrations Using External Forces; ASME Conference of Mechanical Vibration and Noise, 1989.

[23] Russell, Bertrand: Vagueness; Australian Journal of Psychology and Philosophy, 1, 1923

[24] Black, Max; Vagueness: An Exercise in Logical Analysis; Philosophy of Science, 4, 1937

[25] Lukasiewicz, Jan; In Defense of Logistics; Selected Works, L. Borkowski Ed., London, North Holland, 1970

[26] Zadeh, Lotfi: Fuzzy Sets; Information and Control; June 1965

[27] Zadeh, Lotfi: Fuzzy Sets and Systems; System Theory, Fox, J. ed., Polytechnic Press; 1965

[28] Mamdani, E.H.: Application of Fuzzy Algorithms for Control of Dynamic Plant; Proceedings of the Institution of Electrical Engineers, September, 1974

[29] Lee, Chuen Chien: Fuzzy Logic in Control Systems: Fuzzy Logic Controller; IEEE Transactions on Systems, Man and Cybernetics, Vol. 20, No. 2, March/April, 1990

[30] Murayana, Y., Terano, T., Masui, S. and Akiyama, N.: Optimizing Control of a Diesel Engine; Industrial Application of Fuzzy Control, Sugeno, Michio, ed., 1985

[31] Larkin, Lawrence I.: A Fuzzy Logic Controller for Aircraft Flight Control; Industrial Application of Fuzzy Control, Sugeno, Michio, ed., 1985

[32] Yasunobu, Seiji and Miyamoto, Shoji: Automatic Train Operating System By Predictive Fuzzy Control; Industrial Application of Fuzzy Control, Sugeno, Michio, ed., 1985

[33] Yagashita, O., Itoh, O., and Sugeno, Michio: Application of Fuzzy Reasoning to the Water Purification Process ; Industrial Application of Fuzzy Control, Sugeno, Michio, ed., 1985

[34] Murakami, Shuti, and Maeda, Mikio: Automatic Speed Control Using a Fuzzy Logic Controller; Industrial Application of Fuzzy Control, Sugeno, Michio, ed., 1985

[35] Bartolini, G., Casalino, G., Davoli, F., Mastretta, M., Minciardi, R. and Morten, E.: Development Of Performance Adaptive Fuzzy Controllers with Application to Continuous Casting Plant ; Industrial Application of Fuzzy Control, Sugeno, Michio, ed., 1985

[36] Scharf, E.M. and Mandic N.J.: The Application of A Fuzzy Controller to the control of a Multi-Degree-of-Freedom Robot Arm ; Industrial Application of Fuzzy Control, Sugeno, Michio, ed., 1985

[37] Diken, H and Tadjbakhsh, I.G.; Unbalance Response of Flexible Rotors Coupled with Torsion; Journal of Vibration, Acoustics, Stress, and Reliability in Design Vol III, April 1989

[38] Ross, Timothy J.; Fuzzy Logic with Engineering Applications; McGraw Hill; 1995

[39] Wylie, Benjamin E. and Streeter, Victor L.; Fluid Transients; Mcgraw Hill; 1978

[40] Morehead, James C. III; Sum and Difference Frequencies; Proceedings Thirteenth Annual Meeting, Vibration Inst; 1989

BIBLIOGRAPHY

[1] Nonami, K., DiRusso, E., and Fleming, D.P.,: Active Vibration Control for Flexible Rotor By Optimal Direct-Output Feedback Control; ASME Conference of Mechanical Vibration and Noise, 1989.

[2] Karnop, D., and Allen, Ross R.: Semi-Active Control of Multimode Vibratory Systems using ILSM Concept; ASME Journal of Engineering for Industry, August, 1976

[3] Rakheja, S., and Sankar, S.: Vibration and Shock Isolation Performance of a Semi-Active "On-Off" Damper; ASME Journal of Vibration, Acoustics, Stress and Reliability in Design; October, 1985, Vol. 107.

[4] Karnop, D.: Active and Passive Isolation of Random Vibration; Section 3 of Isolation of Mechanical Vibration Impact and Noise, AMD, Vol 1, Applied Mechanics Div., ASME, 1973

[5] Nestorides, E.J.(editor): Handbook on Torsional Vibration; Cambridge University Press; 1958

[6] Ker Wilson, W.: Practical Solution to Torsional Vibration Problems, Vol 4, Devices for Controlling Vibration; Third Edition; Chapman and Hall; 1968

[7] Karnop, D.: Vibration Control using Semi-Active Force Generators;

[8] Lalanne, M.; and Ferraris, G.: Rotordynamic Prediction in Engineering; Wiley; 1990

[9] Vance, J.M.: Rotordynamics of Turbomachinery; Wiley Interscience; 1987

[10] Den Hartog, J.P.: Mechanical Vibrations; Fourth Edition; McGraw Hill; 1956

[11] Reed, F.E.: Dynamic Vibration Absorbers and Auxiliary Mass Dampers; Shock and Vibration Handbook; Second Edition; McGraw Hill; 1976

[12] Thompson, W.T.: Theory Of Vibration With Applications; Second Edition; Prentice Hall; 1981

[13] Greenwood, D.T.: Classical Dynamics; Prentice Hall; 1977

[14] Timoshenko, S.; and Young, D.H.: Elements Of Strength Of Materials; Fourth Edition; D. Van Nostrand; 1962

[15] Meirovitch, L.: Methods Of Analytical Dynamics; McGraw Hill; 1970

[16] Meirovitch, L.: Analytical Methods in Vibrations; The Macmillan Company; 1967

[17] Miron, Douglas B.: Design of Feedback Control Systems; Harcourt, Brace, Jovanovich, 1989

[18] Kuo, Benjamin C.: Automatic Control Systems; Sixth edition, Prentice Hall, 1991.

[19] Phelan, Richard M.: Dynamics of Machinery; Mcgraw Hill, 1967

[20] Byars and Snyder: Engineered Mechanics of Deformable Bodies; Second Edition, International Textbook Company, 1969.

[21] Gorman, Daniel I.: Free Vibration Analysis of Beams and Shafts; Wiley Interscience, 1975

[22] Harrison and Bollinger : Introduction to Automatic Controls, International Textbook Company, 1969

[23] Maday, Clarence J.: Feedback Control Systems For Time Response; Instrument Society of America, 1987.

[24] Owens, D.H.: Multivariable and Optimal Systems; Academic Press, London, 1982.

[25] Ibrahim, Ahmed M.K.: Modeling and Diagnostics of Beams with Fatigue Cracks; PhD Thesis, CA20NUW 13087M52, University of Waterloo, 1987

[26] Inman, D.J.: Engineering Vibration; Prentice Hall; 1994

[27] Kosko, Bart: Neural Networks and Fuzzy Systems; Prentice Hall; 1992

[28] Yager, Ronald R.; Fuzzy Sets, Neural Networks and Soft Computing; Van Nostrand Reinhold; 1994

[29] Klir, George J. and Yuan Bo; Fuzzy Sets and Fuzzy Logic, Theory and Applications; Prentice Hall; 1995

Appendix I

Prototype: Equations of Motion

In this appendix the equations of motion for the prototype will be derived in detail using the Lagrange method and also the bondgraph method. A reconciliation of the bondgraph equations to the second order equations derived by the first method is then presented.

Lagrange Method

Using the Lagrange method each co-ordinate will have a motion $q_i(t)$ that satisfies

$$d/dt(\partial L/\partial \dot{q}_i) - \partial L/\partial q_i = Q_i \qquad (1 < i < 6) \quad \ldots\ldots\ldots\ldots\ldots\ldots\ldots \quad \text{(A-I.1)}$$

As stated in Chap 4 and referring to Fig 4.1 with the defined numbering scheme, the total kinetic energy, 'T', will be the sum of the kinetic energy for each mass and rotating inertia station. The total kinetic energy is

$$T = \tfrac{1}{2} I_1(\dot{\theta}_1)^2 + \tfrac{1}{2} I_3 (\dot{\theta}_3)^2 + \tfrac{1}{2} I_5 (\dot{\theta}_5)^2 + \tfrac{1}{2} I_7 (\dot{\theta}_7)^2 + \tfrac{1}{2} M_9(\dot{y}_9)^2 + \tfrac{1}{2} M_{11} (\dot{y}_{11})^2 \quad \ldots\ldots\ldots\ldots\ldots\ldots\ldots\ldots \quad \text{(A-I.2)}$$

The potential energy, 'V', is the sum of the strain energy in each of the torsional and axial springs (ref Fig 4.1).

$$V = \tfrac{1}{2} K_2(\theta_1 - \theta_3)^2 + \tfrac{1}{2} K_4 (r_3\theta_3 - r_5 \theta_5 - y_9 - y_{11})^2 + \tfrac{1}{2} K_8 y_9^2 + \tfrac{1}{2} K_{10} y_{11}^2 + \tfrac{1}{2} K_6(\theta_5 - \theta_7)^2 \quad \text{(A-I.3)}$$

The non-conservative torques obtained from the virtual work δW of the drive torque on disk one and the load torque on disk 7 are (with the exception of load torque, no damping terms included here for clarity) :

$$Q_1 = T_1(t) \quad \text{(A-I.4)}$$

$$Q_2 = Q_3 = Q_5 = Q_6 = 0 \quad \text{(A-I.5)}$$

$$Q_4 = - b'_7 \dot{\theta}_7 | \dot{\theta}_7 | \quad \text{(A-I.6)}$$

The term b'_7 is the load torque damping coefficient representing the change in load resistance for small variations in rotating speed. In this particular case the coefficient is assumed to be proportional to the speed squared as would be the case for a centrifugal machine such as a pump or fan.

Now using the Lagrangian equation and the non-conservative torques, we can form the 6 equations of motion for the system. The Lagrangian L, is formed as the difference between the kinetic energy and the potential energy.

$$L = T - V \quad \text{(A-I.7)}$$

Then

$$\partial L/\partial \dot{\theta}_1 = I_1 \ddot{\theta}_1 \quad \text{(A-I.8)}$$

$$d/dt(\partial L/\partial \dot{\theta}_1) = I_1 \ddot{\theta}_1 \quad \text{(A-I.9)}$$

$$\partial L/\partial \theta_1 = -K_2 (\theta_1 - \theta_3) \quad \text{(A-I.10)}$$

The first equation is then

$$I_1 \ddot{\theta}_1 + K_2 (\theta_1 - \theta_3) = T_1(t) \quad \text{(A-I.11)}$$

Similarly, the remaining 5 equations are formed as follows:

$$I_3 \ddot{\theta}_3 + K_2 (\theta_3 - \theta_1) + r_3 K_4 (r_3\theta_3 - r_5\theta_5 - y_9 - y_{11}) = 0 \quad \text{(A-I.12)}$$

$$I_5 \ddot{\theta}_5 + r_3 K_4 (r_5\theta_5 + y_{11} + y_9 - r_3\theta_3) + K_6 (\theta_5 - \theta_7) = 0 \quad \text{(A-I.13)}$$

$$I_7 \ddot{\theta}_7 + K_6 (\theta_7 - \theta_5) = - b'_7 \dot{\theta}_7 | \dot{\theta}_7 | \quad \text{(A-I.14)}$$

$$M_9 \ddot{y}_9 + K_4 (y_9 + r_5\theta_5 + y_{11} - r_3\theta_3) + K_8 y_9 = 0 \quad \text{(A-I.15)}$$

$$M_{11} \ddot{y}_{11} + K_4 (y_9 + r_5\theta_5 + y_{11} - r_3\theta_3) + K_{10} y_{11} = 0 \quad \text{(A-I.16)}$$

Bondgraph Method

The foregoing equations of motion may also be formulated as a series of first order differential equations using a modeling method such as bondgraph. The bondgraph diagram is shown in Fig 4.3. The state variables are momentum of the inertia elements and displacement of the stiffness elements. The equations are formulated as a series of relationships representing the energy flow in state space format as follows:

$$\dot{P}_1 = T_1(t) - K_2\,\theta_2 \quad \text{(A-I.17)}$$

$$\dot{\theta}_2 = 1/I_1\,P_1 - 1/I_3\,P_3 \quad \text{(A-I.18)}$$

$$\dot{P}_3 = K_2\,\theta_2 - r_3\,K_4\,y_4 \quad \text{(A-I.19)}$$

$$\dot{y}_4 = r_3/I_3\,P_3 - r_5/I_5\,P_5 - 1/M_9\,P_9 - 1/M_{11}\,P_{11} \quad \text{(A-I.20)}$$

$$\dot{P}_9 = K_4\,y_4 - K_8\,y_8 \quad \text{(A-I.21)}$$

$$\dot{y}_8 = 1/M_9\,P_9 \quad \text{(A-I.22)}$$

$$\dot{P}_{11} = K_4\,y_4 - K_{10}\,y_{10} \quad \text{(A-I.23)}$$

$$\dot{y}_{10} = 1/M_{11}\,P_{11} \quad \text{(A-I.24)}$$

$$\dot{P}_5 = r_5\,K_4\,y_4 - K_6\,\theta_6 \quad \text{(A-I.25)}$$

$$\dot{\theta}_6 = 1/I_5\,P_5 - 1/I_7\,P_7 \quad \text{(A-I.26)}$$

$$\dot{P}_7 = K_6\,\theta_6 - b'_7\;\theta_7|\theta_7| \quad \text{(A-I.27)}$$

where:

$K = 1/C$

P = momentum of the mass / inertia

$\dot{P}$ = Force / Torque

θ = angular displacement

$\dot{\theta}$ = angular velocity

y = linear displacement

$\dot{y}$ = linear velocity

b' = quadratic load damping coefficient

From a computer simulation standpoint the bondgraph format results in a smaller and more efficient system [A] matrix.

Reconciliation of Methods

Since it is not immediately obvious that the first set of second order equations developed using the Lagrangian method is identical to the second set of first order equations from the energy exchange format of bondgraph, the following reconciliation is presented.

Write the bondgraph displacements in terms of the Lagrangian displacements

$$\theta_2 = \theta_1 - \theta_3 \quad \text{(A-I.28)}$$

$$y_4 = r_3\theta_3 - r_5\theta_5 - y_9 - y_{11} \quad \text{(A-I.29)}$$

$$\theta_6 = \theta_5 - \theta_7 \quad \text{(A-I.30)}$$

$$y_8 = y_9 \quad \text{(A-I.31)}$$

$$y_{10} = y_{11} \quad \text{(A-I.32)}$$

and similarly for the accelerations

$$\ddot{\theta}_2 = \ddot{\theta}_1 - \ddot{\theta}_3 \quad \text{(A-I.33)}$$

$$\ddot{y}_4 = r_3\ddot{\theta}_3 - r_5\ddot{\theta}_5 - \ddot{y}_9 - \ddot{y}_{11} \quad \text{(A-I.34)}$$

$$\ddot{\theta}_6 = \ddot{\theta}_5 - \ddot{\theta}_7 \quad \text{(A-I.35)}$$

$$\ddot{y}_8 = \ddot{y}_9 \quad \text{(A-I.36)}$$

$$\ddot{y}_{10} = \ddot{y}_{11} \quad \text{(A-I.37)}$$

differentiating equation (A-I.18)

$$\dot{\theta}_2 = 1/I_1\,\dot{P}_1 - 1/I_3\,\dot{P}_3 \quad \text{(A-I.38)}$$

and substituting $\dot{P}_1$ and $\dot{P}_3$ from equations (A-I.17) and (A-I.19)

$$\ddot{\theta}_1 - \ddot{\theta}_3 = 1/I_1 (T_1(t) - K_2 \theta_2) - 1/I_3 (K_2 \theta_2 - r_3 K_4 y_4)$$

Separate terms associated with each inertia element

$$\ddot{\theta}_1 = 1/I_1 (T_1(t) - K_2 \theta_2)$$
$$\ddot{\theta}_3 = 1/I_3 (K_2 \theta_2 - r_3 K_4 y_4)$$

and substitute in the displacements from the Lagrangian method

$$\ddot{\theta}_1 = 1/I_1 (T_1(t) - K_2 (\theta_1 - \theta_3)) \quad \text{(A-I.39)}$$
$$\ddot{\theta}_3 = 1/I_3 (K_2 (\theta_1 - \theta_3) - r_3 K_4 (r_3\theta_3 - r_5\theta_5 - y_9 - y_{11})) \quad \text{(A-I.40)}$$

re-arranging the above two equations gives

$$I_1 \ddot{\theta}_1 + K_2(\theta_1 - \theta_3) = T_1(t) \quad \text{(A-I.11)}$$
$$I_3 \ddot{\theta}_3 + K_2(\theta_3 - \theta_1) + r_3 K_4 (r_3\theta_3 - r_5\theta_5 - y_9 - y_{11}) = 0 \quad \text{(A-I.12)}$$

Similarly, differentiating equation (A-I.20)

$$\ddot{y}_4 = r_3/I_3 \dot{P}_3 - r_5/I_5 \dot{P}_5 - 1/M_9 P_9 - 1/M_{11} \dot{P}_{11}$$
$$r_3 \ddot{\theta}_3 - r_5 \ddot{\theta}_5 - \ddot{y}_9 - \ddot{y}_{11} = r_3/I_3 \dot{P}_3 - r_5/I_5 \dot{P}_5 - 1/M_9 \dot{P}_9 - 1/M_{11} \dot{P}_{11}$$

Separating the terms as before

$$r_3 \ddot{\theta}_3 = r_3/I_3 \dot{P}_3$$
$$r_5 \ddot{\theta}_5 = r_5/I_5 \dot{P}_5$$
$$\ddot{y}_9 = 1/M_9 \dot{P}_9$$
$$\ddot{y}_{11} = 1/M_{11} \dot{P}_{11}$$

and making the appropriate substitutions

$$r_5 \ddot{\theta}_5 = r_5 / I_5 (r_5 K_4 \ (r_3\theta_3 - r_5\theta_5 - y_9 - y_{11}) - K_6 (\theta_5 - \theta_7))$$

$$I_5 \ddot{\theta}_5 + r_3 K_4 (r_5\theta_5 + y_{11} + y_9 - r_3\theta_3) + K_6 (\theta_5 - \theta_7) = 0 \quad \ldots\ldots\ldots\ldots\ldots \quad \text{(A-I.13)}$$

$$\ddot{y}_9 = 1/M_9 (K_4 (r_3\theta_3 - r_5\theta_5 - y_9 - y_{11}) - K_8 y_9)$$

$$M_9 \ddot{y}_9 + K_4 (y_9 + r_5\theta_5 + y_{11} - r_3\theta_3) + K_8 y_9 = 0 \quad \ldots\ldots\ldots\ldots\ldots \quad \text{(A-I.15)}$$

$$\ddot{y}_{11} = 1/M_{11} (K_4 (r_3\theta_3 - r_5\theta_5 - y_9 - y_{11}) - K_{10} y_{11})$$

$$M_{11} \ddot{y}_{11} + K_4 (y_9 + r_5\theta_5 + y_{11} - r_3\theta_3) + K_{10} y_{11} = \quad \ldots\ldots\ldots\ldots\ldots \quad \text{(A-I.16)}$$

for the last second order equation, differentiate equation (16), substitute and take the $\ddot{\theta}_7$ term

$$\ddot{\theta}_6 = 1/I_5 \dot{P}_5 - 1/I_7 \dot{P}_7$$

$$\ddot{\theta}_5 - \ddot{\theta}_7 = 1/I_5 \dot{P}_5 - 1/I_7 \dot{P}_7$$

$$\ddot{\theta}_7 = 1/I_7 K_6 (\theta_5 - \theta_7) - b'_7 \dot{\theta}_7 | \dot{\theta}_7 |$$

$$I_7 \ddot{\theta}_7 + K_6(\theta_7 - \theta_5) = - b'_7 \dot{\theta}_7 | \dot{\theta}_7 | \quad \ldots\ldots\ldots\ldots\ldots\ldots\ldots \quad \text{(A-I.14)}$$

Prototype with Damper

The following state space equations are for the prototype with the damper attached. Some damping terms are included

$$\dot{P}_1 = T_1(t) - K_2 \theta_2 \quad \text{(A-I.41)}$$

$$\dot{\theta}_2 = 1/I_1 P_1 - 1/I_3 P_3 \quad \text{(A-I.42)}$$

$$\dot{P}_3 = K_2 \theta_2 - r_3 K_4 y_4 - K_{12} \theta_{12} - b_{23}/I_3 P_3 \quad \text{(A-I.43)}$$

$$\dot{\theta}_{12} = 1/I_3 P_3 - 1/I_{13} P_{13} - K_{12}/R_{25} \theta_{12} \quad \text{(A-I.44)}$$

$$\dot{P}_{13} = K_{12} \theta_{12} - b_{26}/I_{13} P_{13} \quad \text{(A-I.45)}$$

$$\dot{y}_4 = r_3/I_3 P_3 - r_5/I_5 P_5 - 1/M_9 P_9 - 1/M_{11} P_{11} \quad \text{(A-I.46)}$$

$$\dot{P}_9 = K_4 y_4 - K_8 y_8 - b_{21}/M_9 P_9 \quad \text{(A-I.47)}$$

$$\dot{y}_8 = 1/M_9 P_9 \quad \text{(A-I.48)}$$

$$\dot{P}_{11} = K_4 y_4 - K_{10} y_{10} - b_{22}/M_{11} P_{11} \quad \text{(A-I.49)}$$

$$\dot{y}_{10} = 1/M_{11} P_{11} \quad \text{(A-I.50)}$$

$$\dot{P}_5 = r_5 K_4 y_4 - K_6 \theta_6 - b_{24}/I_5 P_5 \quad \text{(A-I.51)}$$

$$\dot{\theta}_6 = 1/I_5 P_5 - 1/I_7 P_7 \quad \text{(A-I.52)}$$

$$\dot{P}_7 = K_6 \theta_6 - b'_7 \dot{\theta}_7 |\dot{\theta}_7| \quad \text{(A-I.53)}$$

where:

K, P, $\dot{P}$, θ, $\dot{\theta}$, y, $\dot{y}$, b' as before

R = coefficient of inter-element damping

b = coefficient of damping to ground

Appendix II

Prototype State Space Matrices

A bondgraph is a precise pictorial representation of the energy exchange mechanisms active in a dynamic system. The power bonds allow the interchange of energy between the elements in the network. The system equations are developed for each of the junctions in the bondgraph based on the equivalent of Kirchoff circuit laws. Essentially the series junctions have constant flow (angular and linear velocity in this case) while the parallel junctions have constant effort (torque and force).

Selecting the state variables for the system as momentum of the inertia elements and displacement of the stiffness elements, a set of first order differential equations can be generated which allows the direct set-up of the system matrices as shown below. The element constitutive equations are described in Section 4.1.2.

The following development of system matrices is a straight forward interpretation of equations A-I.17 to A-I.27 as listed in Appendix I.

The vector matrix system equations are set in the standard state space format as follows (ref Sect 3.4):

$$\dot{q} = A\,q + B\,u \quad \ldots\ldots\ldots\ldots\ldots\ldots\ldots\ldots\ldots\ldots\ldots\ldots\ldots\ldots\ldots\ldots \text{(A-II.1)}$$

$$y = C\,q + D\,u \quad \ldots\ldots\ldots\ldots\ldots\ldots\ldots\ldots\ldots\ldots\ldots\ldots\ldots\ldots\ldots\ldots \text{(A-II.2)}$$

The [A] system matrix is given on the second page following.

The [B] coefficient matrix for the input vector defines the forces / torques applied to this single input system. The [B] matrix is a 11 x 1 column vector, in this case, with a value of 1 in the first entry position and with zeros in the remaining positions.

$$B = [1\ 0\ 0\ 0\ 0\ 0\ 0\ 0\ 0\ 0\ 0]^T$$

And similarly for the output coefficient matrix for the state vector as defined by the [C] matrix, e.g.

$C = [1\ 0\ 0\ 0\ 0\ 0\ 0\ 0\ 0\ 0\ 0]$ - for the vibratory torque output of the drive motor inertia disk

$C = [0\ 1\ 0\ 0\ 0\ 0\ 0\ 0\ 0\ 0\ 0]$ - for the angular displacement of the pinion shaft

$C = [0\ 0\ 0\ 1\ 0\ 0\ 0\ 0\ 0\ 0\ 0]$ - for the linear displacement of the pinion mass

The feed forward matrix [D] is [0] for this case.

Prototype system [A] matrix:

	P_1	θ_2	P_3	y_4	P_9	y_8	P_{11}	y_{10}	P_5	θ_6	P_7
$\dot{P}_1$	0	$-k_2$	0	0	0	0	0	0	0	0	0
$\dot{\theta}_2$	$\frac{1}{I_1}$	0	$\frac{-1}{I_3}$	0	0	0	0	0	0	0	0
$\dot{P}_3$	0	k_2	0	$-r_3k_4$	0	0	0	0	0	0	0
$\dot{y}_4$	0	0	$\frac{r_3}{I_3}$	0	$\frac{-1}{M_9}$	0	$\frac{-1}{M_{11}}$	0	$\frac{-r_5}{I_5}$	0	0
$\dot{P}_9$	0	0	0	k_4	0	$-k_8$	0	0	0	0	0
$\dot{y}_8$	0	0	0	0	$\frac{1}{M_9}$	0	0	0	0	0	0
$\dot{P}_{11}$	0	0	0	k_4	0	0	0	$-k_{10}$	0	0	0
$\dot{y}_{10}$	0	0	0	0	0	0	$\frac{1}{M_{11}}$	0	0	0	0
$\dot{P}_5$	0	0	0	r_5k_4	0	0	0	0	0	$-k_6$	0
$\dot{\theta}_6$	0	0	0	0	0	0	0	0	$\frac{1}{I_5}$	0	$\frac{-1}{I_7}$
$\dot{P}_7$	0	0	0	0	0	0	0	0	0	k_6	0

Appendix III

Fuzzy Control Software

The computer programs included in this appendix were written to perform the unique fuzzy control developed for this application. The control is basically a three step procedure to locate the minimum lateral response of an offset geared machine train by varying mass addition and torsional damping. This was accomplished via a semi-active torsional damper / absorber attached to the free end of the pinion shaft. The control device is a dry-friction, electromagnetically actuated clutch with a sliding flywheel arrangement. The control program finds the optimum torsional damping for any set speed in the operating range using a reversing fuzzy associative matrix in conjunction with the fuzzy inferencing procedure to determine output voltage corrections for the actuator. The programs were developed in version 6 of the Turbo Pascal environment as supplied by Borland International software company. A flow diagram for the program "FuzzyControl" is included in the main body of the report as Fig 5.26.

```
Program FuzzyControl;
uses
   crt,turbo3,scrstuff,general, files, tp4d16;
const
   NumInputVar = 3;
   const max_buffer = 2000;
   numav = 1000;
Type
   VariableName = String[20];
   String16 = string[16];
   String4 = string[4];
   MShip = array[1 .. 4] of real;
   MFPoints = array[1 .. NumInputVar] of array[1 .. 4] of real;
   MFunc = array[1 ..4] of char;
   MemF = array[1..4] of string[2];
   MovAvgPts= array[1..5] of real;
Var
  I,J,K,N,m,Num,Num_Readings,r,
  OutCount                    : integer;
  Area,AreaMom                : MShip;
  TotalArea,AreaMoment,
  OutputSignal,Rdata,OutVoltsPre  : real;
  A, B, C, D, E, F, G         : char;
  NM,NL,NS,ZE,PS,PM,PL        : MFPoints;
  Keyboard,Quit,First,Pos,
  Neg,Cond,test,Second,Third  : Boolean;
  OutFile                     : text;
  FileName                    : string16;
  DelOmega,DelVib,Omega,Vib,VibPre,
  OmegaPre,C_Volts,DDVib,Speedref,
  DelVibPre1,DelVibPre2,DelVibPre3,
  OutSigPre1,OutsigPre2,OutSigPre3,
  CurveVolts,ChkVolts,SpeedDif  : real;
  Vibr                        : MovAvgPts;
  MemShip,OutMS               : MShip;
  MemFunc                     : MFunc;
  OutMF                       : MemF;
  InMF                        : array[1..4] of string[15];

  {declarations for the metrobyte board}
   involts, outvolts, rate, rpm,ad_data6,ad_data7: real;
   count, mode, cycle, trigger,
   base_adr, err_code, int_level, dma_level,
   board_num, chanOut, chanlo, chanhi  : integer;
   dataval                     : longint;
   datavector                  : array[0..max_buffer] of integer;

{$I C:\TP6\Fuzzy.mod}   (* input data for Universe of Discourse*)

PROCEDURE MemberShip(P1,P2,P3,P4,InputVar: real);   { determine input membership value }
begin
```

```
if (InputVar > P1) and (InputVar < P2) then
   MemShip[I]:= 1/(P2-P1)*(InputVar-P1)
else
  if (InputVar > P3) and (InputVar <= P4) then
   MemShip[I]:= 1-(InputVar-P3)/(P4-P3)
  else
   Memship[I]:= 1;
end;

PROCEDURE MemShipFunction(InputVar:real);          { determine Input membership functions }
begin
if (InputVar > NL[J,1]) and (InputVar <= NL[J,4])  then
  begin
   MemFunc[I]:= 'A'; {NL}
   MemberShip(NL[J,1],NL[J,2],NL[J,3],NL[J,4],InputVar);
   I:=I+1;
   MemFunc[I]:= 'B'; {NM}
   memship[I]:= 1- memship[I-1];
  end
else if (InputVar > NM[J,1]) and (INputVar <= NM[J,4]) then
    begin
      MemFunc[I]:= 'B'; {NM}
      MemberShip(NM[J,1],NM[J,2],NM[J,3],NM[J,4],InputVar);
      I:=I+1;
      MemFunc[I]:= 'C'; {NS}
      memship[I]:= 1- memship[I-1];
    end
else if (InputVar > NS[J,1]) and (INputVar <= NS[J,4]) then
    begin
      MemFunc[I]:= 'C'; {NS}
      MemberShip(NS[J,1],NS[J,2],NS[J,3],NS[J,4],InputVar);
      I:=I+1;
      MemFunc[I]:= 'D'; {ZE}
      memship[I]:= 1- memship[I-1];
    end
else if (InputVar > ZE[J,1]) and (INputVar <= ZE[J,4]) then
    begin
      MemFunc[I]:= 'D'; {ZE}
      MemberShip(ZE[J,1],ZE[J,2],ZE[J,3],ZE[J,4],InputVar);
      I:=I+1;
      MemFunc[I]:= 'E'; {PS}
      memship[I]:= 1- memship[I-1];
    end
else if (InputVar > PS[J,1]) and (INputVar <= PS[J,4]) then
    begin
      MemFunc[I]:= 'E'; {PS}
      MemberShip(PS[J,1],PS[J,2],PS[J,3],PS[J,4],InputVar);
      I:=I+1;
      MemFunc[I]:= 'F'; {PM}
      memship[I]:= 1- memship[I-1];
    end
```

```
else if (InputVar > PM[J,1]) and (INputVar <= PM[J,4]) then
   begin
    MemFunc[I]:= 'F'; {PM}
    MemberShip(PM[J,1],PM[J,2],PM[J,3],PM[J,4],InputVar);
    I:=I+1;
    MemFunc[I]:= 'G'; {PL}
    memship[I]:= 1- memship[I-1];
   end
else if (InputVar > PL[J,2]) and (INputVar <= PL[J,4]) then
   begin
    MemFunc[I]:= 'G'; {PL}
    memship[I]:= 1;
    I:=I+1;
    MemFunc[I]:= 'G'; {PL}
    memship[I]:= 1- memship[I-1];
   end;
end;

PROCEDURE MemberShipOut(var InMS,OutMS:MShip);  {determine output membership value}
begin
if InMS[1] < InMS[3] then OutMS[1] := InMS[1]
              else OutMS[1] := InMS[3];
if InMS[1] < InMS[4] then OutMS[3] := InMS[1]
              else OutMS[3] := InMS[4];
if InMS[2] < InMS[3] then OutMS[2] := InMS[2]
              else OutMS[2] := InMS[3];
if InMS[2] < InMS[4] then OutMS[4] := InMS[2]
                  else OutMS[4] := InMS[4];
end;

PROCEDURE Defuzz(I:integer;p1,p2,p3,p4,OutMS:real;OMF:String;
            var Area,AMom: MShip);                    {defuzzification routine}
var
  Atotal,Aupper : real;
begin
   OutMF[I] := OMF;
   Atotal := 0.5*(p2-p1) + 0.5*(p4-p3) + (p3-p2);
   Aupper := (0.5*(p2-p1) + 0.5*(p4-p3))*(1-OutMS)*(1-OutMS)
          + (p3-p2)*(1-OutMS);
   Area[I] := Atotal - Aupper;
   AMom[I] := Area[I] * (p2 + 0.5 * (p3-p2));
end;

PROCEDURE MemberFuncOut(var MemFunc:MFunc); {determine output membership function}
var
  K,J : integer;
  InMF1, InMF2 : char;
begin
for I := 1 to 4 do
 begin
  case I of
```

```
 1 : begin K:=1; J:=3; end;
 2 : begin K:=2; J:=3; end;
 3 : begin K:=1; J:=4; end;
 4 : begin K:=2; J:=4; end;
 end; {case}
 InMF1 := MemFunc[K];
 InMF2 := MemFunc[J];
 case InMF1 of
 'A' : case InMF2 of          {Fuzzy Associative Matrix}
  'A':Defuzz(I,PL[3,1],PL[3,2],PL[3,3],PL[3,4],OutMS[I],'PL',Area,AreaMom);
  'B':Defuzz(I,PL[3,1],PL[3,2],PL[3,3],PL[3,4],OutMS[I],'PL',Area,AreaMom);
  'C':Defuzz(I,PL[3,1],PL[3,2],PL[3,3],PL[3,4],OutMS[I],'PL',Area,AreaMom);
  'D':Defuzz(I,PM[3,1],PM[3,2],PM[3,3],PM[3,4],OutMS[I],'PM',Area,AreaMom);
  'E':Defuzz(I,PM[3,1],PM[3,2],PM[3,3],PM[3,4],OutMS[I],'PM',Area,AreaMom);
  'F':Defuzz(I,PS[3,1],PS[3,2],PS[3,3],PS[3,4],OutMS[I],'PS',Area,AreaMom);
  'G':Defuzz(I,PS[3,1],PS[3,2],PS[3,3],PS[3,4],OutMS[I],'PS',Area,AreaMom);
  end; {of second case}
  'B' : case InMF2 of
  'A':Defuzz(I,PL[3,1],PL[3,2],PL[3,3],PL[3,4],OutMS[I],'PL',Area,AreaMom);
  'B':Defuzz(I,PM[3,1],PM[3,2],PM[3,3],PM[3,4],OutMS[I],'PM',Area,AreaMom);
  'C':Defuzz(I,PM[3,1],PM[3,2],PM[3,3],PM[3,4],OutMS[I],'PM',Area,AreaMom);
  'D':Defuzz(I,PM[3,1],PM[3,2],PM[3,3],PM[3,4],OutMS[I],'PM',Area,AreaMom);
  'E':Defuzz(I,PS[3,1],PS[3,2].PS[3,3],PS[3,4],OutMS[I],'PS',Area,AreaMom);
  'F':Defuzz(I,PS[3,1],PS[3,2],PS[3,3],PS[3,4],OutMS[I],'PS',Area,AreaMom);
  'G':Defuzz(I,PS[3,1],PS[3,2],PS[3,3],PS[3,4],OutMS[I],'PS',Area,AreaMom);
  end; {of second case}
  'C' : case InMF2 of
  'A':Defuzz(I,PM[3,1],PM[3,2],PM[3,3],PM[3,4],OutMS[I],'PM',Area,AreaMom);
  'B':Defuzz(I,PM[3,1],PM[3,2],PM[3,3],PM[3,4],OutMS[I],'PM',Area,AreaMom);
  'C':Defuzz(I,PM[3,1],PM[3,2],PM[3,3],PM[3,4],OutMS[I],'PM',Area,AreaMom);
  'D':Defuzz(I,PS[3,1],PS[3,2],PS[3,3],PS[3,4],OutMS[I],'PS',Area,AreaMom);
  'E':Defuzz(I,PS[3,1],PS[3,2],PS[3,3],PS[3,4],OutMS[I],'PS',Area,AreaMom);
  'F':Defuzz(I,ZE[3,1],ZE[3,2],ZE[3,3],ZE[3,4],OutMS[I],'ZE',Area,AreaMom);
  'G':Defuzz(I,ZE[3,1],ZE[3,2],ZE[3,3],ZE[3,4],OutMS[I],'ZE',Area,AreaMom);
  end; {of second case}
 'D' : case InMF2 of
  'A':Defuzz(I,PS[3,1],PS[3,2],PS[3,3],PS[3,4],OutMS[I],'PS',Area,AreaMom);
  'B':Defuzz(I,PS[3,1],PS[3,2],PS[3,3],PS[3,4],OutMS[I],'PS',Area,AreaMom);
  'C':Defuzz(I,ZE[3,1],ZE[3,2],ZE[3,3],ZE[3,4],OutMS[I],'ZE',Area,AreaMom);
  'D':Defuzz(I,ZE[3,1],ZE[3,2],ZE[3,3],ZE[3,4],OutMS[I],'ZE',Area,AreaMom);
  'E':Defuzz(I,ZE[3,1],ZE[3,2],ZE[3,3],ZE[3,4],OutMS[I],'ZE',Area,AreaMom);
  'F':Defuzz(I,NS[3,1],NS[3,2],NS[3,3],NS[3,4],OutMS[I],'NS',Area,AreaMom);
  'G':Defuzz(I,NS[3,1],NS[3,2],NS[3,3],NS[3,4],OutMS[I],'NS',Area,AreaMom);
  end; {of second case}
 'E' : case InMF2 of
  'A':Defuzz(I,PM[3,1],PM[3,2],PM[3,3],PM[3,4],OutMS[I],'PM',Area,AreaMom);
  'B':Defuzz(I,PM[3,1],PM[3,2],PM[3,3],PM[3,4],OutMS[I],'PM',Area,AreaMom);
  'C':Defuzz(I,PS[3,1],PS[3,2],PS[3,3],PS[3,4],OutMS[I],'PS',Area,AreaMom);
  'D':Defuzz(I,NS[3,1],NS[3,2],NS[3,3],NS[3,4],OutMS[I],'NS',Area,AreaMom);
  'E':Defuzz(I,NS[3,1],NS[3,2],NS[3,3],NS[3,4],OutMS[I],'NS',Area,AreaMom);
  'F':Defuzz(I,NS[3,1],NS[3,2],NS[3,3],NS[3,4],OutMS[I],'NS',Area,AreaMom);
```

```
  'G':Defuzz(I,NM[3,1],NM[3,2],NM[3,3],NM[3,4],OutMS[I],'NM',Area,AreaMom);
  end;{of second case}
 'F' :  case InMF2 of
  'A':Defuzz(I,PL[3,1],PL[3,2],PL[3,3],PL[3,4],OutMS[I],'PL',Area,AreaMom);
  'B':Defuzz(I,PL[3,1],PL[3,2],PL[3,3],PL[3,4],OutMS[I],'PL',Area,AreaMom);
  'C':Defuzz(I,PM[3,1],PM[3,2],PM[3,3],PM[3,4],OutMS[I],'PM',Area,AreaMom);
  'D':Defuzz(I,NM[3,1],NM[3,2],NM[3,3],NM[3,4],OutMS[I],'NM',Area,AreaMom);
  'E':Defuzz(I,NM[3,1],NM[3,2],NM[3,3],NM[3,4],OutMS[I],'NM',Area,AreaMom);
  'F':Defuzz(I,NM[3,1],NM[3,2],NM[3,3],NM[3,4],OutMS[I],'NM',Area,AreaMom);
  'G':Defuzz(I,NL[3,1],NL[3,2],NL[3,3],NL[3,4],OutMS[I],'NL',Area,AreaMom);
  end;{of second case}
 'G' :  case InMF2 of
  'A':Defuzz(I,PL[3,1],PL[3,2],PL[3,3],PL[3,4],OutMS[I],'PL',Area,AreaMom);
  'B':Defuzz(I,PL[3,1],PL[3,2],PL[3,3],PL[3,4],OutMS[I],'PL',Area,AreaMom);
  'C':Defuzz(I,PL[3,1],PL[3,2],PL[3,3],PL[3,4],OutMS[I],'PL',Area,AreaMom);
  'D':Defuzz(I,NL[3,1],NL[3,2],NL[3,3],NL[3,4],OutMS[I],'NL',Area,AreaMom);
  'E':Defuzz(I,NL[3,1],NL[3,2],NL[3,3],NL[3,4],OutMS[I],'NL',Area,AreaMom);
  'F':Defuzz(I,NL[3,1],NL[3,2],NL[3,3],NL[3,4],OutMS[I],'NL',Area,AreaMom);
  'G':Defuzz(I,NL[3,1],NL[3,2],NL[3,3],NL[3,4],OutMS[I],'NL',Area,AreaMom);
  end;{of second case}
 end;{of first case}
end;
TotalArea := 0;
AreaMoment:= 0;
for I := 1 to 4 do
begin
  TotalArea := TotalArea + Area[I];
  AreaMoment:= AreaMoment + AreaMom[I];
end;
OutputSignal := AreaMoment / TotalArea ;                    {output signal}
end;

PROCEDURE InitBoard;                                        {initialize the metrobyte board}
begin
 board_num := 0; int_level := 4;  dma_level := 3;
 base_adr := $300;
 d16_init(board_num,base_adr,int_level,dma_level,err_code);
 chanlo := 6; chanhi := 7; chanOut := 1; rate := 2000.0;
 cycle := 0; mode := 0; {polled mode}
 trigger := 1;
end;

PROCEDURE MovAvg;                          {find the moving average of the applicable signal}
begin
 for k := 1 to Num_Readings-1 do
   Vibr[k] := Vibr[k+1];
 Vibr[Num_Readings] := Vib;
 Vib := 0;
 for k := Num_Readings downto 1 do
   Vib :=Vib + Vibr[k]/(Num_Readings+1-r);
 dec (r);
```

```
 if r < 1 then r := 1;
end;

PROCEDURE Average;                    {determine the average value of the digitized signal}
begin
 Omega:= 0;
 Vib  := 0;
 for k := 1 to (2 * numav ) do
 begin
  dataval:=datavector[k-1];
  Omega := Omega + dataval/numav;
  dataval := datavector[k];
  Vib := Vib + dataval/numav;
  inc(k);
 end;
 Rdata:= 0;
 k:=1;
 while (k < 2*numav) do
 begin
  Rdata := Rdata + sqr(Vib-datavector[k])/numav;
  inc(k,2);
 end;
 Omega := ((Omega*1000/409.5)-6.832185)/5.406629;
 if Omega < 0 then Omega := 0;
 if test then
  Vib := sqrt(Rdata)/409.5/10
 else
  Vib := sqrt(Rdata)/409.5;
 DelVib := Vib - VibPre;
 DelOmega := Omega - OmegaPre;
end;

PROCEDURE Output1;                    {output screen giving fuzzy inference detail}
begin
 for i:= 1 to 4 do
 begin
  write('Input Membership function ',I,' is ',InMF[I]);
  writeln(' with membership ',MemShip[I]:4:3);
 end;
 writeln;
 for I := 1 to 4 do
 begin
  write('Output Membership function ',I,' is ',OutMF[I]);
  writeln(' with membership ',OutMS[I]:4:3);
 end;
 writeln;
 for I := 1 to 4 do
 begin
  write(' area ',I,' is ', Area[I]:5:3);
  writeln(' area moment ',I,' is ', AreaMom[I]:5:3);
 end;
```

```
 writeln;
 write(' Total area is ', TotalArea:5:3);
 writeln('   area moment is ', AreaMoment:5:3);
 writeln;
 writeln('Delta output signal = ',OutputSignal:5:3) ;
 write(' Hit any key to continue... ');
 readln;
end;

PROCEDURE Output3;                          {create file of vibration signal against output volts}
begin
  append(OutFile);
  writeln(OutFile);
  write(Outfile,Omega:4:1,',',Vib:7:4,',',DelVib:10:6,
      ',',N:3,',',m:3,',',Num:3,',');
  {for i:= 1 to 4 do
   write(Outfile,InMF[I]:3,',',MemShip[I]:7:3,',');
  for I := 1 to 4 do
   write(Outfile,OutMF[I]:3,',',OutMS[I]:7:3,',');
  writeln(Outfile);
  for I := 1 to 4 do
   write(Outfile, Area[I]:7:3,',',AreaMom[I]:7:3,',');}
  write(Outfile, TotalArea:7:3,',',AreaMoment:7:3,',',OutVoltsPre:7:3,',',
      OutputSignal:7:3,',',OutVolts:7:3);
  close(Outfile);
end;

PROCEDURE Output2;                          {output screen with general control information}
begin
 clrscr;
 gotoxy(0,10);
 writeln('The machine speed in Hz is ',Omega:4:1,
      '  with change ',DelOmega:5:3);
 writeln;
 writeln('The vib level is ',Vib:6:4);
 writeln('   DelVib this step is ',DelVib:8:6);
 writeln;
 writeln('Delta output voltage this step is ',OutputSignal:8:4);
 writeln('Delta output voltage prev step is ',OutSigPre2:8:4);
 writeln;
 writeln('Total Output Voltage this step is       ',(OutVolts):8:4);
 writeln('Total Output Voltage for previous step is ',(OutVoltsPre):8:4);
 C_Volts := 4.450279 * OutVolts + 0.821645;
 writeln('Output Voltage to clutch is ',(C_Volts):6:2);
 writeln;
 writeln(' N = ',N:3,'       m = ',m:3,'       Num =',Num:3);
end;

PROCEDURE FuzzyMinimize;                                {fuzzy inferencing procedure}
begin
  if (Vib > 0.0030) and (Omega > 35) then
```

```
 begin
  MovAvg;
  DelVib := Vib - VibPre;
  I:=1;
  J:=1;
  MemShipFunction(Vib);
  I:=3;
  J:=2;
  MemShipFunction(DelVib);
  MemberShipOut(MemShip, OutMS);
  MemberFuncOut(MemFunc);
  for I := 1 to 4 do
   case MemFunc[I] of
    'A': InMF[I] := 'NL';
    'B': InMF[I] := 'NM';
    'C': InMF[I] := 'NS';
    'D': InMF[I] := 'ZE';
    'E': InMF[I] := 'PS';
    'F': InMF[I] := 'PM';
    'G': InMF[I] := 'PL';
   end;  {of case}
 end;
 if test then OutPut1;
 if m < 3 then inc (m);                    {count the 1st and 2nd times through}
end;

PROCEDURE PreMinimize;                     {initial attempt at locating the minimum response}
begin
  if num = 4 then
  begin
   FuzzyMinimize;
   if third then N := -N;
  end
  else
  begin
   OutputSignal := 0.2;
   if (delvib > 0) and (Num = 2)  then
   begin
    N := -N;
    OutputSignal := 0.4;
    second := true;
   end;
   if (delvib > 0) and (Num = 3)  then
   begin
    N := -N;
    if second then
    begin
     OutputSignal :=  0.3;
     third := true;
    end
    else
```

```
      Outputsignal := 0.1;
    end;
    if(Num =3) and (DelVib<0)  then
    begin
     Outputsignal := 0.1;
     if (abs(DelVib)<DelVibPre1) and second then
       N := -N;
    end;
    if Num <4 then inc(Num);
  end;
end;

PROCEDURE BoardOut;                                  {output analog signal for control}

{4095/10 = 409.5 is the appropriate scaling factor for a 10V }
{(+_5)full range translated into 0-4095 converter counts}
begin
 dataval:= round(OutVolts *4095/5);   {0 to 5 volts}
 d16_aous(board_num,chanOut,dataval,err_code);
 if err_code <> 0 then
   writeln('Execution error ',err_code:4)
end;

PROCEDURE Init_PreCond;                              {initialize conditions}
begin
 DelVibPre1:=0; DelVibPre2:=0; DelVibPre3:=0;
 Pos := false;  Neg := false; Cond := false;
 Second := false;  Third := false;
 OutSigPre1:=0; OutSigPre2:=0; OutSigPre3:=0;
end;

PROCEDURE Speed_Corr;                                {to estimate the volts output vs speed}
begin
 SpeedDif := (Omega-SpeedRef);
 if abs(SpeedDif) > 2 then
 begin
   SpeedRef := omega;
   CurveVolts := 0.04*Omega;
   OutVolts := CurveVolts;
   OutputSignal := 0;
   Init_PreCond;
   num:=1;
   m := 0;
   if ((SpeedDif>0) and (DelVib<0)) or ((SpeedDif<0) and (DelVib>0))
    then n := 1
    else n := -1;
 end;
end;

PROCEDURE Collect_Data;                              {data acquisition routine}
begin
```

```
   d16_ainsc(board_num,chanlo,chanhi,mode,cycle,trigger,count, rate,
        datavector[0],err_code);
   if err_code <> 0 then
    d16_print_error(err_code)
   {else
   begin
    test:= true;
    for i := 0 to count-1 do
    begin
     write('Enter value for dataVector[',i,']');
     readln(datavector[i]);
    end;
   end;}
end;

Procedure Init_Variables;
begin
 quit := false;     {conditional for quitting program}
 First := false;    {conditional for counting Vib increases}
 test:= false;      {office test condition to increase resolution of vib}
 Num :=0;           {counter for Vib increases}
 Num_Readings := 3; {num of readings in moving average}
 r := 3;            {counter for the first three readings}
 m:=1;              {counter for FuzzyMinimize procedure}
 N:=1;              {pos/neg changeover in minimize routines}
 OutCount:=0;       {count of file output data}
 Delvib:=0;
 Init_PreCond;
 DelOmega:=0;
 OmegaPre := 35;    {Hz}
 VibPre := 0.0030;  {volts a/c portion of signal}
 OutVolts := 1.80;  {low voltage init}
 OutVoltsPre := 0;
 Vibr[5]:=0;        {latest reading in the moving average}
 for k:=4 downto 1 do  {init all variables in moving average}
  Vibr[k] := Vibr[k+1];
 for i := 1 to 4 do
 begin
    InMF[I]:='Z'; MemShip[I]:=0; OutMF[I]:='Z'; OutMS[I]:=0;
    Area[I]:=0; AreaMom[I]:=0;
 end;
 TotalArea :=0; AreaMoment:=0; OutputSignal:=0;
 CreateFile(OutFile,Filename);
 write(Outfile,' Om, Vb, DlVb, N, m, Nu,');
 {for i:= 1 to 4 do
  write(Outfile,' IMF[',I,'],',' MS[',I,'],');
 for I := 1 to 4 do
  write(Outfile,' OMF[',I,'],',' MS[',I,'],');
 writeln(OutFile);
 for I := 1 to 4 do
  write(Outfile,' A[',I,'],',' AM[',I,'],');}
```

```
  write(Outfile,' ToA,',' AMo,',' OVP,',' OSig,',' PrV');
  close(OutFile);
end;

PROCEDURE Conditionals;          {signal examination for determining the value of N}
begin
   if (m > 0) and (m < 3) and (DelVib > 0) then Cond := true;
   if (OutSigPre3 >0) and (OutSigPre2 >0) and (OutSigPre1 >0) then
     Pos := true;
   if (OutSigPre3 <0) and (OutSigPre2 <0) and (OutSigPre1 <0) then
     Neg := true;
   if (DelVibPre1>0) and (DelVibPre2>0) and (Pos or Neg) then Cond:= true;
   if (OutVolts = 1.0) and Neg then Cond := true;
   if (OutVolts = 5.0) and Pos then Cond := true;
   if Cond then
   begin
    N := -N;
    Init_PreCond;        {re-initialize pre_conditions}
   end;
end;

PROCEDURE Output;
begin
  OmegaPre := Omega;
  VibPre := Vib;
  if Num > 1 then                    {going thru PreMinimize}
  begin
    DelVibPre3 := DelVibPre2;
    DelVibPre2 := DelVibPre1;
    DelVibPre1 := DelVib;
    OutSigPre3 := OutSigPre2;
    OutSigPre2 := OutSigPre1;
    OutSigPre1 := OutputSignal * N;  {this step value with existing N}
    if m > 0 then                    {going thru FuzzyMinimize}
      Conditionals;                  {determine this step value for N + or -}
  end;
  OutputSignal :=OutputSignal * N;
  OutVolts := OutVolts + OutputSignal;
  OutSigPre1 := OutputSignal;        {Actual Delta volts for this step}
  if OutVolts < 1.6 then OutVolts := 1.6
  else if OutVolts >5 then OutVolts := 5;
  BoardOut;
  Output3;                           {output to file}
  Output2;                           {output to screen}
  OutVoltsPre:= OutVolts;            {set for next step output}
  delay(500);
end;
```

```
{**********  main program  **********}
begin
SelectInputMode(Keyboard);
if KeyBoard then KeyBoardInput
        else ReadFile;
InitBoard;                          {begin data acquisition section}
write('The input sample frequency in Hz is ',rate:8:0);
writeln;
writeln('The number of averages is presently ',numav);
count := 2 * numav;
Init_Variables;                     {initialize the program variables}
BoardOut;
repeat
 Collect_data;                      {acquire data for speed and vibration}
 Average;                           {return with rms values for Omega and Vib}
 if (Vib < 0.001) or (Omega < 10) then
 begin
  clrscr;
  gotoxy(0,10);
  writeln('....cycling... ');
 end
 else
 begin
  Speed_Corr;                       {check rough location of speed vs output volts}
  if (abs(SpeedDif) <= 2) and (Omega > 35)  then
   PreMinimize;
  Output;
  { writeln;
  write('Hit any key to continue; <Q>uit to end: ');
  Quit := upcase(ReadKey)= 'Q';}
 end;
 until Keypressed;{ Quit;}
end.
```

```
{FUZZY.MOD}
{NOTE: this group of procedures is written as an include file for the program fzcntl.pas}
{the procedures given here allow the applicable fuzzy membership function data along the } {universe of
discourse to be input via the keyboard and subsequently written in a file to disc.}

PROCEDURE SelectInputMode(var Keybord:Boolean);
VAR
 answer : CHAR;
BEGIN
 ClrScr;
 gotoxy (0,10);
 WRITELN ('Do you want to input the file from the keyboard or from');
 WRITE ('a file?  (K or F)  ');
```

```
  EchoKF (answer);
  IF answer IN ['F' , 'f'] THEN
    KeyBord := FALSE
  ELSE
    KeyBord := TRUE
END;

PROCEDURE ReadFile;  { from a file }
type
   string10 = string[10];
   string3  = string[3];
VAR
  i,j  : INTEGER;
  SourceFile : TEXT;
  Title : String10;
  MF : string3;
BEGIN
  WRITELN;
  IF  GetFile (SourceFile)  THEN
    BEGIN
     RESET (SourceFile);
     Repeat
     READLN (SourceFile, Title,j);
     READ(SourceFile ,MF);
     FOR  i := 1  TO  4  DO
        READ (SourceFile , NL[j,i]); readln(SourceFile);
     READ(SourceFile ,MF);
     FOR  i := 1  TO  4  DO
        READ (SourceFile , NM[j,i]);readln(SourceFile);
     READ(SourceFile ,MF);
     FOR  i := 1  TO  4  DO
        READ (SourceFile , NS[j,i]);readln(SourceFile);
     READ(SourceFile ,MF);
     FOR  i := 1  TO  4  DO
        READ (SourceFile , ZE[j,i]);readln(SourceFile);
     READ(SourceFile ,MF);
     FOR  i := 1  TO  4  DO
        READ (SourceFile , PS[j,i]);readln(SourceFile);
     READ(SourceFile ,MF);
     FOR  i := 1  TO  4  DO
        READ (SourceFile , PM[j,i]);readln(SourceFile);
     READ(SourceFile ,MF);
     FOR  i := 1  TO  4  DO
        READ (SourceFile , PL[j,i]);readln(SourceFile);
     Until EOLN (SourceFile) OR (j=NumInputVar);
     READLN (SourceFile)
     END;
     CLOSE (SourceFile);
     end;

PROCEDURE StoreFile;    { store file on disk}
```

```
type
   InputVar = integer:
var
  answer: char;
  FileName: string16;
  OutFile : text;
begin
 WRITE ('Do you want to store the membership function points on disk? ');
 WRITE ('  (Y or N)   ');
EchoYN (answer);
 IF answer IN ['Y', 'y'] THEN
  BEGIN
   CreateFile (OutFile, FileName);
   REWRITE (OutFile);
   For I :=1 to NumInputVar do
   begin
     WRITELN (OutFile, 'Input Var ',InputVar(I));
     write(Outfile,'NL');
     FOR J := 1 to 4 DO
     WRITE(OutFile, NL[I,J]:6:1); writeln(OutFile);
     write(OutFile,'NM');
     FOR J := 1 to 4 DO
     WRITE(OutFile, NM[I,J]:6:1);   writeln(Outfile);
     write(OutFile,'NS');
     FOR J := 1 to 4 DO
     WRITE(OutFile, NS[I,J]:6:1);   writeln(OutFile);
     write(OutFile,'ZE');
     FOR J := 1 to 4 DO
     WRITE(OutFile, ZE[I,J]:6:1);   writeln(OutFile);
     write(OutFile,'PS');
     FOR J := 1 to 4 DO
     WRITE(OutFile, PS[I,J]:6:1);   writeln(OutFile);
     write(OutFile,'PM');
     FOR J := 1 to 4 DO
     WRITE(OutFile, PM[I,J]:6:1);   writeln(OutFile);
     write(OutFile,'PL');
     FOR J := 1 to 4 DO
     WRITE(OutFile, PL[I,J]:6:1);   writeln(OutFile);
   end;
  CLOSE (OutFile)
 end;
end;

PROCEDURE KeyBoardInput; {input Universe of Discourse via keyboard}
type
   string14 = string[14];
   InputVar = integer;
var
  answer: char;
  FileName: string14;
  OutFile : text;
```

```
begin
   for I := 1 to NumInputVar do
   begin
      write('Enter the input variable number: ');
      readln(InputVar(I));
      for J:= 1 to 4 do
      begin
         write('Enter point ',J,' for NL(',I,',',J,'):');
         readln(NL[I,J])
      end;
      for J:= 1 to 4 do
      begin
         write('Enter point ',J,' for NM(',I,',',J,'):');
         readln(NM[I,J])
      end;
      for J:= 1 to 4 do
      begin
         write('Enter point ',J,' for NS(',I,',',J,'):');
         readln(NS[I,J])
      end;
      for J:= 1 to 4 do
      begin
         write('Enter point ',J,' for ZE(',I,',',J,'):');
         readln(ZE[I,J])
      end;
      for J:= 1 to 4 do
      begin
         write('Enter point ',J,' for PS(',I,',',J,'):');
         readln(PS[I,J])
      end;
      for J:= 1 to 4 do
      begin
         write('Enter point ',J,' for PM(',I,',',J,'):');
         readln(PM[I,J])
      end;
      for J:= 1 to 4 do
      begin
         write('Enter point ',J,' for PL(',I,',',J,'):');
         readln(PL[I,J])
      end;
   end;
   StoreFile
   end;
```

Appendix IV

Torsional Lateral Mode Shapes

The torsional lateral mode shapes presented herein were identified by finite element analysis (Cosmos M program) and confirmed with results from Matlab. The finite element model was constructed of appropriate mass elements to represent the rotary inertia and mass stations, and with 3-d beam elements for the connecting shafting. The model is illustrated in Fig A-IV 1. The offset of the shafting provided by the pinion and gear radii is indicated as r1 and r2 respectively in the above figure. The finite element model included solid elements, to represent the gear and pinion structure, which allowed no distortion of these members. The gear / pinion mesh stiffness is represented by a longitudinal spring element of stiffness K_t = 1.84 e8 N/m^2. The bearing supports are modeled as stiff.

The mass elements are single node elements with up to 6 degrees of freedom. The rotational inertia elements are about the 'z' axis only (axial) for the drive motor, pinion, damper, gear, and load inertias. Lateral motion of the mass elements for the pinion and gear stations was allowed in the 'y' direction (vertical) while being constrained in the 'z' and 'x'.

The beam elements representing the shafting are 3-node uniaxial elements having 6 degrees of freedom (3 translational and 3 rotational) per node. Bending motion of the beam elements is allowed in the 'y' direction only and with torsional motion about 'z'.

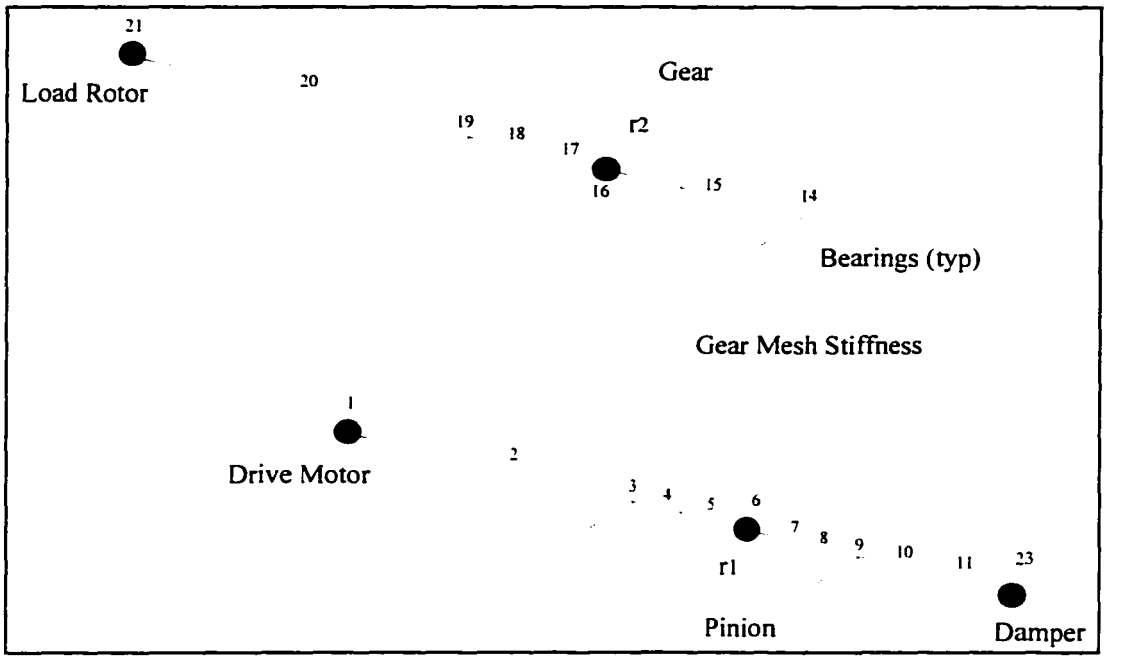


Figure A-IV 1: Finite Element Model

The linear spring utilized for the gear mesh is a 2 node, uniaxial element in which 2 degrees of freedom (one translational and one rotational) are considered for each node. In this model only the translational motion is allowed.

The figures included in this appendix describe the first two significant modes (modes 2 and 3, Fig A-IV 2- 5) of the rotor in the free damper condition, as well as the first three significant modes (modes 2, 3 and 4, Fig A-IV 6 - 11) for the rotor in the locked damper condition. The first mode in each case for the semi-definite system is a zero frequency rigid body torsional mode.

Each of the above significant modes is described by two figures. The first figure presents the coupled mode shape plot from the finite element program. In this figure, the lateral mode shape is well defined but unfortunately, the torsional motion is only indicated at the gear mesh. To further define the actual torsional mode shape across the full length of the rotors, a second plot for each frequency is given together with a supporting tabulation of the applicable relative node displacements for each mode. Reference Fig A-IV 1 for the relative node distribution used in the model.

The following observations are noted with respect to the figures presented in this appendix which show the coupling of the torsional and lateral model shapes.

Free damper condition:

mode 2

- Some minor bending is indicated in Fig A-IV 2 for this mode.
- A significant torsional deflection is indicated between the gear and load for this mode in Fig A-IV 3.

mode 3

- A significant bending contribution at both the pinion and gear stations is evident in Fig A-IV 4.
- An unequal torsional distortion (because of coupling with the significant bending) of the pinion and gear inertias is shown in Fig A-IV 5.

Locked damper condition:

mode 2

- A significant bending contribution at both the pinion and gear stations is indicated in Fig A-IV 6.

- Some minor torsional deflection is evident between the gear and pinion, as well as significant torsional deflection is indicated between the pinion and damper inertias in Fig A-IV 7.

mode 3

- Negligible bending deflection is indicated in Fig A-IV 8 for this mode.
- A significant torsional deflection now occurs between both the gear and load inertias, and the pinion and damper inertias (ref Fig A-IV 9).
- The torsional deflection between the gear and pinion in Fig A-IV 9 is equal and opposite, indicative of the small bending component for this mode.

mode 4

- A significant bending contribution is indicated at both the pinion and gear stations in Fig A -IV 10.
- Again, unequal torsional distortion of the pinion and gear inertias is shown for this mode in Fig A -IV 11 because of coupling with the significant bending component.

The mode shape information presented indicates clearly the interaction between the torsional and lateral regimes throughout the operation speed range of similar offset geared machine arrangements.

Table A-IV 1: Relative Node Displacements (free mode 2)

Rotor	Node	y - displacement	x - rotation
P i n i o n	1	0	9.244591
	2	-0.003104748	8.824897
	3	7.89238E-05	8.649157
	4	0.01376909	8.598946
	5	0.02047806	8.565472
	6	0.02354754	8.52865
	7	0.02258535	8.667172
	8	0.01756034	8.681356
	9	7.911046E-05	8.709725
	10	-0.004439518	8.823199
	11	-0.000414575	9.192789
	23	0	9.270111
G e a r	14	-8.970164E-05	-7.678134
	15	-0.01349344	-7.678134
	16	-0.0196791	-7.678134
	17	-0.01911436	-6.310566
	18	-0.0132682	-4.299436
	19	-7.127804E-05	-1.564299
	20	9.358076E-05	20.96036
	21	0	23.71796

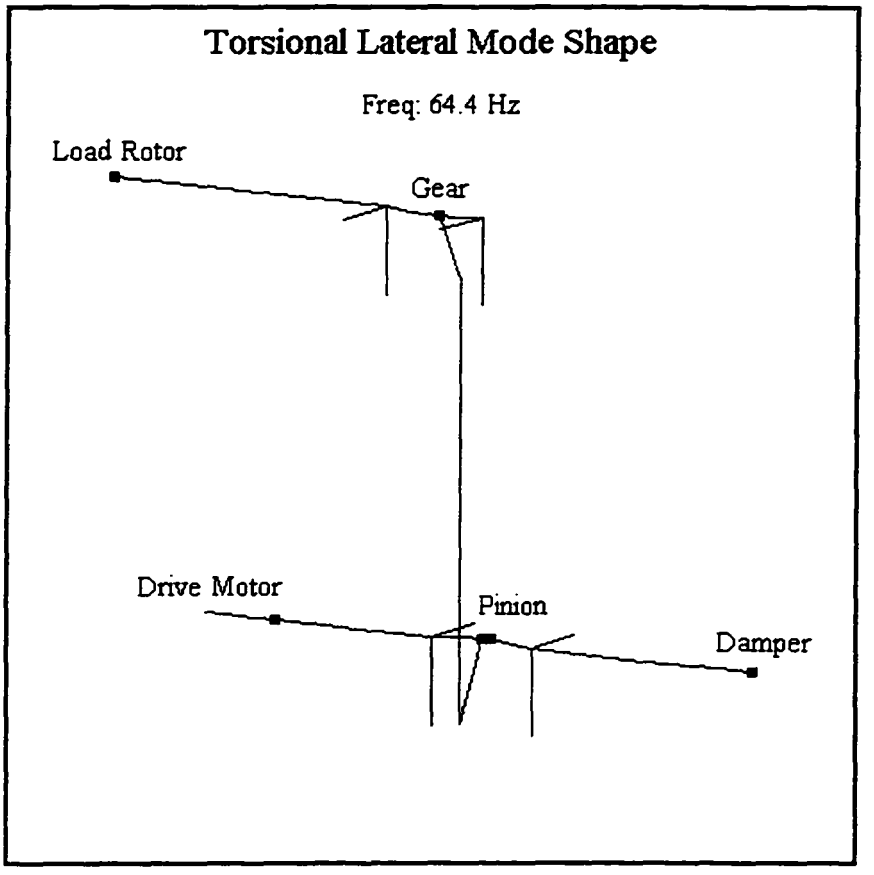


Figure A-IV 2: Free Mode 2, Coupled Mode Shape

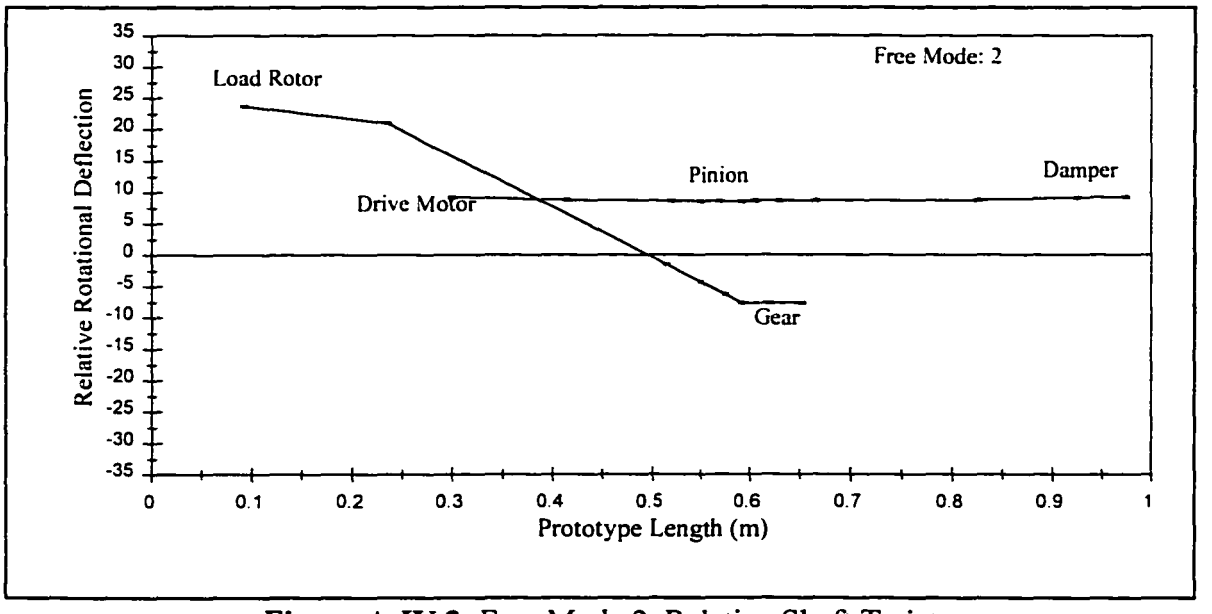


Figure A-IV 3: Free Mode 2, Relative Shaft Twist

Table A-IV 2: Relative Node Displacements (free mode 3)

Rotor	Node	y - displacement	x - rotation
	1	0	23.35116
P	2	-0.06125739	18.05014
i	3	0.001514193	15.83043
n	4	0.2720601	15.19622
i	5	0.4060949	14.77342
o	6	0.4709022	14.30834
n	7	0.4552942	15.58581
	8	0.3569315	15.76252
	9	0.00168605	16.11594
	10	-0.09066494	17.52961
	11	-0.008466602	22.13399
	23	0	23.09728
	14	-0.002495785	5.687778
	15	-0.3754304	5.687778
G	16	-0.547535	5.687778
e	17	-0.5318223	5.395933
a	18	-0.3691635	4.966749
r	19	-0.001983181	4.383058
	20	0.002603714	-0.4238065
	21	0	-1.01229

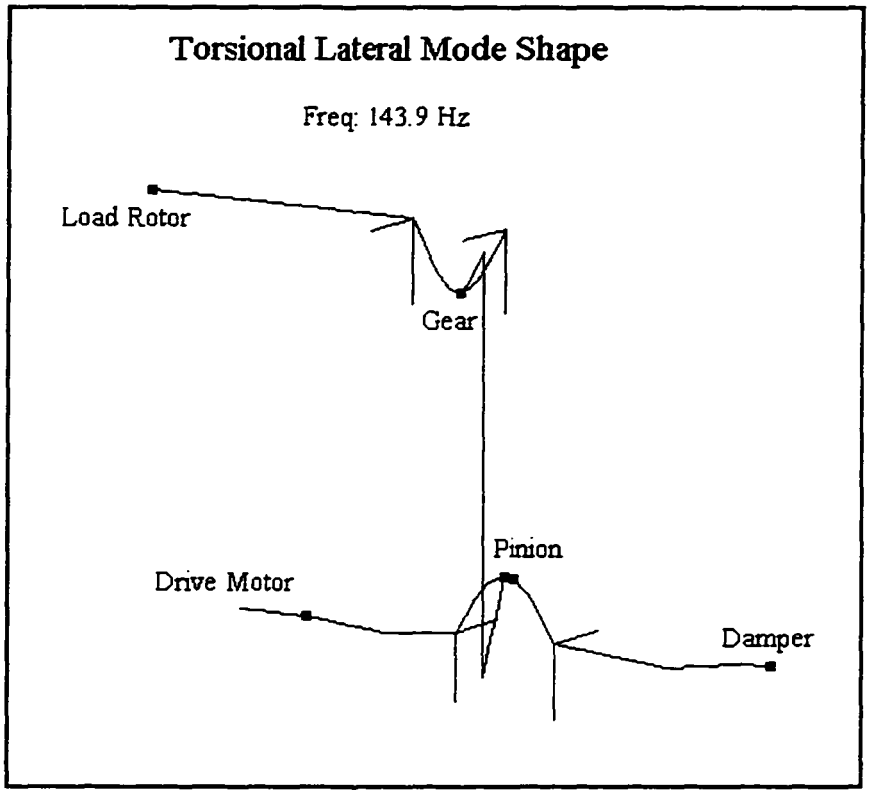


Figure A-IV 4: Free Mode 3, Coupled Mode Shape

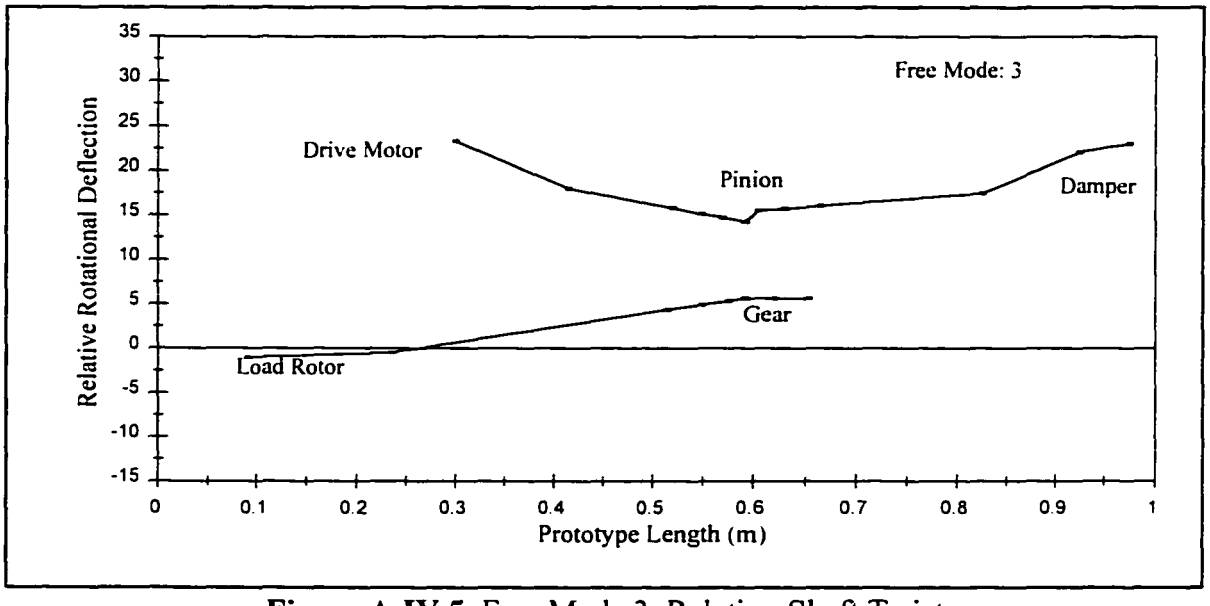


Figure A-IV 5: Free Mode 3, Relative Shaft Twist

Table A-IV 3: Relative Node Displacements (locked mode 2)

Rotor	Node	y - displacement	x - rotation
	1	0	0.3053509
P	2	-0.005357514	0.2957484
i	3	0.0001364722	0.2917276
n	4	0.02375719	0.2905788
i	5	0.03532317	0.2898129
o	6	0.04059196	0.2889704
n	7	0.03890944	0.7967116
	8	0.03023322	1.565184
	9	0.0001356902	3.10213
	10	-0.007640608	9.249911
	11	-0.0007135017	29.27343
	23	0	33.46257
	14	-0.0001531503	1.171018
	15	-0.02303775	1.171018
G	16	-0.03359871	1.171018
e	17	-0.03263452	1.734306
a	18	-0.0226532	2.562671
r	19	-0.0001216951	3.689247
	20	0.0001597732	12.96693
	21	0	14.10276

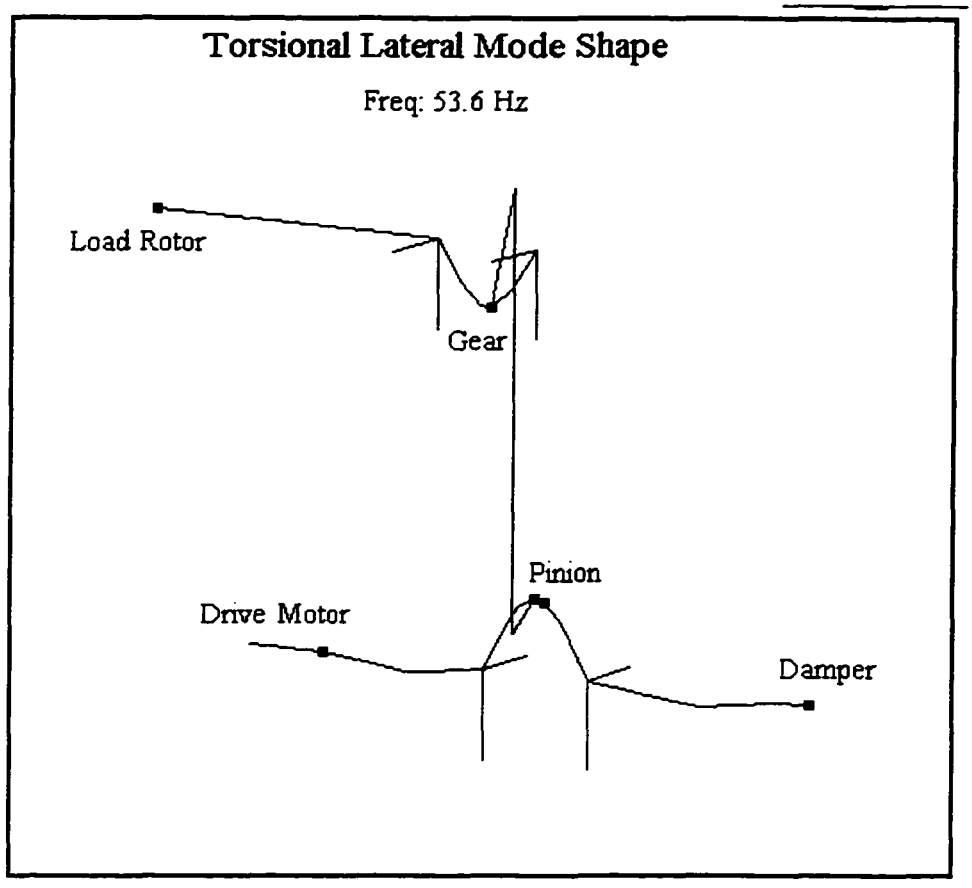


Figure A-IV 6: Locked Mode 2, Coupled Mode Shape

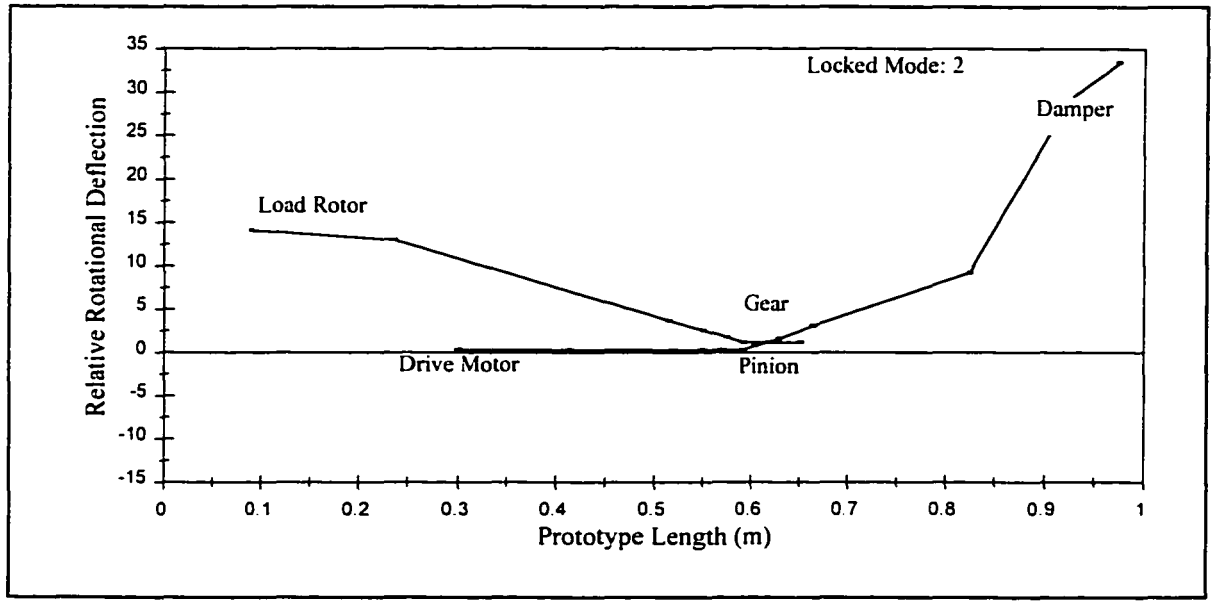


Figure A-IV 7: Locked Mode 2, Relative Shaft Twist

Table A-IV 4: Relative Node Displacements (locked mode 3)

Rotor	Node	y - displacement	x - rotation
	1	0	9.895093
P	2	0.0006071572	9.396136
i	3	-1.54226E-05	9.187206
n	4	-0.002692756	9.127512
i	5	-0.004005193	9.087716
o	6	-0.004606594	9.04394
n	7	-0.004419337	8.816686
	8	-0.003436868	8.242307
	9	-1.550428E-05	7.093547
	10	0.0008690069	2.498513
	11	8.115038E-05	-12.46766
	23	0	-15.59874
	14	1.761293E-05	-9.210596
	15	0.002649439	-9.210596
G	16	0.003863994	-9.210596
e	17	0.003753108	-7.956243
a	18	0.002605213	-6.111604
r	19	1.399545E-05	-3.602897
	20	-1.837459E-05	17.05705
	21	0	19.58636

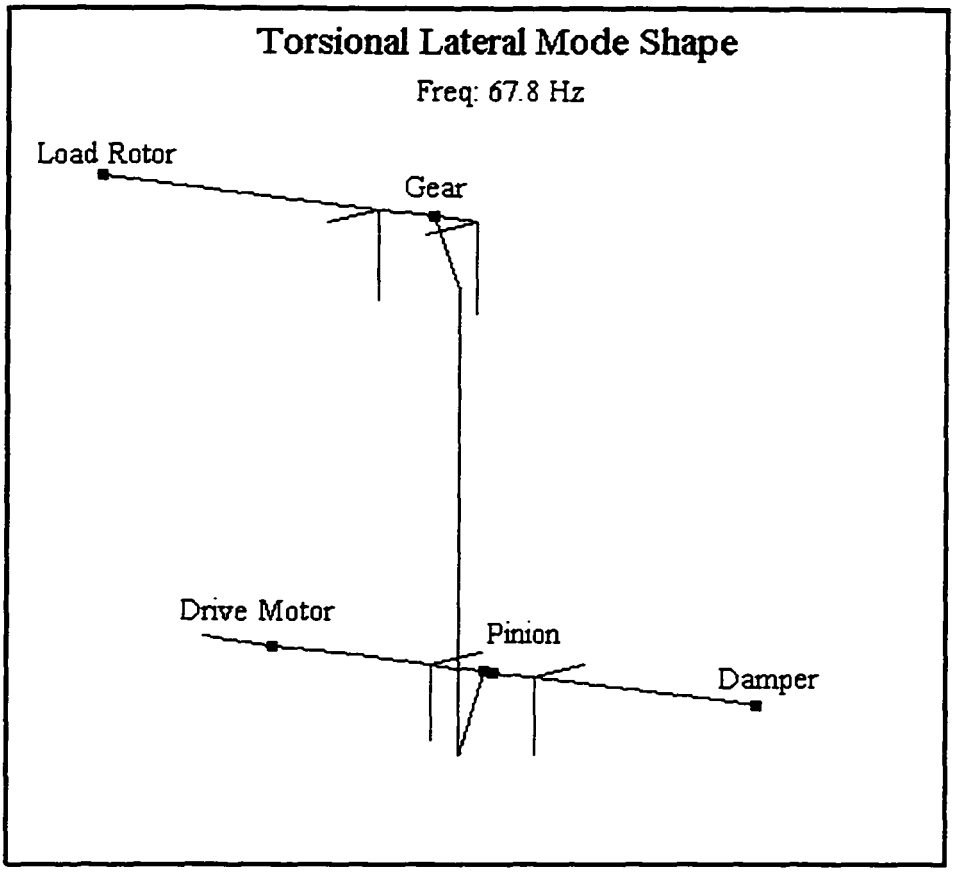


Figure A-IV 8: Locked Mode 3, Coupled Mode Shape

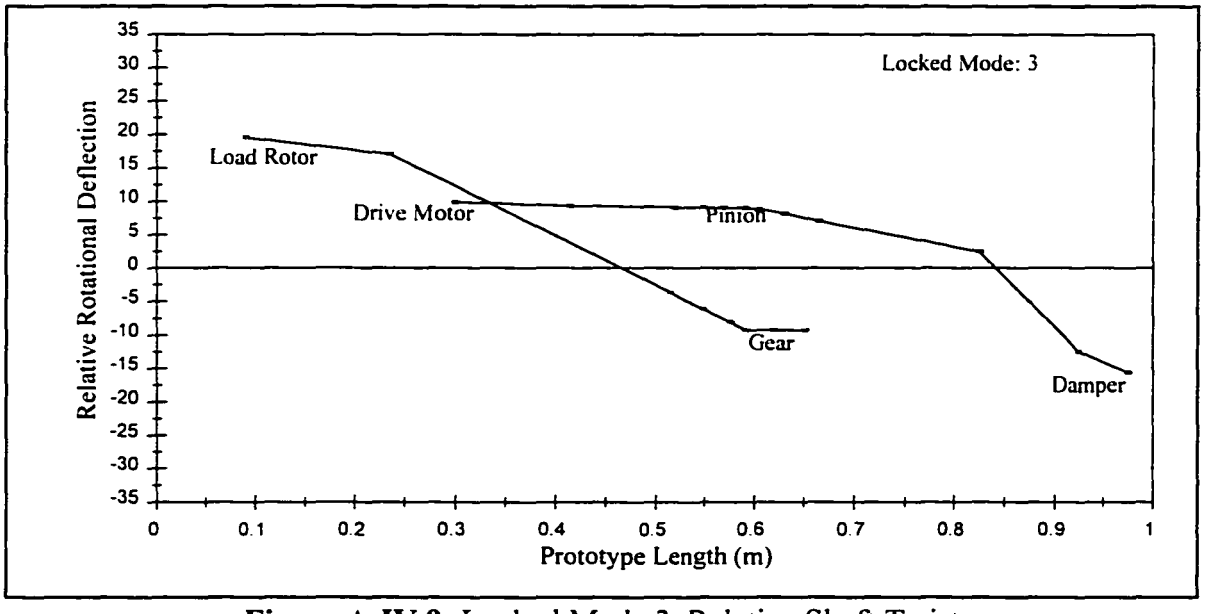


Figure A-IV 9: Locked Mode 3, Relative Shaft Twist

Table A-IV 5: Relative Node Displacements (locked mode 4)

Rotor	Node	y - displacement	x - rotation
P i n i o n	1	0	25.11657
	2	-0.05997672	19.19755
	3	0.001480486	16.71907
	4	0.266391	16.01093
	5	0.397703	15.53884
	6	0.4613579	15.01954
	7	0.4462373	15.97352
	8	0.3499682	15.53823
	9	0.00165677	14.66765
	10	-0.08891596	11.18533
	11	-0.008303279	-0.1567214
	23	0	-2.529597
G e a r	14	-0.00255517	5.042848
	15	-0.3843634	5.042848
	16	-0.5605632	5.042848
	17	-0.5444765	4.785774
	18	-0.3779475	4.407724
	19	-0.00203037	3.893575
	20	0.002665667	-0.3405905
	21	0	-0.8589608

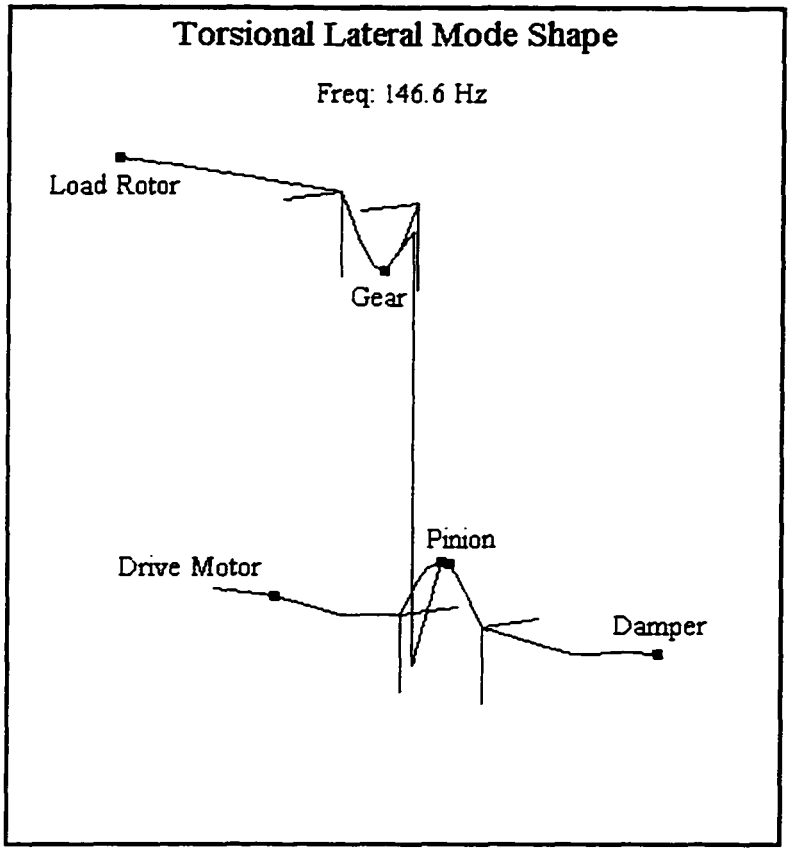


Figure A-IV 10: Locked Mode 4, Coupled Mode Shape

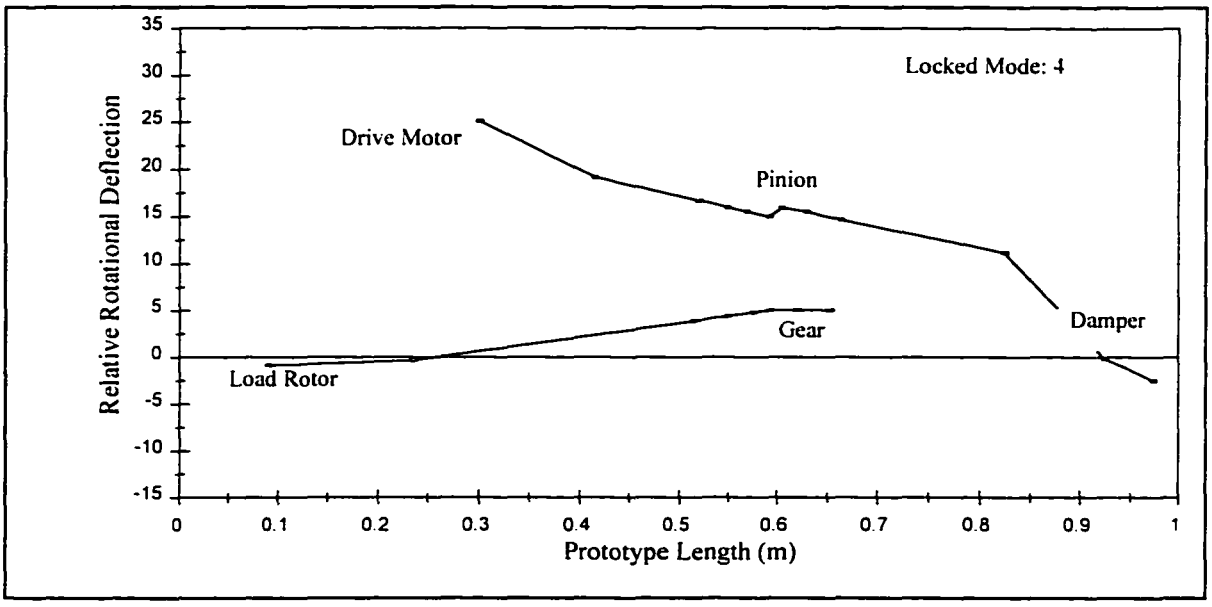


Figure A-IV 11: Locked Mode 4, Relative Shaft Twist

Appendix V

Metrabyte Model DAS-16 Card

A Metrabyte model DAS-16 card was installed in a lab PC (80286 AT) desktop computer to perform the data acquisition function for this project. Board-specific utility software routines in Turbo Pascal, developed by Quinn Curtis, were utilized to access the analog to digital (A/D) conversion functionality of the card.

The Metrabyte model DAS-16 card is a multifunction high speed analog / digital I/O expansion board for 8088, 80286, 80386 series computers. It is a full length board that installs internally in an expansion slot of a the PC and allows fast high precision data acquisition for signal analysis, control, etc. The board has a multi-layer construction with integral ground plane to minimize noise and crosstalk at high frequencies.

The DAS 16 uses an industry standard (HI-67A) 12 bit successive approximation converter with a 12 microsecond conversion time giving a maximum throughput rate if 60 kHz in DMA mode. The channel input configuration is switch selectable on the board, providing a choice between 16 single ended channels or 8 differential channels with 90 dB common mode rejection and +/- 10 v common mode range.

The A/D conversions may be initiated in any one of 3 ways, by software command, by internal programmable interval timer or by direct external trigger to the A/D. At the end

of the A/D conversion, it is possible to transfer the data in any of 3 ways, by program transfer, by interrupt or by DMA. All operating modes are selected by a control register on the DAS-16 and are also supported by the utility software.

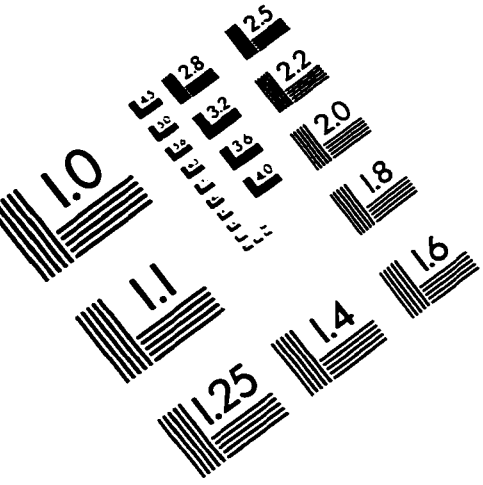
High input impedance ranges of +1v, +2v, +5v and +10 v unipolar and +/-0.5 v, +/-1v, +/-2.5v, +/-5v and +/-10v bipolar are switch selectable. These ranges are common to all channels and are controlled by the gain of the input instrumentation amplifier. Other ranges may be realized with a single user installed resistor. All inputs are multiplexed through a low drift, fast settling instrumentation amplifier / sample-hold combination.

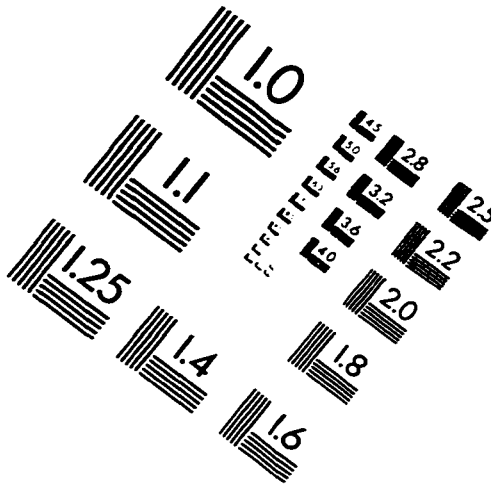
A three channel programmable interval (Intel 8254) provides trigger pulses for the A/D at any rate from 250 Khz to 1 pulse/hr. Two channels are operated in a fixed divider configuration from an internal 1 MHz clock. The third channel is uncommitted and provides a gated 16 bit binary counter that can be used for event or pulse counting, delayed triggering, and in conjunction with the other channels for frequency and period measurement.

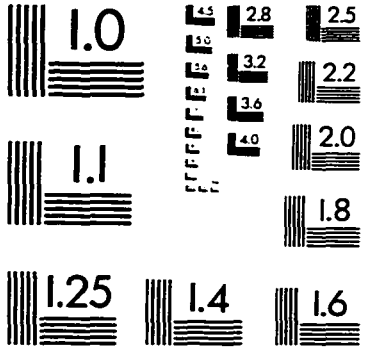
The card offers two channels of multiplying 12 bit D/A output. The D/A converters may be operated with a fixed -5v reference available from the DAS-16 board to give a 0 to +5v output. Alternatively an external dc or ac reference may be used to give different output ranges or programmable attenuator action on an ac signal. The D/A's are double-buffered to provide instantaneous single step update.

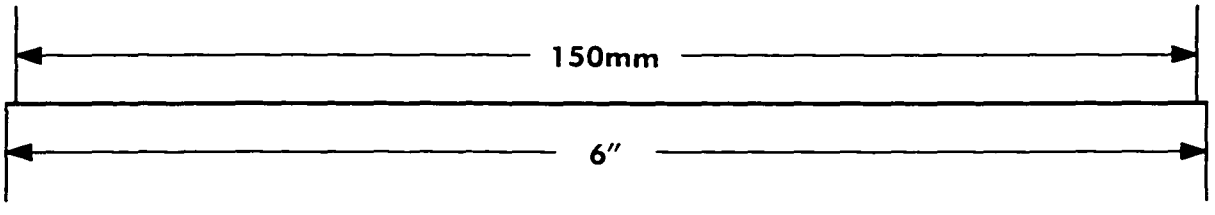
A -5v (+/-0.05v) precision reference voltage output is derived from the A/D converter reference. Typical uses are providing a dc reference for the D/A converters and offsets, and bridge excitation to user supplied circuits.

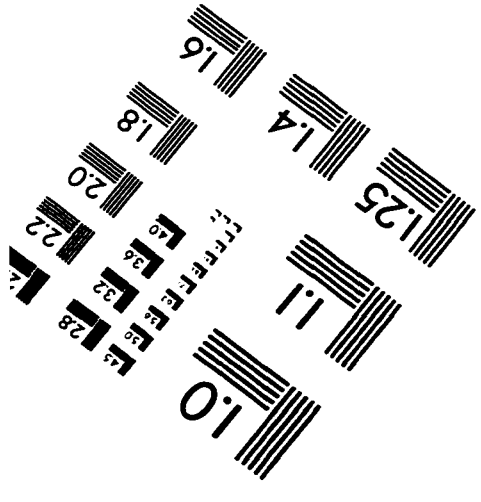
IMAGE EVALUATION
TEST TARGET (QA-3)

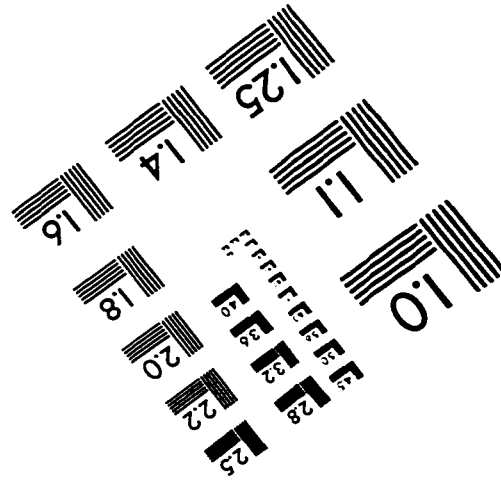












APPLIED IMAGE, Inc
1653 East Main Street
Rochester, NY 14609 USA
Phone: 716/482-0300
Fax: 716/288-5989

© 1993, Applied Image, Inc., All Rights Reserved